NCL 71-32R

NORTHROP CORPORATE LABORATORIES

KINETIC MODEL AND THEORETICAL CALCULATIONS FOR STEADY STATE ANALYSIS OF ELECTRICALLY EXCITED CO LASER AMPLIFIER SYSTEM FINAL REPORT: PART II

NO RECORD OF PART I

Prepared by

W. B. Lacina
Northrop Corporate Laboratories

Office of Naval Research
Contract No. N00014-71-C-0037
1 August 1970 through 31 July 1971

Sponsored by
Advanced Research Projects Agency
Order No. 306

UNCLASSIFIED

Security Classification

DOCUMENT CONTROL DATA - R & D

(Security classification of title, body of abstract and indexing annotation must be entered when the overall report is classified)

1. ORIGINATING ACTIVITY (Corporate author) NORTHROP CORPORATE LABORATORIES 3401 WEST BROADWAY HAWTHORNE, CALIFORNIA	2a. REPORT SECURITY CLASSIFICATION UNCLASSIFIED 2b. GROUP -

3. REPORT TITLE

KINETIC MODEL AND THEORETICAL CALCULATIONS FOR STEADY STATE ANALYSIS OF ELECTRICALLY EXCITED CO LASER AMPLIFIER SYSTEM - FINAL REPORT: PART II

4. DESCRIPTIVE NOTES (Type of report and inclusive dates)

FINAL REPORT: PART II

5. AUTHOR(S) (First name, middle initial, last name)

LACINA, W. B.

6. REPORT DATE AUGUST 1971	7a. TOTAL NO. OF PAGES 108	7b. NO. OF REFS 74
8a. CONTRACT OR GRANT NO. Contract N00014-71-C-0037 b. PROJECT NO. ARPA ORDER NO. 306 c. d.	9a. ORIGINATOR'S REPORT NUMBER(S) NCL 71-32R 9b. OTHER REPORT NO(S) (Any other numbers that may be assigned this report) --	

10. DISTRIBUTION STATEMENT

DISTRIBUTION OF THIS DOCUMENT IS UNLIMITED.

11. SUPPLEMENTARY NOTES NONE	12. SPONSORING MILITARY ACTIVITY OFFICE OF NAVAL RESEARCH DEPARTMENT OF THE NAVY ARLINGTON, VIRGINIA 22217

13. ABSTRACT

A qualitative and quantitative discussion of several aspects of electrically excited CO laser systems is presented. Topics included are molecular spectroscopy and radiative properties, molecular kinetics, and plasma characteristics. Special emphasis is on description of a steady state molecular kinetic model which has been constructed for calculation of the vibrational population distributions and resulting radiative properties for a CO laser amplifier system. The master equation for the vibrational populations is formulated, with several pumping, relaxation, cross-relaxation, and stimulated emission processes included. A computer program for cw operation with an arbitrary number of vibrational levels has been constructed for numerical solution of the master equation, and preliminary results for a variety of parameters are presented. The importance of plasma characteristics is discussed, although calculations for the electron kinetics have not yet been undertaken. Future efforts should be made to analyze the coupled system of electron and molecular kinetics on a consistent and equal basis. (U)

DD FORM 1 NOV 68 1473 (PAGE 1)

S/N 0101-607-6801

UNCLASSIFIED

Security Classification

KEY WORDS	LINK A		LINK B		LINK C	
	ROLE	WT	ROLE	WT	ROLE	WT
Molecular Kinetics						
CO Laser						
Anharmonic Pumping						
Stimulated Emission						
Vibrational Populations						
Saturation Intensity						
Radiative Characteristics						
Laser Amplifier						
Electrically Excited Laser						
Quantum Efficiency						
V-V and V-T Relaxation						
CO Spectroscopy						

NCL 71-32R

KINETIC MODEL AND THEORETICAL CALCULATIONS FOR STEADY STATE ANALYSIS OF ELECTRICALLY EXCITED CO LASER AMPLIFIER SYSTEM

FINAL REPORT: PART II

AUGUST 1971

Office of Naval Research
Contract No. N00014-71-C-0037
1 August 1970 through 31 July 1971

Prepared by

W. B. Lacina

Sponsored by
Advanced Research Projects Agency
Order No. 306

Principal Investigator: Dr. M. L. Bhaumik
Tel: AC 213 675-4611 Ext 4925

NORTHROP CORPORATE LABORATORIES
3401 West Broadway
Hawthorne, California 90250

NOTICE

The views and conclusions contained in this document are those of the authors and should not be interpreted as necessarily representing the official policies, either expressed or implied, of the Advanced Research Projects Agency or the U. S. Government.

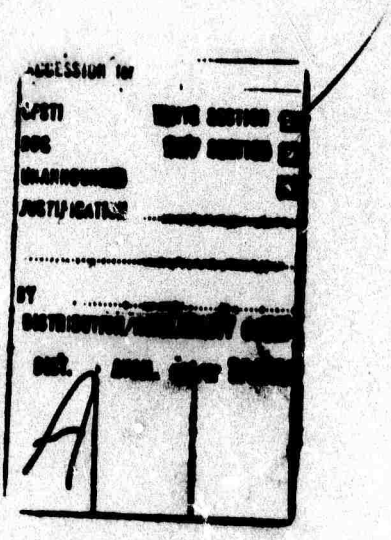

TABLE OF CONTENTS

1.0 INTRODUCTION

Molecular gas lasers have been unsurpassed for obtaining high efficiencies with high average power operation. For example, up to 30% has been realized for the CO_2 laser, and since this is basically a three-level system, the upper limit is the 40% quantum efficiency. However, diatomic molecular lasers can offer significant advantages for obtaining operation at even higher efficiencies, and CO, a particularly promising candidate, has recently attracted the interest of several workers.[1-20] Since a diatomic molecule has only one ladder of energy levels corresponding to a single vibrational mode (in contrast to CO_2, which has three different modes) it is possible to attain quantum conversion efficiencies of nearly 100%. The reason for this is that the lower laser level of a given transition can serve as the upper level of a subsequent transition, thus permitting the vibrational energy to be extracted as coherent radiation through several pairs of levels for which the populations are sufficiently inverted. For CO, it should be noted that, as a result of the rapid redistribution of vibrational energy among the levels, a molecule reaching a terminal laser level can be re-excited, and thus the absence of lasing on the lower levels need not limit the efficiency. This advantage is in contrast to the CO_2 system, for which the energy of the lower laser level is rapidly dissipated as heat energy through VT collisional relaxation.

A very serious problem which exists for some diatomic molecules (e.g., HF, HBr, NO) is the fast vibration-translation (VT) collisional relaxation processes, which cause molecules to lose vibrational energy quickly as heat. Among the diatomic molecules which are useful for laser applications, CO is unique in that respect, since its VT lifetimes are relatively long. For a diatomic molecule, the ladder of vibrational levels has energy spacings which are nearly resonant except for the anharmonic defect, and

thus, efficient vibrational cross-relaxation processes are possible. In fact, for the CO laser, it is these rapid near-resonant vibration-vibration exchange collisions (VV) that dominate the molecular kinetics and predominantly determine the structure of the vibrational population distribution.

A thorough understanding of the characteristics of the electrically excited CO laser involves molecular spectroscopy, radiative properties, molecular kinetics, electron kinetics, and discharge chemistry. The general purpose of this report is to summarize our understanding of the physical mechanisms of the CO laser, as well as to provide a useful compilation of the mathematical relations that are frequently required for CO laser system calculations. These results form the basis for the molecular kinetic model and computer program that was developed to analyze the performance of an electrically excited, steady state CO laser amplifier system, and which will be described in more detail in a subsequent section. A summary of several detailed experimental measurements performed at NCL to determine CO laser characteristics under different operating conditions are described in a separate report.[21]

The radiative characteristics for CO are treated in Section 2.0, where molecular spectroscopy, spontaneous and stimulated emission, and laser gain and saturation are discussed. Section 3.0 is devoted to a description of the pumping and relaxation processes which are important for the molecular kinetics, and contains results of the computer calculations which were performed for a variety of parametric cases. In Section 4.0, the electron kinetics of a weakly ionized plasma are treated briefly, although we have

not yet attempted numerical calculations of electron energy distribution functions. Since the plasma and molecular properties are coupled through electron-molecule collisions, calculations for the electron energy distribution would be desirable in order to obtain a more complete theoretical understanding of electrically excited CO laser systems.

2.0 RADIATIVE AND SPECTROSCOPIC CHARACTERISTICS

2.1 Energy Levels and Spectroscopy of the CO Molecule. The spectroscopy of carbon monoxide has been studied extensively because of its natural occurrence as a combustion product in flames. An excellent up-to-date review[22] can be found in the NBS monograph entitled "The Band Spectrum of Carbon Monoxide." Additional discussions and description of earlier work can be found in Herzberg's classic book[23] on diatomic molecules. Another useful reference for molecular spectroscopy is the book by Penner.[24]

The energy level diagram of CO molecules is shown in Figure 2.1. The visible spectrum of CO, arising out of electronic transitions between the upper electronic states, are dominated by three prominent band systems:

$A^1\pi - X^1\Sigma^+$	Fourth Positive System (2800-1140Å)
$b^3\Sigma^+ - a^3\pi$	Third Positive System (2800-1140Å)
$B^1\Sigma^+ - A^1\pi$	Angstrom System (6600-4100Å)

Among these, the A-X Fourth Positive System in the UV is the most pronounced and is easily excitable.

Although CO laser action with low power output has been reported by Mathias and Parker[20] on the Angstrom band electronic transitions, the primary interest lies in the high output power infrared CO laser involving transitions between the vibrational-rotational levels of the ground electronic state. These levels are described below in greater detail.

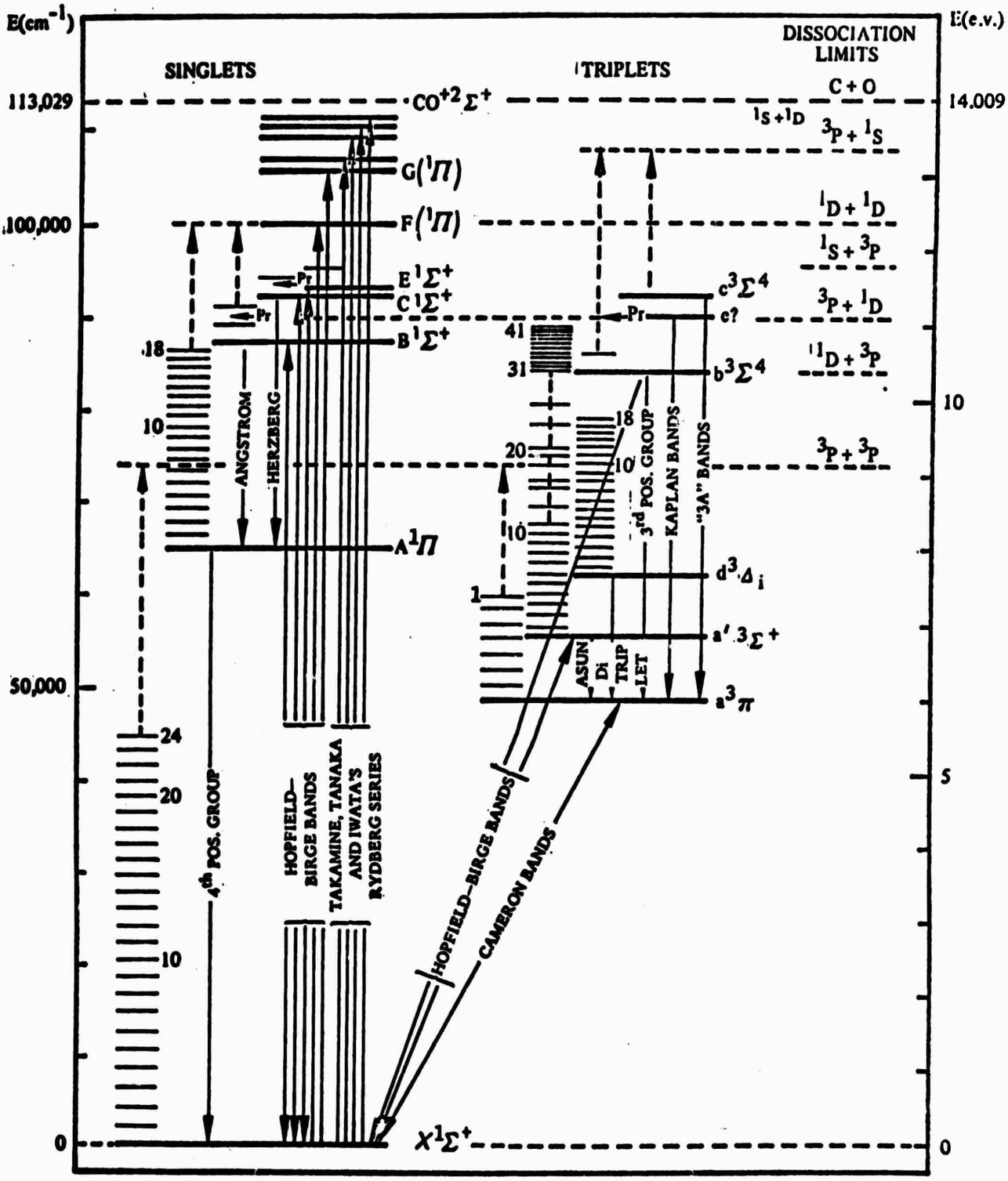

Figure 2.1. Energy Level Diagram of the CO Molecule.

2.1.1 Vibrational-Rotational Levels. Figure 2.2 shows the vibrational-rotational levels of the ground electronic states of CO. Basically, the vibrational-rotational levels in a given electronic state can be considered to arise from a superposition of harmonic oscillator and rigid rotator energy levels, and can be labeled with three quantum numbers, v, J, and M. The vibrational energy of a harmonic oscillator consists of the terms $G(v) = (v + 1/2)\,\omega_e$, where ω_e is the vibrational frequency, and v = 0, 1, 2,... labels the vibrational quantum levels. The energy of a rigid rotator is given by $F(J) = B\,J(J + 1)$, where B, the rotational constant, is related to the inverse of the moment of inertia, and J, the rotational angular momentum quantum number, assumes the values J = 0, 1, 2, ... Each of the rotational levels are degenerate, and are labeled by a quantum number M = -J, -(J - 1), ... 0, 1, 2, ... (J - 1), J. The total degeneracy of a rotational state with rotational quantum number J is, therefore, $g_J = (2J + 1)$. This leads to a spectrum of molecular energy levels given by

$$E(v, J, M) = E(v, J) = G(v) + F(J). \tag{2.1}$$

However, in practice, the vibrational energy of molecules is more accurately described by an anharmonic oscillator, and (due to centrifugal forces) the rotational spectrum is actually that of a non-rigid rotator. Consequently, it can be shown[23] that the vibrational and rotational terms are

$$G(v) = (v + 1/2)\,\omega_e - (v + 1/2)^2\,\omega_e x_e + (v + 1/2)^3\,\omega_e y_e + (v + 1/2)^4\,\omega_e z_e \tag{2.2}$$

and

$$F(J) = BJ(J + 1) - DJ^2\,(J + 1)^2, \tag{2.3}$$

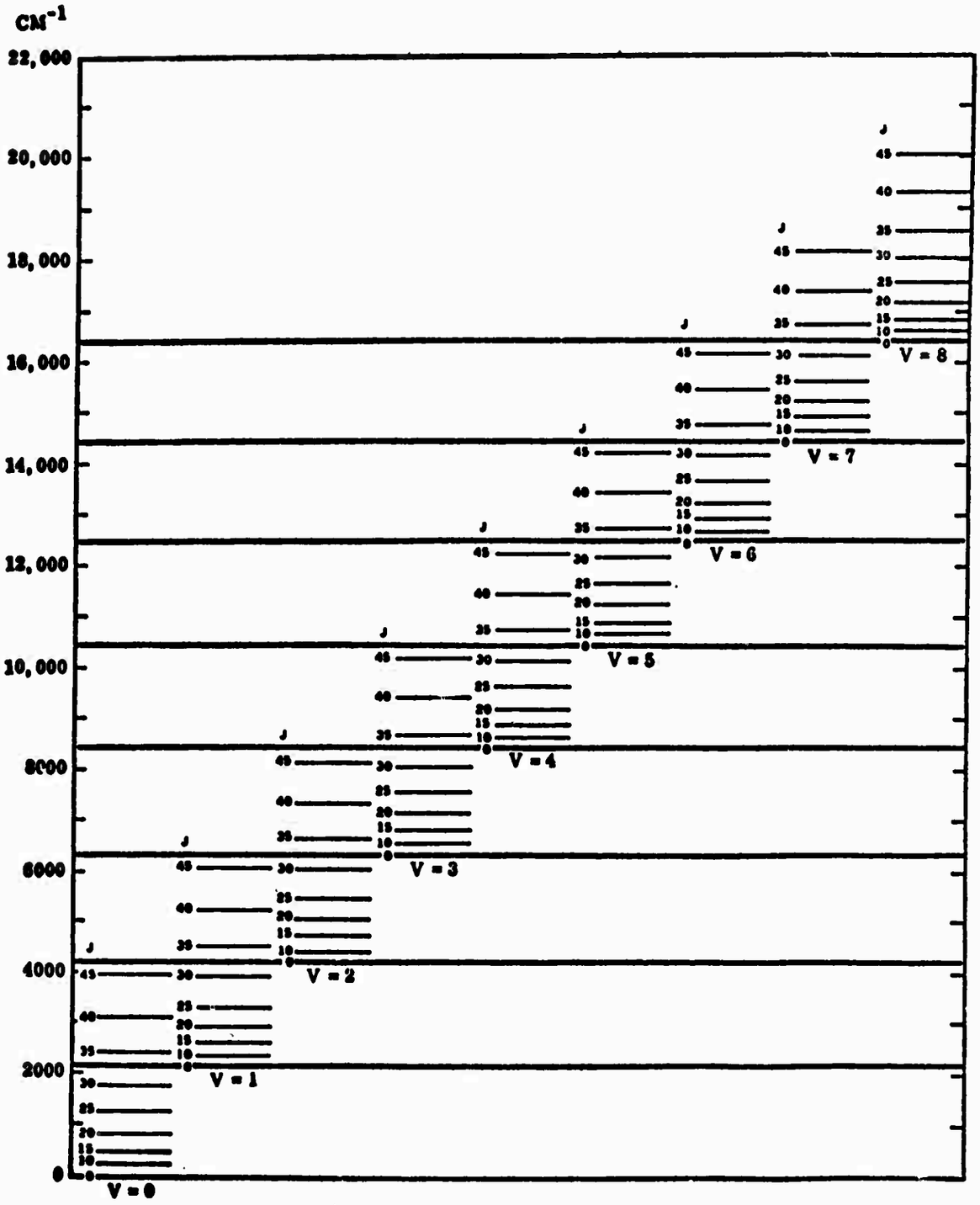

Figure 2.2. Vibrational-Rotational Levels of the Electronic Ground State ($X^1 \Sigma^+$) of CO.

where D is positive and $\ll$ B, and $\omega_e z_e \ll \omega_e y_e \ll \omega_e x_e \ll \omega_e$. Furthermore, it is usually not possible to completely ignore the interaction between the vibrational and rotational motions. If these two systems are coupled, the energy cannot be given simply as a sum of G(v) and F(J). Since the molecule is simultaneously vibrating and rotating, the internuclear distance is changing, and thus the moment of inertia, which is related to 1/B, is also changing. However, because the rotational frequencies are low compared to the vibrational frequencies, it is usually plausible to use mean values B_v and D_v for the rotational constants when the molecule is in a given vibrational state v. Thus, if the rotational-vibrational coupling is not too strong. it is satisfactory to retain [23] the expression (2.1) for E(v, J), with B_v and D_v given by

$$B_v = B_e - \alpha(v + 1/2) + \gamma(v + 1/2)^2 \qquad (2.4)$$

$$D_v = D_e + \beta(v + 1/2) . \qquad (2.5)$$

For CO, the vibrational constants ω_e, $\omega_e x_e$, $\omega_e y_e$, and $\omega_e z_e$ have been determined by Patel[6,7], and the rotational constants α, β, γ, B_e, and D_e have been given by Benedict et al.[25] These are summarized in Table 2.1 below.

ω_e	2169.82
$\omega_e x_e$	13.292
$\omega_e y_e$	.01082
$\omega_e z_e$	5.72×10^{-5}
B_e	1.93141
D_e	6.18×10^{-6}
α	.017520
β	-1.76×10^{-9}
γ	2.96×10^{-6}

Table 2.1. Vibrational and Rotational constants of the CO molecule in wavenumbers (cm^{-1}).

2.1.2 Infrared Transitions for CO. The first order allowed infrared spectrum for CO results from transitions between the vibrational-rotational levels, subject to certain selection rules. The selection rules for electric dipole radiation lead to allowed transitions for $v' = v \pm 1$, and $J' = J \pm 1$. The reason for this is that the first order electric dipole moment is proportional to the displacement, and is a vector. This leads to the vector addition rule for the change in J values, and to $\Delta v = \pm 1$, characteristic of harmonic oscillators. (The fact that the vibrational motion is slightly anharmonic will relax this selection rule somewhat, although transitions for which $\Delta v \neq \pm 1$ will be much weaker.) The transitions for which $(J - 1) \rightarrow J$ or $(J + 1) \rightarrow J$ are referred to as P(J) or R(J) branches, respectively, with the label J denoting the angular momentum of the final state. (There is no Q(J) branch, corresponding to transitions $J \rightarrow J$, for CO. This is a consequence of the fact that the total angular momentum is equal to the rotational angular momentum, with no electronic contribution. The selection rule on J then arises from a Clebsch-

Gordon coefficient, C(J, 1, J'; M, . .), which vanishes for J = J'.)
The first-order allowed transition frequencies for the two branches are given by

P(J) Branch:

$$\tilde{\nu} = E(v, J-1) - E(v-1, J) = G(v) - G(v-1) + F'_v(J-1) - F_{v-1}(J) \qquad (2.6)$$

R(J) Branch:

$$\tilde{\nu} = E(v, J+1) - E(v-1, J) = G(v) - G(v-1) + F_v(J+1) - F_{v-1}(J) \qquad (2.7)$$

and these can be combined into a single expression,

$$\tilde{\nu} = \tilde{\nu}_o + (B_v + B_{v-1})\, m + (B_v - B_{v-1} - D_v + D_{v-1})\, m^2 \qquad (2.8)$$
$$-2(D_v + D_{v-1})\, m^3 - (D_v - D_{v-1})\, m^4$$

where $\tilde{\nu}_o = G(v) - G(v-1)$, and where m = -J or (J + 1) for the P(J) or R(J) branch, respectively. (Throughout, we shall use the convention that ν represents frequency in sec^{-1}, and $\tilde{\nu} = \nu/c$ represents frequency in wavenumbers, cm^{-1}.) A computer program was written to calculate the P(J) and R(J) transition frequencies and air wavelengths for v = 1 to 30 and J = 1 to 50, and to sort them into numerical order. This enabled the experimentally observed CO laser output lines to be quickly and readily identified.

2.2 Spontaneous Emission. From the quantum theory of radiation, the transition rate for spontaneous radiation of a molecule from an initial vibration-rotation state (v', J', M') to a final state (v, J, M) is given by the Einstein A-coefficient,

$$A_{v', J', M' \to v, J, M} = \frac{64\pi^4 \nu^3 (v', J' \to v, J)}{3hc^3} \left| \mu (v', J', M' \to v, J, M) \right|^2 \qquad (2.9)$$

where $\left| \mu(v', J', M' \rightarrow v, J, M) \right|^2$ is the square of the dipole matrix element, and where the frequency $\nu(v', J', M' \rightarrow v, J, M)$, which is independent of the quantum numbers M', M, was given by Eq. (2.8) for $v = v' - 1$ for both P and R branches. Since a priori knowledge of the initial and final degenerate quantum numbers M' and M is not possible, the total spontaneous radiation rate for the transition $v' \rightarrow v$, $J' \rightarrow J$ can be obtained from Eq. (2.9) by averaging over the initial M' states, and summing over the final M states. Since the initial M' states all have equal probability of occurence, viz. $1/g_{J'}$, where $g_{J'} = (2J' + 1)$ is the rotational degeneracy of the initial state, we obtain

$$A_{v', J' \rightarrow v, J} = \sum_{M'M} (1/g_{J'}) A_{v', J', M' \rightarrow v, J, M} . \qquad (2.10)$$

For CO, it can be shown that (cf. Ref. 24, p. 130-133),

$$\sum_{M'M} \left| \langle v', J', M' \right| \mu \left| v, J, M \rangle \right|^2 = \left| \langle v' \right| R \left| v \rangle \right|^2 \times$$

$$\left\{ J \delta(J, J'+1) + J' \delta(J+1, J') \right\}, \qquad (2.11)$$

and from this expression, it is apparent that the two possible decay modes correspond to a P and R transition. Thus, the transition rate (2.10) becomes, finally,

$$A_{v', J' \rightarrow v, J} = \frac{64\pi^4 \nu^3 (v', J' \rightarrow v, J)}{3hc^3 (2J' + 1)} \left| \langle v' \right| R \left| v \rangle \right|^2 \times$$

$$\left\{ J \delta(J, J' +1) + J' \delta(J+1, J') \right\}, \qquad (2.12)$$

The <u>total</u> spontaneous decay rate for $v' \rightarrow v$ can be obtained by averaging over all initial J' levels, and summing over all final J levels. Thus, if $\rho(v', J')$ denotes the probability that the initial rotational level is J', we obtain

$$A_{v' \rightarrow v} = \sum_{J'J} \rho(v', J')\, A_{v'J' \rightarrow v, J} \tag{2.13}$$

For example, if the rotational levels are in thermal equilibrium at some temperature T_{rot}, the initial probability coefficients $\rho(v', J')$ will be Maxwell-Boltzmann factors,

$$\rho(v', J') = \frac{(2J' + 1)}{Q^{rot}_{v'}} \exp\left[-B_{v'} J'(J' + 1)/kT_{rot}\right], \tag{2.14}$$

where

$$Q^{rot}_{v'} = \sum_{J'} (2J' + 1) \exp\left[-B_{v'} J'(J' + 1)/kT_{rot}\right] \tag{2.15}$$

is the rotational partition function of the initial vibrational level v'. If the sum over J in Eq. (2.13) is carried out first, we obtain

$$A_{v' \rightarrow v} = \frac{64\pi^4}{3h} \left|\langle v' \left| R \right| v \rangle\right|^2 \sum_{J'} \left(\rho(v', J')/g_{J'}\right) X$$

$$\left\{(J'+1)\, \tilde{\nu}^3 (v', J' \rightarrow v, J'+1) + J' \tilde{\nu}^3 (v', J' \rightarrow v, J'-1)\right\}, \tag{2.16}$$

which involves the P(J'+1) and R(J'-1) frequencies. From Eq. (2.8), these are given by

$$\tilde{\nu}(v', J' \rightarrow v, J'+1) \approx \tilde{\nu}_o(v', v) - (J'+1)(B_{v'} + B_v) \tag{2.17}$$

$$\tilde{\nu}(v', J' \rightarrow v, J'-1) \approx \tilde{\nu}_o(v' v) + J'(B_{v'} + B_v) \tag{2.18}$$

and thus, the expression in brackets in Eq. (2.16) becomes

$$(J'+1)\,\tilde{\nu}_o^3 - 3(J'+1)^2\,\tilde{\nu}_o^2\,(B_{v'} + B_v) + J'\tilde{\nu}_o^3 + 3J'^2\,\tilde{\nu}_o^2(B_{v'} + B_v) + \ldots \approx (2J'+1)\left[\tilde{\nu}_o^3 - 3\tilde{\nu}_o^2(B_{v'}+B_v)\right]. \quad (2.19)$$

Since the rotational constants $B_{v'}$ and B_v are negligible compared with $\tilde{\nu}_o$, the second term in expression (2.19) can be neglected, and Eq. (2.16) reduces, finally, to

$$A_{v' \to v} \equiv \tau_{v'v}^{-1} = \frac{64\pi^4\,\tilde{\nu}_o\,(v', v)^3}{3h}\;|R_{v'v}|^2, \quad (2.20)$$

where $\tilde{\nu}_o(v', v)$ is the energy (frequency) difference in cm^{-1} between the levels v' and v, and $\tau_{v', v}$ denotes the spontaneous lifetime for the radiative decay from $v' \to v$. (Note that, after the sum over J in Eq. (2.13) was carried out, the sum over J' collapsed to the trivial sum of $\rho(v', J')$, which is just equal to unity. Thus, the total spontaneous radiative decay rate of a level v' is independent of the distribution of the rotational J' levels.) For a harmonic oscillator, the vibrational matrix elements $|R_{v, v-1}|^2$ are approximately equal to $v\,|R_{10}|^2$. For CO, it has been shown[24] that a Morse potential describes the matrix elements $|R_{v, v-1}|^2$ more accurately than a quadratic potential, and that gives the result

$$\left|R_{v'\,v}/R_{10}\right|^2 = \frac{v'!}{v!}\;\frac{(1/x_e - 2v' - 1)\,(1/x_e - 2v - 1)}{\prod_{t=0}^{v'-v-1}(1/x_e - v' + t)\,(v' - v)^2\,(1/x_e - 3)}\;\times$$

$$(1/x_e - 2)^2/(1/x_e - v' - v - 1)^2, \quad (2.21)$$

where x_e is a measure of the anharmonicity of the molecule, and is defined by

$$x_e = \omega_e x_e / \omega_e \quad . \tag{2.22}$$

The expression is valid for $v' > v$; for $v' < v$, the corresponding expression can be obtained simply by interchanging v' and v in Eq. (2.21). It is easy to verify that this result reduces, to a first approximation, to the form $|R_{v,v-1}|^2 = v\,|R_{10}|^2$ which is characteristic of a harmonic oscillator. From Eq. (2.20), it follows that the transition rate $A_{v' \to v}$ can be expressed in terms of A_{10}, and the ratio of the squares of the transition dipole moments, as given by Eq. (2.21):

$$A_{v' \to v} = A_{10} \left(\tilde{\nu}_o (v'|v) / \tilde{\nu}_{10} \right)^3 |R_{v',v}/R_{10}|^2 \quad . \tag{2.23}$$

This equation, in conjunction with Eq. (2.21), is useful, since it allows the radiative decay rates for $\Delta v = 1$ and $\Delta v = 2$ to be calculated for high vibrational levels in terms of the basic rate A_{10}. For these cases, Eq. (2.23) becomes

$$|R_{v,v-1}/R_{10}|^2 = v[(1/x_e - 2)/(1/x_e - 2v)]^2 \; X$$

$$\left\{ \frac{(1/x_e - 2v - 1)(1/x_e - 2v + 1)}{(1/x_e - 3)(1/x_e - v)} \right\}, \tag{2.24}$$

and

$$|R_{v,v-2}/R_{10}|^2 = \frac{1}{4}\, v(v-1)\,[(1/x_e - 2)/(1/x_e - 2v + 1)]^2 \; X$$

$$\left\{ \frac{(1/x_e - 2v - 1)(1/x_e - 2v + 3)}{(1/x_e - 3)(1/x_e - v)(1/x_e - v + 1)} \right\} \quad . \tag{2.25}$$

The value of the transition dipole moment R_{10} for the CO molecule is $R_{10}(CO) = 9.906 \times 10^{-20}$ esu, which corresponds to a spontaneous radiation rate

$$A_{10} = 1/\tau_{sp} = \frac{64\pi^4 \tilde{\nu}_{10}^{\ 3}}{3h} |R_{10}|^2 = 30.3 \text{ sec}^{-1} \qquad (2.26)$$

2.3 Stimulated Emission. In the presence of external radiation, the rates for stimulated emission or absorption of electromagnetic energy by excited molecules will be expressed in terms of the Einstein B-coefficients. The probability per second that incident monochromatic radiation at frequency ν induces a molecular transition from an initial state (v', J', M') to a final state $(v, J. M)$ is given by

$$\Gamma^{i}_{v', J', M' \to v, J. M} = \frac{I(\nu)}{c} S(\nu, \nu_{12}) B_{v'J'M' \to V, J, M} \qquad (2.27)$$

where $I(\nu)$ is the radiant power per unit area, $S(\nu, \nu_{12})$ is the normalized line shape function for the molecular resonance centered at frequency $\nu_{12} = \nu(v', J' \to v, J)$, and $B_{v', J', M' \to v, J, M}$ is the Einstein B-coefficient, defined by

$$B_{v', J', M' \to v, J, M} = A_{v', J', M' \to v, J, M} / (8\pi h \tilde{\nu}_{12}^{\ 3}). \qquad (2.28)$$

It is a fundamental characteristic of quantum theory that the transition rates for each elementary process and its inverse are equal, assuming that certain invariance conditions are satisfied. This is, in substance, the principle of detailed balancing, according to which the rates for forward and reverse microscopic processes are equal for a system in statistical equilibrium. Therefore,

$$B_{v', J', M' \to v, J, M} = B_{v, J, M \to v', J', M'}. \qquad (2.29)$$

Again, it can be argued that, since there can be no knowledge of the initial of final degenerate quantum numbers M and M', it is more relevant to consider only the total stimulated rates for the processes $(v', J') \rightarrow (v, J)$ and $(v, J) \rightarrow (v', J')$. These can again be defined, as for the case of the A-coefficient in the previous section, as an average over initial and sum over final M states:

$$B_{v', J' \rightarrow v, J} = \sum_{M'M} (1/g_{J'}) B_{v'J'M' \rightarrow v, J, M} \tag{2.30a}$$

$$B_{v, J \rightarrow v'J'} = \sum_{MM'} (1/g_J) B_{v, J, M \rightarrow v'J'M'} \tag{2.30b}$$

It follows immediately from Eq. (2.30) that the reduced Einstein B-coefficients satisfy the relation,

$$g_J B_{v, J \rightarrow v', J'} = g_{J'} B_{v', J' \rightarrow v, J} \tag{2.31}$$

Furthermore, they can be expressed in terms of the reduced A-coefficient, given by Eq. (2.12), as

$$B_{v', J' \rightarrow v, J} = A_{v', J' \rightarrow v, J} / (8\pi h \tilde{\nu}_{12}^3). \tag{2.32}$$

A particular case, which will be required later for the discussion of laser gain, are the B-coefficients for the P(J) and R(J) branches of a transition $v \rightarrow v - 1$:

$$B_{v, J-1 \rightarrow v-1, J} = \frac{8\pi^3 J}{3h^2 g_{J-1}} |R_{v, v-1}|^2, \tag{2.33a}$$

and

$$B_{v, J+1 \rightarrow v-1, J} = \frac{8\pi^3 (J+1)}{3h^2 g_{J+1}} |R_{v, v-1}|^2. \tag{2.33b}$$

As Eq. (2.27) shows, the stimulated emission properties of the molecular system depend upon the resonance line shape function $S(\nu)$. Therefore, before proceeding with a discussion of gain and saturation characteristics, it will be useful to summarize some basic information about line broadening mechanisms in molecular gas lasers.

2.4 Line Shape. One of the important factors that determines the stimulated radiative characteristics of the laser gain medium is the width and shape of the spectral emission line. In general, the radiative transition will not be monochromatic in frequency, but will be broadened due to lifetime effects, collisional effects, or medium inhomogeneities. The probability density that the observed emission will be in the frequency interval $(\nu, \nu + d\nu)$ will be described by a line shape distribution function $g(\nu)$, which shall always be assumed to be normalized to unity:

$$\int_{-\infty}^{\infty} d\nu g(\nu) = 1. \tag{2.34}$$

In this section, a brief discussion of the broadening mechanisms important for molecular gas lasers will be given, with a summary of several useful relations. In general, a Lorentz line shape results from processes that limit the lifetime of excited states, modulate their energy levels, or induce nonradiative transitions between them; it also occurs for collisional processes that interrupt the phase of the radiating molecules, and thereby modulate the emission frequency. Alternatively, medium inhomogeneities may produce a distribution of emission frequencies, and this usually results in a Gaussian line shape. For molecular gas lasers, this can arise from Doppler shift of the transition frequencies of molecules whose velocity distribution is Boltzmann. The nature of homogeneous broadening is fundamentally different from that of

inhomogeneous broadening; in the former case, all of the molecules in the medium share the same basic emission properties, while in the latter case, all of the molecules are different. This has important consequences for saturation effects, both in regard to gain characteristics and line shape distribution. In the homogeneous case, saturating radiation near resonance can be distributed to all of the molecules of the medium, while in the latter case, different molecules behave independently. For molecular gas lasers, natural line broadening due to spontaneous radiation or nonradiative decay induced by collisions is always negligible; the only two mechanisms that are important are Doppler and pressure broadening, which shall be discussed in more detail below.

2.4.1 Doppler Broadening. For conventional gas lasers, operating at total pressures typically less than 20 torr, inhomogeneous Doppler broadening is the dominant mechanism that determines the radiative linewidth. If it is assumed that the molecular velocities are distributed according to a Maxwell-Boltzmann function, then the fractional number of molecules in $(v_x, v_x + dv_x)$ is given by

$$dn(v_x, v_x + dv_x)/n = (M/2\pi RT)^{1/2} \exp[-Mv_x^2/2RT]dv_x. \quad (2.35)$$

If the x-direction is chosen as the line of sight, the observed emission frequency from molecules having a velocity component v_x will be Doppler-shifted to

$$\nu = \nu_o (1 + v_x/c), \quad (2.36)$$

where ν_o is the center frequency of the transition. The probability that the observed emission lies in the frequency interval $(\nu, \nu + d\nu)$ is defined to be

$d\nu g_D(\nu, \nu_o) = dn(v_x, v_x + dv_x)/n$, so that $g_D(\nu, \nu_o)$ can be obtained directly from Eq. (2.35) by substituting the result (2.36) and $dv_x = d\nu/\tilde{\nu}_o$, where $\tilde{\nu}_o = \nu_o/c$ is the center frequency expressed in wavenumbers (cm^{-1}). Thus, the line shape function for Doppler broadening is given by

$$g_D(\nu, \nu_o) = \frac{1}{\Delta\nu_D\sqrt{\pi}} \exp\left[- \frac{(\nu - \nu_o)^2}{\Delta\nu_D^2} \right], \qquad (2.37)$$

where

$$\Delta\nu_D = \tilde{\nu}_o \left(\frac{2RT}{M} \right)^{1/2} \qquad (2.38)$$

is the half-width of the distribution, measured at the 1/e point. (Note that the $\Delta\nu_D$ defined here omits the $\sqrt{\ln 2}$ factor which often occurs in the literature, and which would correspond to the half-width at the half-power points.)

2.4.2 Pressure Broadening. At higher pressures, collision broadening provides the dominant contribution to the linewidth. Collisional processes represent a homogeneous broadening mechanism, with a line shape function given by[26,27]

$$g_P(\nu, \nu_o) = (\Delta\nu_c/\pi)\left[(\nu - \nu_o - \delta\nu_c)^2 + \Delta\nu_c^2\right]^{-1}, \qquad (2.39)$$

where $\delta\nu_c$ is a pressure-induced shift of the center frequency ν_o, and where $\Delta\nu_c$ is the pressure-broadened linewidth. Except for extremely high pressures ($\gtrsim$ several atm), the frequency shift $\delta\nu_c$ is negligible, so that the pressure-broadened line shape function can be expressed by

$$g_P(\nu, \nu_o) = (\Delta\nu_c/\pi)\left[(\nu - \nu_o)^2 + \Delta\nu_c^2\right]^{-1}, \qquad (2.40)$$

where

$$\Delta \nu_c = f_c/(2\pi) \tag{2.41}$$

is the half-width at half-power points. Here, f_c is the collision frequency, given by

$$f_c = \sum_X \sigma_{opt}(CO,X)\, n_X \langle v_{rel}(CO,X)\rangle_T, \tag{2.42}$$

where

$$\langle v_{rel}(CO,X)\rangle_T = [(8RT/\pi)(M_{CO}^{-1} + M_X^{-1})]^{1/2} \tag{2.43}$$

is the relative thermal velocity between CO and X molecules at temperature T, $R = 8.317 \times 10^7$ erg/mole/$^\circ$K is the gas constant, M's are molecular weights, n_X is the number of X molecules/cm^3, and $\sigma_{opt}(CO,X)$ is the optical collision cross section for the pair of molecules (CO, X). The "hard sphere" collision cross section,

$$\sigma(X,Y) = \pi(d_X + d_Y)^2/4 \tag{2.44}$$

determined from kinetic experiments is usually a good approximation for the effective optical cross section, since every collision interrupts the phase of a radiating molecule. (In fact, even "softer" collisions suffice, since the optical cross section is typically slightly larger than the hard sphere cross section.) Thus, if reliable data on the optical collision cross sections is lacking, the "hard sphere" diameters d_X, which are tabulated in the table below for several molecules of interest, can often be used.

X	M	d_X(A)
CO_2	44	4.00
CO	28	3.59
N_2	28	3.68
Ar	40	3.42
He	4	2.58

Table 2.2

2.4.3 Combined Doppler and Pressure Broadening. In the pressure and temperature region where the effects of collision and Doppler broadening are comparable, a more complicated line shape function results. For this intermediate case, the radiative line shape function will reflect the combined effects of both broadening mechanisms, and will be expressed in terms of a convolution of the two distributions given by Eq. (2.37) and (2.40). The relative number of molecules whose emission frequency lies in $(\nu', \nu' + d\nu')$ due to Doppler shift from a center transition frequency ν_o is $d\nu' g_D(\nu', \nu_o)$; the relative number of molecules whose emission frequency is shifted from ν' to the interval $(\nu, \nu + d\nu)$ because of collisional effects is $d\nu g_P(\nu, \nu')$. Hence, the relative number of molecules whose emission frequency is in $(\nu, \nu + d\nu)$ for a transition centered at ν_o, Doppler-shifted to ν', will be given by a distribution function $S(\nu, \nu_o; \nu')$, defined by $d\nu S(\nu, \nu_o; \nu') = d\nu g_P(\nu, \nu')\, d\nu' g_D(\nu', \nu_o)$. Integration over all of the intermediate frequencies ν' will then produce the line shape function for combined pressure and Doppler broadening,

$$S(\nu, \nu_o) = \int_{-\infty}^{\infty} d\nu' \, g_P(\nu, \nu') \, g_D(\nu', \nu_o) \, . \qquad (2.45)$$

Since all of the distribution functions discussed here depend only upon the difference of the frequencies, Eq. (2.45) can be written

$$S(\nu - \nu_o) = \int_{-\infty}^{\infty} d\nu' \; g_P([\nu - \nu_o] - \nu') \, g_D(\nu'), \tag{2.46}$$

which is the familiar convolution integral form. To evaluate this distribution function, it is convenient to introduce the Fourier transforms,

$$g(\tau) = \int d\nu \, e^{i\nu\tau} g(\nu). \tag{2.47}$$

which can be shown to be

$$g_P(\tau) = \exp\left[i\nu_o\tau - \Delta\nu_c|\tau| \right] \tag{2.48a}$$

and

$$g_D(\tau) = \exp\left[i\nu_o\tau - \tau^2 \Delta\nu_D{}^2/4 \right]. \tag{2.48b}$$

for the pressure and Doppler broadened line shapes, respectively. The convolution integral (2.46) for $S(\nu)$ can then be expressed as the inverse Fourier transform of the product of $g_P(\tau)\, g_D(\tau)^*$:

$$S(\nu) = \frac{1}{2\pi} \int_{-\infty}^{\infty} d\tau \, e^{-i\nu\tau - \Delta\nu_c|\tau|} \exp(-\tau^2 \Delta\nu_D{}^2/4). \tag{2.49}$$

This integral can be related to the real part of an error function of complex argument. The resonance line shape function at the center frequency, S(0), becomes

$$S(0) = \frac{1}{\pi} \int_0^\infty d\tau \exp\left[- \Delta\nu_c \tau - \tau^2 \Delta\nu_D{}^2/4\right] \qquad (2.50)$$

$$= \frac{2}{\pi \Delta\nu_D} \exp(x^2) \int_x^\infty d\xi e^{-\xi^2} \qquad (2.51)$$

$$= \frac{1}{\Delta\nu_D \sqrt{\pi}} \exp(x^2) \operatorname{erfc}(x), \qquad (2.52)$$

where

$$x = \Delta\nu_c / \Delta\nu_D, \qquad (2.53)$$

and erfc(x) is the complementary error function,

$$\operatorname{erfc}(x) = \frac{2}{\sqrt{\pi}} \int_x^\infty d\xi\, e^{-\xi^2} . \qquad (2.54)$$

It is easily verified that the line shape factor at resonance reduces to the results for pure Doppler or pressure broadening, if the limit $x \to 0$ or $x \to \infty$ is taken in Eq. (2.52):

1) Doppler broadened limit: $x \to 0$, and

$$S(0) \to \frac{1}{\Delta\nu_D \sqrt{\pi}} \qquad (2.55a)$$

2) Pressure broadened limit: $x \to \infty$, and

$$S(0) \to \frac{1}{\pi \Delta\nu_c} , \qquad (2.55b)$$

where the asymptotic relation $\exp(x^2) \operatorname{erfc}(x) \simeq 1/(x\sqrt{\pi})$ has been invoked.

2.5 Laser Gain Characteristics. Theoretical discussions of the gain coefficient have been given by Patel for CO[6,7] and CO_2[28] lasers. The gain can be calculated as follows: the net increase dI in power/unit area of an incident beam of frequency ν travelling a thickness dx of an active medium, neglecting spontaneous emission (which is emitted over all solid angles, and is a characteristic of the medium with or without incident radiation) is given by

$$dI = h\nu\, dx\, [\, N_2\, \Gamma^i_{21} - N_1\, \Gamma^i_{12}\,] \tag{2.56}$$

where N_1, N_2 are the number of molecules per unit volume in states 1 and 2, and Γ^i_{12}, Γ^i_{21} are the probabilities per unit time for induced transitions from states 1 and 2 with the emission (or absorption) of a photon with energy $h\nu$. Expressions for Γ^i_{12}, Γ^i_{21} have been given by Eq. (2.27) in a previous section in terms of the Einstein B-coefficients B_{12} and B_{21}. If the gain is defined by

$$\alpha = \frac{1}{I}\left(\frac{dI}{dx}\right), \tag{2.57}$$

we obtain

$$\alpha = (h\nu/c)\,[N_2\, B_{21} - N_1\, B_{12}\,]\, S(\nu, \nu_{12})\ . \tag{2.58}$$

For the vibrational-rotational transitions of the CO molecule, the gain for $(v, J \pm 1) \rightarrow (v\text{-}1, J)$ (i.e, the P(J) and R(J) branches of the $v \rightarrow (v-1)$ transition) can be obtained from Eq. (2.33), and becomes

$$\alpha_{v, J\pm1 \rightarrow v-1, J} = \frac{8\pi^3 \nu\,(v, J\pm1 \rightarrow v\text{-}1, J)}{3hc}\, S_J\, |R_{v, v-1}|^2\ X$$

$$\left\{ \frac{n_{v, J\pm1}}{g_{J\pm1}} - \frac{n_{v-1, J}}{g_J} \right\} S(\nu), \tag{2.59}$$

where

$$S_J = \begin{cases} J, & \text{for P(J) transitions} \\ (J+1), & \text{for R(J) transitions} \end{cases} \qquad (2.60)$$

The population densities of the intial and final vibrational-rotational levels have been denoted by $n_{v,J}$. Since the rotational energy level spacings are small compared to the average kinetic energies of the molecules under typical temperature conditions ($kT \gtrsim 60\ cm^{-1}$ for $T \gtrsim 77^{\circ}K$), molecular collisions will rapidly thermalize the population distribution of the rotational levels in any given vibrational state. For CO_2 lasers, with $B \sim .4\ cm^{-1}$, this rotational cross relaxation is very fast, and the J levels can always be assumed to attain a thermal equilibrium described by a Maxwell-Boltzmann distribution of the form given in Eq. (2.14), with $T_{rot} \sim T$ (the kinetic temperature). For CO, the value of B is $\sim 2\ cm^{-1}$, which is five times larger than that for CO_2; thus, for CO, rotational cross relaxation would be expected to be slower, since larger amounts of rotational energy have to be exchanged between colliding molecules to thermalize the distribution. If rotational cross relaxation is extremely fast compared to other pumping rates and to stimulated emission rates, then even though gain may exist for several transitions simultaneously, the line with the highest gain will begin to oscillate first, and the other rotational levels will be depleted through a single transition. On the other hand, if the rotational cross relaxation is slow, it is possible for several rotational branches of a single $v \rightarrow v - 1$ transition to oscillate simultaneously. Since rotational energy exchange occurs by collisional processes, its rate is directly proportional to the gas pressure.

It is usually a good approximation to assume that the populations $n_{v,J}$ are given by the Boltzmann distribution (2.14), with the rotational temperature T_{rot} equal to the kinetic temperature T:

$$n_{v,J} = \frac{n_v g_J}{Q_v^{rot}} \exp\left[-B_v J(J+1)/kT\right], \tag{2.61}$$

where n_v denotes the total population density of level v, and where the rotational partition function Q_v^{rot} for level v is given by

$$Q_v^{rot} = \sum_J g_J \exp\left[-B_v J(J+1)/kT\right] \tag{2.62}$$

$$\approx \int_0^\infty dx \exp\left(-B_v x/kT\right) \approx \frac{kT}{B_v} . \tag{2.63}$$

The latter approximation holds because $B_v \ll kT$ for typical gas kinetic temperatures. The Boltzmann constant $k = .6945\ cm^{-1}/^oK$ shall always be understood to be expressed in these units throughout this work unless otherwise specified.

Under the present assumptions, the expression (2.59) for the P and R branch gains for the transition $v \rightarrow v-1$ become, using Eq. (2.61):

$$\alpha_{v,J' \rightarrow v-1,J} = \frac{A_{10}\, \tilde{\nu}(v,J' \rightarrow v-1,J)\, S(\nu)}{8\pi \tilde{\nu}_{10}^{\,3}\, kT} S_J \left|R_{v,v-1}/R_{10}\right|^2 \times$$

$$\left\{ n_v B_v \exp\left[-B_v J'(J'+1)/kT\right] \right.$$

$$\left. - n_{v-1} B_{v-1} \exp\left[-B_{v-1} J(J+1)/kT\right] \right\} . \tag{2.64}$$

One of the interesting characteristics of molecular lasers is that the P-branch transitions can show gain even when the total vibrational populations between the initial and final levels are not inverted. This situation is known as partial inversion. It can be shown that the R-branch transitions can never exhibit gain under partial inversion conditions. However, if the total vibrational populations are sufficiently inverted, some R-branch transitions can show gain, although it is always less than that for P-branch lines. Even for the case of partial inversion, there are generally several transitions that have suitable gain for laser oscillation. However, due to strong competition effects between transitions, only a small number of lines may result in the output. Therefore, for CO laser systems pumped by methods that do not produce high total inversions, it is only the P-branch transitions that are of interest. For the P-branch, the gain equation can be obtained from Eq. (2.64) by setting $J' = (J-1)$ and $S_J = J$. The structure of Eq. (2.64) shows that the gain is a sensitive function of the populations, temperature, and J values, and consequently, the spectral output of the laser depends critically on the operating conditions. Figure 2.3 shows the dependence of the normalized gain for CO as a function of J-branch at $T = 100^{\circ}K$ for $v = 6 \rightarrow v = 5$ transitions, and for a variety of relative inversions.

Note here that Eq. (2.64) is valid for both small-signal or saturated gain, provided that the line is homogeneously broadened, i.e., it depends only upon the populations of the vibrational levels. Saturation effects will enter naturally into Eq. (2.64), depending upon whether or not rates of stimulated emission for the system are comparable to pumping and relaxation processes, and if so, they would have to be included in the kinetic equations which determine the vibrational populations. For the situation where the small-signal region is inhomogeneously broadened, the gain equation for saturation effects is not given simply by (2.64), but requires an integration over the inhomogeneous distribution. This is discussed in more detail for a simple two-level example in Section 2.7.

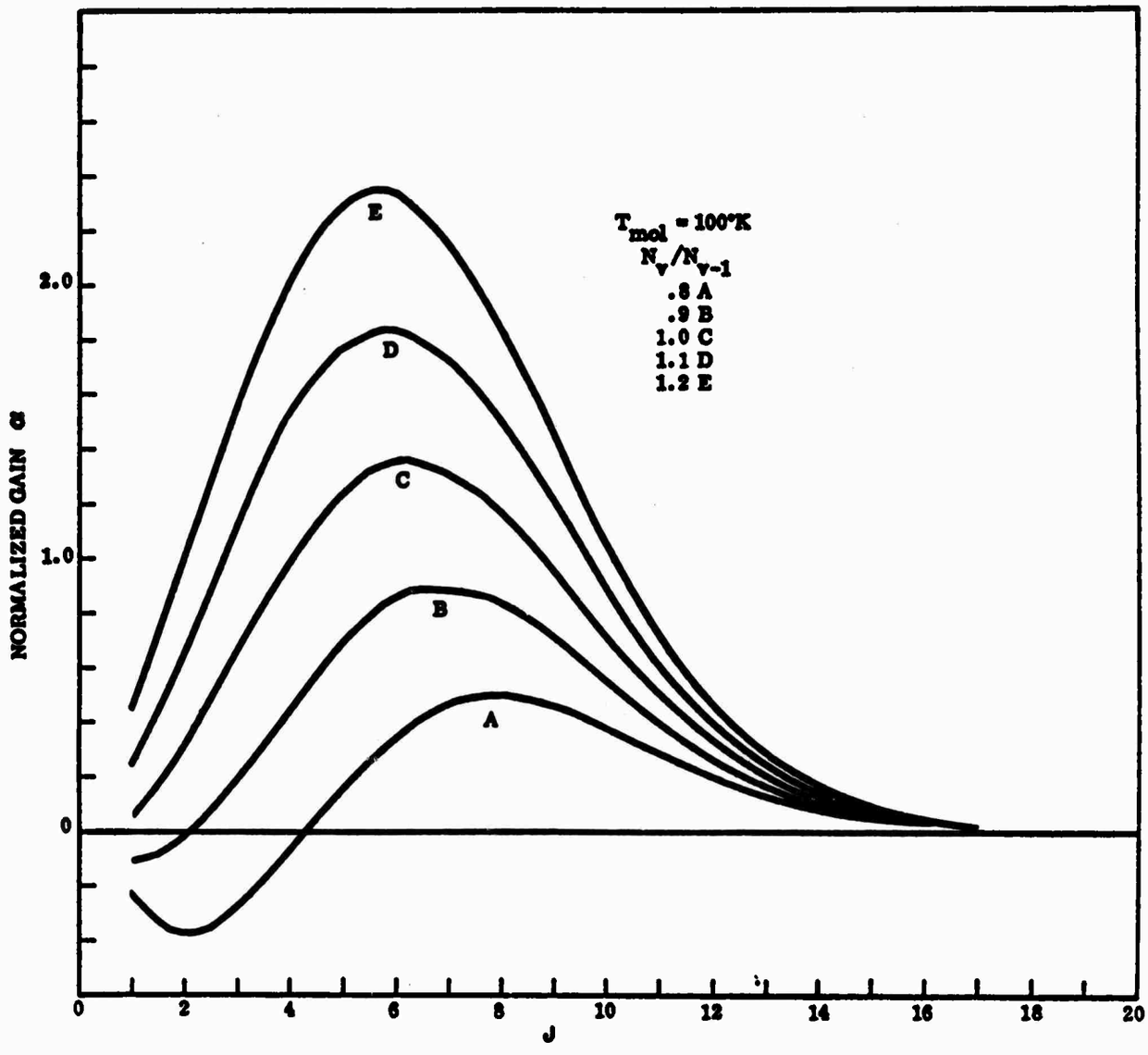

Figure 2.3. Normalized small-signal gain for the 6→5 P(J) transitions, for T = 100°K and various inversion ratios.

2.6 Radiative Contribution to Molecular Kinetics. The effects of spontaneous and stimulated emission have to be included in the set of kinetic equations, which will be discussed in more detail later, for the molecular vibrational level populations. In this section, expressions for the radiative excitation and decay rates that will be required later are developed. In the following discussion, it shall be assumed that the radiative processes include spontaneous emission with $\Delta v = 1$ and $\Delta v = 2$, and stimulated emission due to an arbitrary number of external radiation fields of intensities $I(\nu, \nu_v^J)$ at frequencies ν near the resonant frequencies ν_v^J that correspond to P(J), v → v-1 transitions.

The contribution of spontaneous radiation with $\Delta v = 1$ and 2 to the vibrational population of level r is $dn_r/dt = R_r^{sp}$, given by

$$R_r^{sp} = -n_r (A_{r \to r-1} + A_{r \to r-2}) + n_{r+2} A_{r+2 \to r} + n_{r+1} A_{r+1 \to r} \qquad (2.65)$$

where the Einstein A-coefficients have been given by Eq. (2.23). Spontaneous decay represents a pure loss mechanism, with only downward transitions, and for the CO laser, it can only represent an important relaxation mechanism for high vibrational levels in very low pressure systems. For the case of stimulated radiation processes, there are both downward and upward transitions (emission and absorption), with the rate $dn_r/dt = R^{stim}$ for the vibrational level r given by

$$R^{stim} = - \sum_J n_{r,J-1} \Gamma^i_{r,J-1 \to r-1,J} + \sum_J n_{r-1,J} \Gamma^i_{r-1,J \to r,J-1}$$

$$- \sum_J n_{r,J} \Gamma^i_{r,J \to r+1,J-1} + \sum_J n_{r+1,J-1} \Gamma^i_{r+1,J-1 \to r,J}. \qquad (2.66)$$

Thus,

$$R_r^{stim} = -n_r S_{r \to r-1} + n_{r-1} S_{r-1 \to r} - n_r S_{r \to r+1} + n_{r+1} S_{r+1 \to r} \qquad (2.67)$$

where

$$S_{r \to r-1} = \frac{S(\nu, \nu_r^J)\, A_{10}\, B_r}{8\pi hc(kT)\, \tilde{\nu}_{10}^3} \left| \frac{R_{r,r-1}}{R_{10}} \right|^2 \sum_J J \exp\left\{ -B_r J(J-1)/kT \right\} I(\nu_r^J), \quad (2.68a)$$

$$S_{r-1 \to r} = \frac{S(\nu, \nu_r^J)\, A_{10} B_{r-1}}{8\pi hc\,(kT)\, \tilde{\nu}_{10}^3} \left| \frac{R_{r,r-1}}{R_{10}} \right|^2 \sum_J J \exp\left\{ -B_{r-1} J(J+1)/kT \right\} I(\nu_r^J) \quad (2.68b)$$

(Note that, since k = .6945 is expressed in $cm^{-1}/^oK$, the quantity hck = 1.38 x 10^{-16} erg/^oK. Thus, the intensities I which are conventionally expressed in units of watt/cm^2 must be multiplied by a factor of 10^7 to convert them to erg/sec/cm^2.) If there is only a single external radiation field present, with frequency ν_v^J, the expression for the rates of stimulated emission and absorption for level v become

$$S_{v \to v-1} = \frac{S(\nu, \nu_r^J)\, A_{10} B_v}{8\pi hckT\, \tilde{\nu}_{10}^3}\, J \left| R_{v,v-1}/R_{10} \right|^2 \exp\left\{ -B_v J(J-1)/kT \right\} I(\nu_v^J) \quad (2.69a)$$

$$S_{v-1 \to v} = \frac{S(\nu, \nu_v^J)\, A_{10}\, B_{v-1}}{8\pi hckT\, \tilde{\nu}_{10}^3}\, J \left| R_{v,v-1}/R_{10} \right|^2 \exp\left\{ -B_{v-1} J(J+1)/kT \right\} I(\nu_v^J) \quad (2.69b)$$

It is often convenient to define optical cross sections $\sigma_{21}(v, J)$ and $\sigma_{12}(v, J)$ by the definition,

$$\frac{\sigma_{21}(v, J)\, I(\nu_v^J)}{h\, \nu_v^J} = S_{v \to v-1} \quad (2.70a)$$

and

$$\frac{\sigma_{12}(v, J)\, I(\nu_v^J)}{h\, \nu_v^J} = S_{v-1 \to v} \quad (2.70b)$$

so that

$$\sigma_{21}(v,J) = \frac{S(\nu,\nu_v^J)\,\tilde{\nu}_v^J\,A_{10}B_vJ}{8\pi kT\,\tilde{\nu}_{10}^3}\,|R_{v,v-1}/R_{10}|^2\,\exp\left\{-B_vJ(J-1)/kT\right\} \qquad (2.71a)$$

$$\sigma_{12}(v,J) = \frac{S(\nu,\nu_v^J)\,\tilde{\nu}_v^J\,A_{10}B_{v-1}J}{8\pi kT\,\tilde{\nu}_{10}^3}\,|R_{v,v-1}/R_{10}|^2\,\exp\left\{-B_{v-1}J(J+1)/kT\right\} \qquad (2.71b)$$

In terms of these cross sections, the gain for the $v \rightarrow v-1$, P(J) transition can be written

$$\alpha_{v,J-1\rightarrow v-1,J} = n_v\,\sigma_{21}(v,J) - n_{v-1}\,\sigma_{12}(v,J) \qquad (2.72)$$

The cross section is often a useful parameter for discussing the saturation characteristics of the laser medium. Eq. (2.67) and (2.65) will be required later for the discussion of the kinetic equations that determine the vibrational level populations.

2.7 Saturation Effects. When the rates of stimulated emission and absorption become comparable to or greater than rates of pumping and relaxation, the laser medium will display saturation characteristics, since then the level populations of the material medium are substantially affected by the radiative processes. In the limit that external radiation fields are small, stimulated radiation can be neglected in the kinetic equations that determine the vibrational population densities. For the CO laser system, the effects of saturation and cross-saturation will be discussed in more detail in a subsequent section. At this point, a simple derivation of the saturation characteristics of a homogeneously and inhomogeneously broadened two-level system will be presented in order

to summarize some of the basic considerations that are involved. For the low pressure regime, much of the experimental results for the CO laser have typically been in the Doppler broadened region, so measurements of saturation parameters have to be interpreted differently than would be the case for the pressure broadened region.

The rate equations for the populations of a simple two-level system will be assumed to be of the form

$$\dot{N}_2 = -N_2/\tau_2 + R_2 - (N_2\ \sigma_{21} - N_1\ \sigma_{12})I(\upsilon)/h\upsilon \qquad (2.73a)$$

$$\dot{N}_1 = -N_1/\tau_1 + R_1 + (N_2\ \sigma_{21} - N_1\ \sigma_{12})I(\upsilon)/h\upsilon \qquad (2.73b)$$

where τ_1 and τ_2 are relaxation rates, R_1 and R_2 are pumping rates, and σ_{21} and σ_{12} are cross sections for stimulated emission, analogous to those defined earlier in Eq. (2.70). We shall assume initially that the system is homogeneously pressure broadened, with a Lorentzian line shape function $g_p(\upsilon, \upsilon_{12})$, where υ_{12} is the resonance frequency between levels 1 and 2. The form of g_p was given by Eq. (2.40) for a collision broadened line. For the moment, we shall think of the two levels as being vibrational levels of the CO laser, although the kinetics for the CO system are much more complicated than the simple model to be discussed here. Nevertheless, the saturation characteristics can be understood best by an initial appeal to a simple derivation, which will serve to illustrate the basic concepts. In the steady

state, the solution of these equations for the gain, $\alpha(I) = (N_2 \sigma_{21} - N_1 \sigma_{12})$, becomes

$$\alpha(I, \nu) = \frac{R_2 \tau_2 \sigma_{21} - R_1 \tau_1 \sigma_{12}}{1 + \frac{I(\nu)}{h\nu} (\tau_1 \sigma_{12} + \tau_2 \sigma_{21})} \tag{2.74}$$

$$= \frac{\alpha_o}{\left[1 + \frac{I(\nu)}{I_s(\nu)}\right]} \tag{2.75}$$

where α_o, the small-signal gain corresponding to negligibly small external field intensity $I(\nu)$, is given by

$$\alpha_o = R_2 \tau_2 \sigma_{21} - R_1 \tau_1 \sigma_{12} \tag{2.76}$$

and where the saturation intensity $I_s(\nu)$ is defined by

$$I_s(\nu) = h\nu/(\tau_1 \sigma_{12}(\nu) + \tau_2 \sigma_{21}(\nu)). \tag{2.77}$$

The physical interpretation of the saturation intensity I_s is that $\alpha_o I_s$ represents the maximum possible extraction of power per unit volume from the homogeneously broadened laser medium.

As Eq. (2.70) shows, the stimulated emission cross sections σ_{21} and σ_{12} depend upon the frequency ν through the line shape factor. For a purely homogeneously broadened medium, therefore, the gain will saturate according to Eq. (2.75) as the input radiation increases in intensity. If we assume that the levels 2 and 1 represent v and v-1 in the CO system, and that the transition ν_{12} is the P(J) branch, then the cross sections

will be given by Eq. (2.71). Let ρ_1 and ρ_2 be defined as the rotational Boltzmann factors, Eq. (2.14), so that the cross sections can be written

$$g_2\,\sigma_{21}(\nu) = g_P(\nu,\ \nu_v^J)\,(h\nu/c)\,\rho_2\,\frac{8\pi^3 J}{3h^2}\,|R_{v,\ v-1}|^2 \tag{2.78a}$$

$$g_1\sigma_{12}(\nu) = g_P(\nu,\ \nu_v^J)\,(h\nu/c)\,\rho_1\,\frac{8\pi^3 J}{3h^2}\,|R_{v,\,v-1}|^2. \tag{2.78b}$$

Then the expression for saturated gain becomes

$$\alpha\,(I,\nu) = \frac{\beta\, g_P(\nu,\ \nu_v^J)}{1 + \gamma\, I(\nu)\, g_P(\nu,\ \nu_v^J)}, \tag{2.79}$$

where

$$\beta = (R_2\,\tau_2\,\rho_2/g_2 - R_1\,\tau_1\,\rho_1/g_1)\,\frac{8\pi^3\,\nu J}{3hc}\,|R_{v,\,v-1}|^2, \tag{2.80}$$

and

$$\gamma = (\tau_2\,\rho_2/g_2 + \tau_1\,\rho_1/g_1)\,\frac{8\pi^3 J}{3h^2 c}\,|R_{v,\,v-1}|^2. \tag{2.81}$$

Using the collision-broadened expression Eq. (2.40) for the line shape function $g(\nu,\ \nu_v^J)$ gives

$$\alpha\,(I,\nu) = \frac{(\beta\Delta\nu_c/\pi)}{(\nu - \nu_v^J)^2 + \Delta\nu_c^2 + \gamma\, I(\nu)\,\Delta\nu_c/\pi} \tag{2.82}$$

which shows that the gain line is broadened (i.e., its <u>shape</u> is changed) as the intensity is increased. The important thing to notice from Eq. (2.82) is

that the width of the Lorentzian depends upon the intensity I -- that is, in the region where saturation effects become important, the homogeneous line is both collision and intensity broadened. The form of the saturated gain equation, (2.75), has been derived here for a simple two level system, but it is typical of the behavior in many systems.

If there is an inhomogeneous distribution of frequencies, then the saturated gain expression (2.82) becomes

$$\alpha(I, \nu) = \int_{-\infty}^{\infty} d\nu' \; \frac{\beta \, g_P(\nu, \nu')}{1 + \gamma I(\nu) \, g_P(\nu, \nu')} \; g_D(\nu', \nu_\nu^J). \tag{2.83}$$

This equation is just the convolution of a Gaussian distribution g_D, given by Eq. (2.37), and a broadened Lorentzian, whose form was given more explicitly in Eq. (2.82). As was shown in Section 2.4.3, the convolution can be evaluated in terms of the complementary error function for the case of exact resonance, $\nu = \nu_{12}$. Using Eq. (2.52), we obtain

$$\alpha(I, \nu_{12}) = \frac{\beta \exp(x^2) \, \mathrm{erfc}(x)}{\sqrt{\pi} \, \Delta\nu_D \, (1 + I/I_s)^{1/2}} \tag{2.84}$$

where the parameter x is defined as

$$x = \Delta\nu_{eff}/\Delta\nu_D, \tag{2.85}$$

in terms of the effective homogeneous width,

$$\Delta_{eff}^2 = \Delta\nu_c^2 \, (1 + I/I_s). \tag{2.86}$$

The parameter

$$I_s = \pi \Delta\nu_c / \gamma \tag{2.87}$$

represents the saturation intensity for the homogeneously broadened line at exact resonance, and in the derivation of Eq. (2.84), account has been taken of the fact that Eq. (2.82) represents a Lorentzian with an effective broadening $\Delta\nu_{eff}$. For the extreme Doppler broadened region, for which $x \ll 1$, Eq. (2.84) for the saturated gain at resonance reduces to

$$\alpha(I) = \frac{(\beta/\sqrt{\pi}\Delta\nu_D)}{(1 + I/I_s)^{1/2}} \tag{2.88}$$

while for $x \gg 1$, which is characteristic of homogeneous broadening, Eq. (2.84) becomes

$$\alpha(I) = \frac{(\beta/\pi\Delta\nu_c)}{(1 + I/I_s)} \tag{2.89}$$

An interesting point to notice is the following: if operation is initially in the extreme Doppler region, the effective spectral "hole width" that is burned out of the frequency distribution by a radiation field is just $\Delta\nu_c$, and the gain begins to saturate according to the expression (2.88). However, as the radiation field intensity I begins to increase, the effective homogeneous linewidth Δ_{eff} given by Eq. (2.86) increases, and when the ratio $x = \Delta\nu_{eff}/\Delta\nu_D$ becomes comparable to or greater than unity, the saturation behavior goes over to the homogeneously broadened limit, characterized by Eq. (2.89). Notice that the quantities $(\beta/\sqrt{\pi}\Delta\nu_D)$ and $(\beta/\pi\Delta\nu_c)$ that occur in the numerators of Eq. (2.88) and (2.89) are just equal to the resonance small-signal gains α_o that are characteristic of the Doppler or pressure broadened regimes (since $1/\sqrt{\pi}\Delta\nu_D = g_D(0)$, and $1/\pi\Delta\nu_c = g_P(0)$, respectively). Since the saturation behavior goes over to the form (2.89) as the intensity I becomes very large, I_s retains the physical significance that $\alpha_o I_s$ represents the limiting extractable energy per unit volume from the

laser medium. Note, however, that to retain this interpretation, α_o must be understood to be the collision broadened small-signal gain -- i.e., $\alpha_o = \beta g_P(0) = \beta / \pi \Delta \nu_c$.

Since the actual experimentally measured small-signal gain is a measure of the combined line shape function S(0) given by Eq. (2.52),

$$\alpha_o = (\beta \sqrt{\pi} \Delta \nu_D) \exp (\Delta \nu_c^2 / \Delta \nu_D^2) \operatorname{erfc} (\Delta \nu_c / \Delta \nu_D), \tag{2.90}$$

it then follows that for any arbitrary region of values $\Delta \nu_c$, $\Delta \nu_D$, and I, that the gain $\alpha(I)$, given by Eq. (2.84), saturates at resonance according to

$$\alpha(I) = \alpha_o \frac{\exp \left(\frac{\Delta \nu_c^2}{\Delta \nu_D^2} \frac{I}{I_s} \right) \operatorname{erfc} \left[\frac{\Delta \nu_c}{\Delta \nu_D} (1 + I/I_s)^{1/2} \right]}{(1 + I/I_s)^{1/2} \operatorname{erfc} (\Delta \nu_c / \Delta \nu_D)}, \tag{2.91}$$

which reduces to the expressions (2.88) and (2.89) in the appropriate limits. It further follows that, if α_o is the actual small signal gain, then the limiting extractable energy per unit volume is given by

$$\alpha_o I_s (\Delta \nu_D \sqrt{\pi} \Delta \nu_c) \exp (-\Delta \nu_c^2 / \Delta \nu_D^2) / \operatorname{erfc} (\Delta \nu_c / \Delta \nu_D) . \tag{2.92}$$

If the experimental measurements of small-signal gain and saturation intensity are carried out in the Doppler broadened region, this expression reduces to

$$\alpha_o I_s (\Delta \nu_D \sqrt{\pi} \Delta \nu_c). \tag{2.93}$$

Physically, the meaning of (2.93) is that, for the Doppler broadened region, only the fraction $(\pi \Delta \nu_c / \sqrt{\pi} \Delta \nu_D)$ of the spectral line is being tapped by the external radiation field. Of course, if the experimental data corresponds

to the pressure broadened region, expression (2.92) for the extractable energy reduces immediately to the familiar form, $\alpha_o I_s$.

3.0 MOLECULAR KINETICS: PUMPING AND RELAXATION MECHANISMS

3.1 Introduction. The program initiated at NCL for the study and development of low pressure electrically excited CO lasers has resulted in a considerable understanding of the relative importance of the operative mechanisms and excitation processes that determine the vibrational populations of CO. In support of the experimental research, a theoretical analysis was undertaken to develop a steady-state kinetic model of an electrically excited CO laser system that would make it possible to predict the CW performance to be expected under arbitrary experimental conditions and variation of parameters. Because of its high efficiency, demonstrated with conventional longitudinal electric discharge configurations, the CO laser is a promising candidate for high power electric discharge systems employing more sophisticated techniques of plasma control for optimization of operation. In terms of excitation and relaxation mechanisms, gas constituents, and quasi-continuous mode of operation, long-pulse transversely-excited E-beam devices that are presently being explored for the CO laser will be fundamentally only an extension of the low pressure longitudinal devices. Therefore, the construction of such a kinetic model represents a valuable approach for extrapolating low pressure results to determine design criteria and performance characteristics for future high energy devices.

A description of the steady-state kinetic model for an electrically excited CO laser amplifier system, and the computer program that has been developed for the calculation of vibrational populations, gains, saturation parameters, rates of energy transfer, and quantum efficiency, will be given below, with a discussion of the numerical techniques employed. At the present time, the status of this work is relatively complete, although

further effort is required to determine certain important constants and to make comparisons between calculations and experimental measurements. Basic experiments for that purpose, such as small signal gain measurements and double-probe and double Q-switching techniques for measurement of vibrational cross relaxation, are discussed more fully in a companion report . Although there is presently a need for improvement in the knowledge of the values and functional dependence of certain parameters of this model, the program has been developed to handle the most general possible input operating conditions. The computer code has been completely debugged, and is performing successfully. In subsequent sections, a description of the mechanisms that have been included will be given, and representative results (based on preliminary assumptions concerning the rate constants) will be presented.

3.2 Steady-State Kinetic Model. As a general theoretical model of the CO laser medium, we consider a mixture of gases A, B, C, ..., excited by an electric discharge, where A represents the active diatomic gas, CO, B a second diatomic gas, and C,.... other monatomic constituents. The energy levels and populations of A and B will be denoted by E_r, n_r ($r = 0,1, 2,...$) and F_R, N_R ($R = 0, 1, 2,...$) respectively. It shall be assumed that the walls of the discharge volume represent a heat reservoir at temperature T with an infinite heat capacity, and that the distribution of translational energies of each of the molecular species is Boltzmann at temperature T. Likewise, the rotational energy levels in each vibrational state are assumed to be in good thermal contact with the translational mode through molecular collision processes, so that we may assume $T_{rot} = T$. The population distributions n_r and N_R of these diatomic systems are determined by a variety of competing pumping and relaxation processes, and satisfy the

master equation,

$$dn_r/dt = R_r^e + R_r^{VT}(A^\dagger, A) + R_r^{VT}(A^\dagger, B, C, \ldots) + R_r^{VVT}(A^\dagger, A^\dagger)$$

$$+ R_r^{VVT}(A^\dagger, B^\dagger) + R_r^{sp} + R_r^{stim} + R_r^{misc} = 0, \qquad (3.1a)$$

with a similar equation for N_R (R = 0, 1, 2...). Although the ultimate source of vibrational excitation is by electron collisions, the method of energy input need not be (and in fact, is not) the dominant mechanism in determining the resulting vibrational population distributions. In the order of their appearance, the terms occurring on the RHS of the master equation represent excitation and relaxation rates for the following processes:

i) electron impact collisions
ii) VT collisions (single quantum) by impact with A
iii) VT collisions (single quantum) by impact with B, C, ...
iv) VVT near resonant exchange collisions with another $A^\dagger$ molecule
v) VVT near resonant exchange collisions with a $B^\dagger$ molecule
vi) spontaneous decay ($\Delta v = 1$ and $\Delta v = 2$)
vii) stimulated emission processes, resulting from input radiation for an arbitrary number of vibrational-rotational lines.
viii) miscellaneous pumping or decay terms

In the steady state, the time derivative can be set equal to zero, yielding a multilevel set of coupled, nonlinear, algebraic simultaneous equations:

$$R_r^e + R_r^{VT}(A^\dagger, A) + R_r^{VT}(A^\dagger, B, C, \ldots) + R_r^{VVT}(A^\dagger, A^\dagger)$$

$$+ R_r^{VVT}(A^\dagger, B^\dagger) + R_r^{sp} + R_r^{stim} + R_r^{misc} = 0 \qquad (3.1b)$$

The processes i) to v) will be described in more detail in the following sections. Spontaneous and stimulated emission have been discussed thoroughly in Section 2.6 on radiative characteristics, with the rates R_r^{sp} and R_r^{stim} given by Eq. 2.65 and Eq. 2.67 respectively.

3.3 Electronic Excitation. The mechanism for vibrational excitation in electrical discharge CO and CO_2 laser systems is by indirect electron impact collisions, which proceed via the formation of intermediate compound excited states due to resonant electron scattering. Although the ultimate source of vibrational excitation is by indirect electron collisions, the method of energy input need not be (and, in fact, is not in the case of the CO laser) the dominant mechanism determing the resulting populational distribution.

The scattering cross sections for vibrational excitation of several molecules, such as CO, N_2, and CO_2, etc., exhibit pronounced peaks for incident electron energies of typically a few electron volts. Shulz[29,30] has measured these cross sections experimentally for several molecules, with the results for CO and N_2 shown in Fig. 3.1. From this Figure, it can be seen that electrons with energies of 1.0 to 3.0 eV are most efficient for vibrational excitation.

Since the vibrational energy levels for CO and N_2 are separated by much smaller amounts (~.2 eV), it follows that the collision process does not correspond to a direct electronic excitation. The existence of the phenomenon suggests that the excitation can be interpreted in terms of indirect resonance electron scattering, which arises from the formation of a temporary, short-lived, intermediate compound state CO^- or N_2^-. The existence of well-defined peaks in the vibrational cross sections can be attributed to resonances of the incident electron wave in the potential well of the molecule. In this

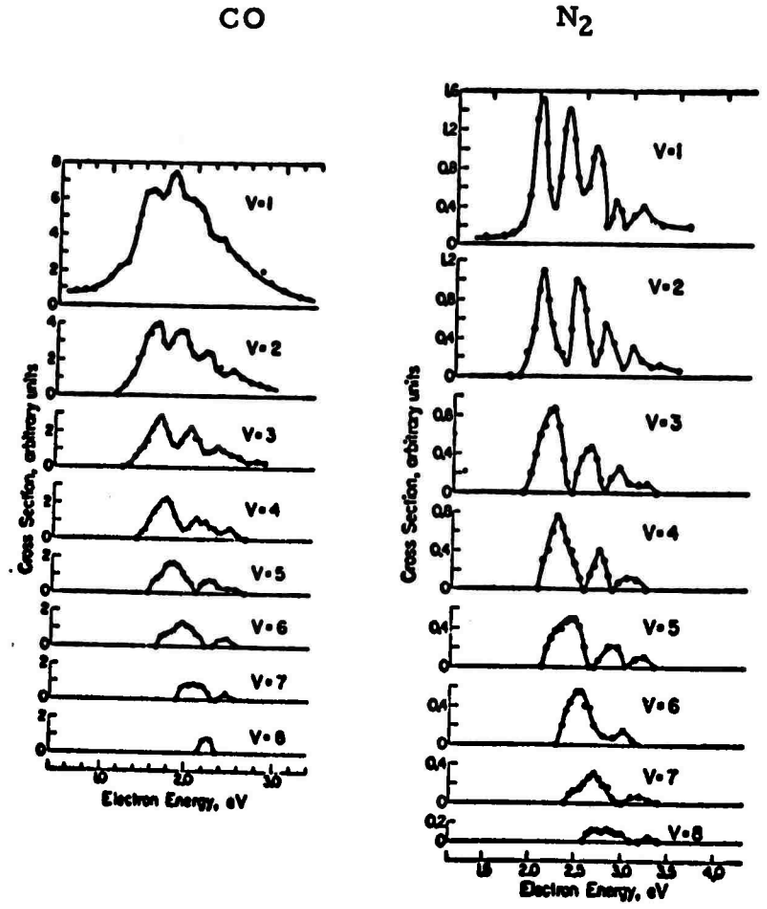

Figure 3.1. Cross-Sections for Vibrational Excitation of CO and N_2 by Electron Collisions, taken from Reference 29.

interaction region, the electron wave function at certain resonance energies is distorted and enhanced, and may form a quasi-bound state of positive energy with the molecule, such as CO^- or N_2^-. There is, however, a finite probability of decay, characterized by the lifetime τ of the complex, with the widths of the cross section peaks corresponding roughly to the inverse of the lifetime τ of the excited state. Herzenberg and Mandl[32] and Chen[33] have investigated the problem of vibrational excitation by electron collision theoretically, and have obtained good agreement with experiments based on this model.

Physically, the process of vibrational excitation can be understood as follows: the incident electron with a favorable resonance energy is trapped in the molecular potential well, forming a negative compound state that lives for some lifetime τ. During that time, the energy of the electron "dissolves" into the available energy modes of the complex, and when the electron is finally re-emitted, the molecule may retain some of this energy in the form of an excited vibrational level. As shown schematically in Fig. 3.2 the energy levels of the compound state are not the same as those of the molecule. Electrons with incident energies of E_o, E_1, E_2, ... will have an enhanced probability of being captured to form the excited compound state, and thus, it is for these energies that the cross section will be expected to display resonance peaks. Basically, therefore, the excitation can be pictured as occurring via a three state process:

1) $e^-(E) + CO \rightarrow CO^-$
2) CO^- lives for time τ, during which time its energy may be redistributed internally among various energy modes
3) $CO^- \rightarrow CO(v) + e^-(E')$

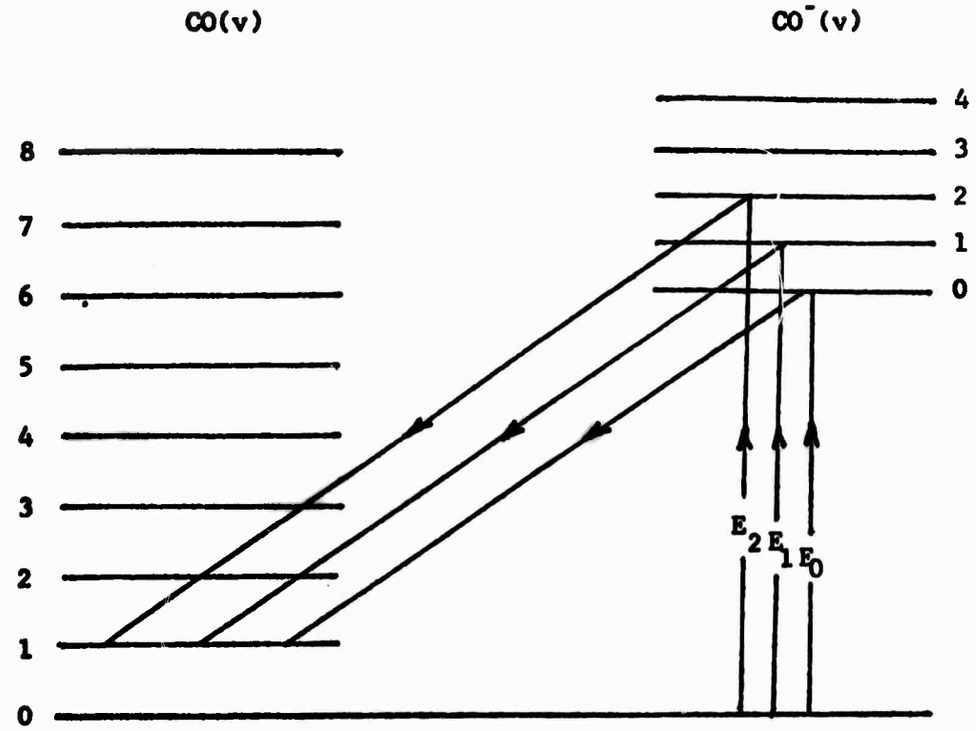

Figure 3.2a: Schematic representation of the vibrational excitation of CO from v = 0 to v = 1 by resonance electron scattering, with formation of CO^- compound state.

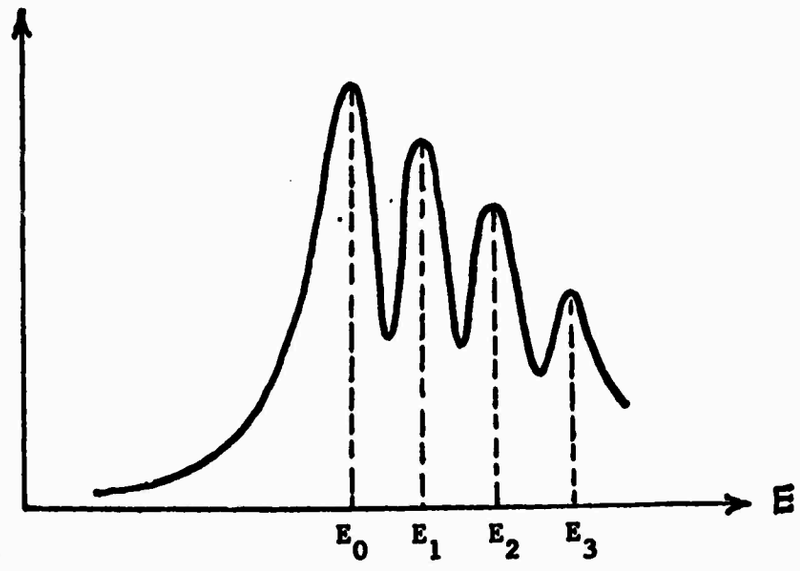

Figure 3.2b: Schematic representation of the resonance structure exhibited by the excitation cross section for the process depicted in (a) above.

The total rate of excitation dw $(r, \vec{k} \to s, \vec{k}')$ into the continuum of final states $d\vec{k}'/(2\pi)^3$ for the scattering processes in which an incident electron of momentum $\hbar\vec{k}$ excites a CO molecule from an initial vibrational level r to a final level s, represented by

$$e^-(\vec{k}) + CO(r) \to CO(s) + e^-(\vec{k}') \tag{3.2}$$

can be expressed in terms of the scattering matrix T as

$$dw(r, \vec{k} \to s, \vec{k}') = \frac{2\pi}{\hbar} |T_{rs}(\vec{k}, \vec{k}')|^2 \delta(E_i - E_f)\, d\vec{k}'/(2\pi)^3, \tag{3.3}$$

where E_i and E_f are the initial and final energies,

$$\begin{aligned} E_i &= E_r + \hbar^2 k^2/2m \\ E_f &= E_s + \hbar^2 k'^2/2m \end{aligned} \tag{3.4}$$

If $f(\vec{k})$ denotes the electron distribution function, so that $n_e f(\vec{k})d\vec{k}$ represents the number of electrons per unit volume in the range $(\vec{k},\ k+d\vec{k})$, where n_e is the electron density, then the total rate of vibrational excitation from r to s is given by

$$\begin{aligned} R^e_{r\to s} = n_e(2\pi/\hbar) \int d\vec{k} f(\vec{k}) \int d\vec{k}'/(2\pi)^3 \ \times \\ |T_{rs}(\vec{k}, \vec{k}')|^2 \ \delta(E_r + \hbar^2 k^2/2m - E_s - \hbar^2 k'^2/2m) \end{aligned} \tag{3.5}$$

which is the transition rate (3.3) averaged over initial and summed over final electron states. The presence of the δ-function insures energy conservation when the integral is carried out over all $\vec{k}$ and $\vec{k}'$. The microscopic principle of detailed balancing for the process (3.2) is

expressed mathematically by

$$\left|T_{rs}(\vec{k},\vec{k}')\right|^2 = \left|T_{sr}(\vec{k}',\vec{k})\right|^2, \tag{3.6}$$

so the rate $R^e_{s\to r}$ for the reverse process can be written exactly the same as Eq. (3.5) with $f(\vec{k}')$ replacing $f(\vec{k})$. Eq. (3.5) demonstrates that the rate of vibrational excitation depends upon the electron kinetics of the plasma, since the electron distribution function $f(\vec{k})$ is involved. If a Boltzmann distribution is assumed for the electrons, characterized by a temperature T_e,

$$f(\vec{v}) = (m/2\pi kT_e)^{3/2} \exp(-mv^2/2kT_e) \tag{3.7}$$

where $\vec{v} = \hbar\vec{k}/m$ is the electron velocity, then it is easy to verify immediately from Eq. (3.5) and the corresponding equation that would apply for the inverse process that

$$R^e_{r\to s} = \exp\left(\frac{E_s - E_r}{kT_e}\right) R^e_{s\to r'} \tag{3.8}$$

which is the usual thermodynamic expression of the principle of detailed balancing for an electron gas that is in thermal equilibrium at temperature T_e.

It is convenient to relate the more familiar quantities such as cross section and differential cross section to the scattering matrix expression given above. The scattering matrix $\left|T_{rs}(\vec{k},\vec{k}')\right|^2$ is a function of the initial electron energy (and thus, k), and of the final scattering angles, specified by $\Omega_{\vec{k}'}$. If the volume element $d\vec{k}$ in Eq. (3.5) is replaced by $k'^2 dk' d\Omega_{\vec{k}'}$, and the integral over k' carried out, the differential scattering cross

section can be defined as

$$v d\sigma_{r\to s}/d\Omega_{\vec{k}'} = \frac{2\pi}{\hbar} \left| T_{rs}(k, \Omega_{\vec{k}'}) \right|^2 \rho(E_f) \tag{3.9}$$

where $\rho(E_f)$, the density of final states, is defined by

$$\rho(E_f) = (1/2\pi)^3 \int dk' k'^2 \delta(E_r + \hbar^2 k^2/2m - E_s - \hbar^2 k'^2/2m) \tag{3.10}$$

and v is the initial electron velocity. It is easy to verify that

$$\rho(E_f) = (m^2/h^3)\, v' \tag{3.11}$$

where v' is the final velocity given by

$$v'^2 = v^2 + 2(E_r - E_s)/m, \tag{3.12}$$

and that $\rho(E_f)$ vanishes if $2(E_s - E_r)/m > v^2$. That is, if the excitation process corresponds to a vibrational change from $r \to s$, the incident electron must have a minimum energy of at least $(E_s - E_r)$ if $s > r$. For de-excitation, of course, there is no minimum energy requirement for the incident electron.

The total cross section is defined as an integration over all solid angle of the differential scattering cross section:

$$\sigma_{r\to s}(E) = \int d\Omega\, (d\sigma_{r\to s}/d\Omega) \tag{3.13}$$

This cross section corresponds to the experimentally measured quantities, such as those obtained by Schulz for CO and N_2, which were shown in Fig. 3.1. It can be seen from Eqs. (3.9) and (3.13) that the total excitation cross sections for forward are reverse processes can be related by

$$(v/v')\,\sigma_{r\to s}(E) = (v'/v)\,\sigma_{s\to r}(E'), \tag{3.14}$$

which is yet another form for expressing the principle of detailed balancing. If the Boltzmann distribution of Eq. (3.7) is assumed for the electrons, it can be shown that the resulting distribution in energy will be given by

$$f(E) = \frac{2}{\sqrt{\pi}}\,(kT_e)^{-3/2}\,E^{1/2}\exp(-E/kT_e) \tag{3.15}$$

and the resulting excitation rates $R^e_{r\to s}$ $(s > r)$ will become

$$R^e_{r\to s} = n_e \langle v_e \rangle /(kT_e)^2 \int_{(E_s-E_r)}^{\infty} dE\,\sigma_{r\to s}(E)\,E\exp(-E/kT_e), \tag{3.16}$$

where

$$\langle v_e \rangle = (8\,kT_e/\pi m)^{1/2} \tag{3.17}$$

is the average thermal electron velocity for temperature T_e. It is instructive to notice that by using the detailed balance relation $v^2\sigma_{r\to s}(E) = v'^2\sigma_{s\to r}(E')$ in conjunction with the energy conservation condition (3.12), Eq. (3.16) can be manipulated to demonstrate the thermodynamic expression of detailed balancing that was given by Eq. (3.8). The net rate of electron excitation of level r is

$dn_r/dt = R_r^e$, where R_r^e is given by

$$R_r^e = -n_r \sum_s R_{r\to s}^e + \sum_s n_s R_{s\to r}^e$$

$$= n_e \sum_s \left[n_s - n_r \exp\left(\frac{E_r - E_s}{kT_e} \right) \right] \langle v(E) \sigma_{s\to r}(E) \rangle_{T_e} \qquad (3.18)$$

Unfortunately, the available experimental data on electron impact excitation of the molecular vibrational levels is restricted to collision processes for which the molecule is initially in the ground state. For CO and N_2, the data of Schulz includes cross sections for processes $0 \to v$, where $v = 1, 2, \ldots 8$. Therefore, for the construction of a molecular kinetic model, some assumptions must be made on excitation rates for which the initial molecular level is not zero. Based on the simple schematic picture of the resonance scattering process discussed above, and represented by Fig. 3.2, it is probably reasonable to assume that for the first few levels, say $r = 1, 2, \ldots 6$, the cross sections are about the same, but with the position of the energy peaks shifted by the initial energy of the molecular state:

$$\sigma_{o\to i}(E) = \sigma_{r\to r+i}(E - E_r) \qquad (3.19)$$

Eq. (3.16) can be numerically integrated to give the electron pumping rates for CO. The rates $R_{r\to s}^e/n_e = \langle v(E) \sigma_{r\to s}(E) \rangle_{T_e}$ obtained for representative temperatures T_e and various levels r, s are shown in Table 3.1. As Eq.(3.16) clearly demonstrates, the electron excitation rates depend very critically upon a favorable overlap between the electron energy distribution function and the cross sections, $\sigma_{r\to s}(E)$. For CO, N_2, and CO_2, it is fortuitous that the cross sections are appreciable for

i	$\langle v\sigma_{o \to i} \rangle$ (cm^3/sec)
1	1.59×10^{-8}
2	6.51×10^{-9}
3	3.63×10^{-9}
4	1.98×10^{-9}
5	1.29×10^{-9}
6	8.50×10^{-10}
7	4.71×10^{-10}
8	1.94×10^{-10}

Table 3.1: Electron excitation rates $\langle v\sigma_{o \to i} \rangle$ for a Boltzmann electron distribution with temperature $T_e = 10,000^{\circ}K$.

electron energies of a few eV, which is characteristic of typical electric discharge conditions. (NO, for example, does not form a compound state NO^-, and thus cannot be exploited as efficiently as CO.) To the extent that it is possible, it is, therefore, always obviously desirable to design the laser system parameters in such a way that this overlap effect will be maximized. The optimization of the plasma characteristics in electric discharge lasers is an important factor that determines the efficiency of electrical energy transfer into the vibrationally excited states of the active molecules, and is, therefore, a fundamental consideration for increasing the conversion efficiency. There are several ways in which the plasma characteristics can be altered to enhance the laser operation; some of them are relatively simple, such as altering the discharge constituents to optimize the gas mixture, while others are relatively sophisticated. Further discussion of some of these considerations will be given in a subsequent section devoted to the electron kinetics of a weakly ionized plasma.

3.4 Vibrational Relaxation and Cross-Relaxation. Collisions between excited molecules can result in excitation or decay of vibrational quanta by so-called V-T processes, such as

$$\begin{aligned} A(r+1) + A &\rightleftarrows A(r) + A + \Delta E = E_{r+1} - E_r \\ B(R+1) + B &\rightleftarrows B(R) + B + \Delta E = F_{R+1} - F_R \\ A(r+1) + B &\rightleftarrows A(r) + B + \Delta E = E_{r+1} - E_r \\ B(R+1) + A &\rightleftarrows B(R) + A + \Delta E = F_{R+1} - F_R \end{aligned} \qquad (3.20)$$

in which the excess energy is supplied or provided by kinetic energy,

or by means of the so-called V-V-T processes, such as

$$A(r+1) + A(s) \rightleftarrows A(r) + A(s+1) + \Delta E = E_{r+1} - E_r + E_s - E_{s+1} \quad (3.21a)$$

$$A(r+1) + B(S) \rightleftarrows A(r) + B(S+1) + \Delta E = E_{r+1} - E_r + F_S - F_{S+1} \quad (3.21b)$$

$$B(R+1) + B(S) \rightleftarrows B(R) + B(S+1) + \Delta E = F_{R+1} - F_R + F_S - F_{S+1} \quad (3.21c)$$

$$A(r+1) + A(s+1) \rightleftarrows A(r) + A(s) + \Delta E = E_{r+1} - E_r + E_{s+1} - E_s \quad (3.21d)$$

$$A(r+1) + B(S+1) \rightleftarrows A(r) + B(S) + \Delta E = E_{r+1} - E_r + F_{S+1} - F_S \quad (3.21e)$$

$$B(R+1) + B(S+1) \rightleftarrows B(R) + B(S) + \Delta E = F_{R+1} - F_R + F_{S+1} - F_S \quad (3.21f)$$

in which vibrational quanta of energy are exchanged between molecules, with the excess energy transferred to or from the kinetic energy. The rates for V-T processes decrease rapidly as the amount of kinetic energy ΔE that must be absorbed by the translational mode increases. Furthermore, the collision rates are predominantly determined from dipole transitions for which $\Delta v = 1$, so it is usually reasonable to neglect all V-T processes but those which convert only a single vibrational quantum of energy. Likewise, V-V-T transitions for processes other than those in which each molecule changes by a single quantum can be neglected.

In the first group of V-V processes, given in Eqs. (3.21a, b, c), one molecule loses energy while the second gains energy; thus, for those cases, the excess energy ΔE exchanged with the translational mode will be small. These represent near-resonant exchange collisions. In contrast, the second group of V-V-T processes are nonresonant exchange collisions, since both molecules gain or lose energy, all of which must be transferred to or from kinetic energy. Since the vibrational energies of CO or N_2 are $\sim 2000\ cm^{-1}$, the translational energy that must be exchanged is $\sim 4000\ cm^{-1} \sim 80\ kT$ (for $T \sim 77^{\circ}K$, for example). Thus, the

transition rate for such processes as represented by Eqs. (3.21d, e, f) would be expected to be very small, and they can be neglected. Only the near-resonant exchange collisions represented by Eqs. (3.21a, b, c) need to be retained.

The V-V-T processes represent the most important mechanism for determing the vibrational population distribution of the CO laser system. Although excitation energy input comes from electron impact collisions, the rates of V-V-T resonant exchange collisions are much faster, and thus, the energy is rapidly redistributed among the vibrational levels. It has, in fact, previously been shown by Treanor, et al[34] and others[35-41] that the kinetics of diatomic molecular gases dominated by rapid V-V-T exchange collisions can lead to highly excited, non-Boltzmann distributions of vibrational level populations.

From the principle of detailed balancing, the transition rates for each of the microscopic reversible processes above will be equal. In the case of the V-T processes (3.20) and the V-V-T processes (3.21a, b, c), excess energy has been transferred to (or from) the thermal reservoir at temperature T, and the initial and final states of the reservoir have been tacitly suppressed in writing these reactions. The heat bath can be considered to be a system with a large number of degrees of freedom, with states $|f>$ that span a continuous energy spectrum. The assumption of thermal equilibrium at temperature T means that the heat bath can be defined as a statistical mixture with probabilities $\rho_f = \exp(-E_f kT)$ for finding it in any of the states $|f>$. (The assumption of infinite heat capacity is equivalent to saying that the probabilities ρ_f do not change if energy is exchanged with the reservoir; i.e., the termperature T does not change.) If V-T processes are written to explicitly include reference to the initial and final states of

the reservoir, then, for example

$$|i> + A(r+1) + A \rightleftarrows |f> + A(r) + A \tag{3.22}$$

$$E_i + E_{r+1} = E_f + E_r \tag{3.23}$$

If the rates for the microscopic process (3.22) are denoted by $p_{r+1,\, i\to r,\, f}$ and $p_{r,\, f\to r+1,\, i}$, the principle of detailed balancing requires that

$$p_{r+1,\, i\to r,\, f} = p_{r,\, f\to r+1,\, i}\,. \tag{3.24}$$

However, since the internal states of the thermal reservoir are not of interest, the total V-T transition rates can be obtained as follows:

$$P_{r+1\to r} = \sum_{i,f} \rho_i\, p_{r+1,\, i\to r,\, f} \tag{3.25a}$$

$$P_{r\to r+1} = \sum_{i,f} \rho_f\, p_{r,\, f\to r+1,\, i} \tag{3.25b}$$

i.e., the total transition probabilities are obtained by summing over all final lattice states, and over all initial states weighted by the <u>a priori</u> probabilities p_i for being in states $|i>$. Since $\rho_f = \rho_i \exp\left[(-E_f + E_i)/kT\right] = \rho_i \exp\left[(E_r - E_{r+1})/kT\right]$, Eqs. (3.24) and (3.25) lead to the thermodynamic expression of the principle of detailed balancing,

$$P_{r+1\to r} = \exp\left[\frac{E_{r+1} - E_r}{kT}\right] P_{r\to r+1}\,. \tag{3.26}$$

Similar equations hold for all of the forward and reverse transition

rates for the V-V-T collisions also; e.g., the rates for (3.21a) are related by

$$P_{r+1,\,s\to r,\,s+1} = P_{r,\,s+1\to r+1,\,s}\exp\left(\frac{E_{r+1} - E_r + E_s - E_{s+1}}{kT}\right), \tag{3.27a}$$

and for (3.21b) by

$$Q_{r+1,\,R\to r,\,R+1} = Q_{r,\,R+1\to r+1,\,R}\exp\left(\frac{E_{r+1} - E_r + F_R - F_{R+1}}{kT}\right). \tag{3.27b}$$

The rate of excitation of level r due to V-T and V-V-T collision processes will be given by

$$\begin{aligned} R_r^{VT}(A^\dagger, A) = {} & P_{r+1\to r}\left[n_{r+1}\,n - \exp\left(-\frac{E_{r+1} - E_r}{kT}\right) n_r n\right] \\ & - P_{r\to r-1}\left[n_r n - \exp\left(-\frac{E_r - E_{r-1}}{kT}\right) n_{r-1} n\right] \end{aligned} \tag{3.28a}$$

$$\begin{aligned} R_r^{VT}(A^\dagger, B) = {} & Q_{r+1\to r}\left[n_{r+1}N - \exp\left(-\frac{E_{r+1} - E_r}{kT}\right) n_r N\right] \\ & - Q_{r\to r-1}\left[n_r N - \exp\left(-\frac{E_r - E_{r-1}}{kT}\right) n_{r-1} N\right] \end{aligned} \tag{3.28b}$$

$$R_r^{VVT}(A^\dagger, A^\dagger) = \sum_s P_{r+1,\,s-1\to r,\,s}\left[n_{r+1}n_{s-1} - \exp\left(-\frac{E_{r+1}+E_{s-1}-E_r-E_s}{kT}\right)n_r n_s\right]$$

$$-\sum_s P_{r,\,s\to r-1,\,s+1} \times \left[n_r n_s - \exp\left(-\frac{E_r+E_s-E_{r-1}-E_{s+1}}{kT}\right)n_{r-1}n_{s+1}\right] \qquad (3.29a)$$

$$R_r^{VVT}(A^\dagger, B^\dagger) = \sum_R Q_{r+1,\,R-1\to r,\,R}\left[n_{r+1}N_{R-1} - \exp\left(-\frac{E_{r+1}-E_r+F_{R-1}-F_R}{kT}\right)n_r N_R\right]$$

$$-\sum_R Q_{r,\,R\to r-1,\,R+1} \times \left[n_r N_R - \exp\left(-\frac{E_r-E_{r-1}+F_R-F_{R+1}}{kT}\right)n_{r-1}N_{R+1}\right] \qquad (3.29b)$$

Before discussing the rates in detail, it is instructive at this point to illustrate the physical significance of fast V-V-T cross-relaxation with a simple example. Javan[42] has shown how the interplay between two nearly resonant 2-level systems in contact with thermal reservoirs at different temperatures (e.g., the electron and translational baths) can lead to interesting equilibrium population distributions under different conditions, depending upon the relative magnitudes of the rates of pumping and relaxation mechanisms. Consider the two systems shown in Fig. 3.3; system s has populations n_a and n_b in levels a and b, which are separated

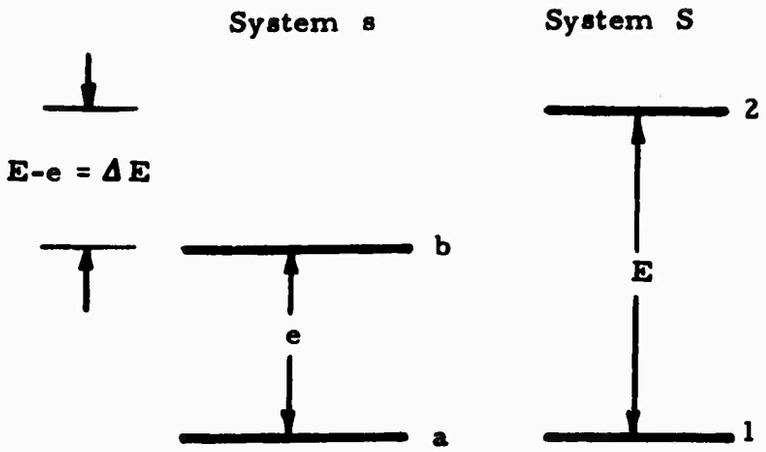

Figure 3.3a. Two simple 2-level systems interacting with near-resonant exchange collisions.

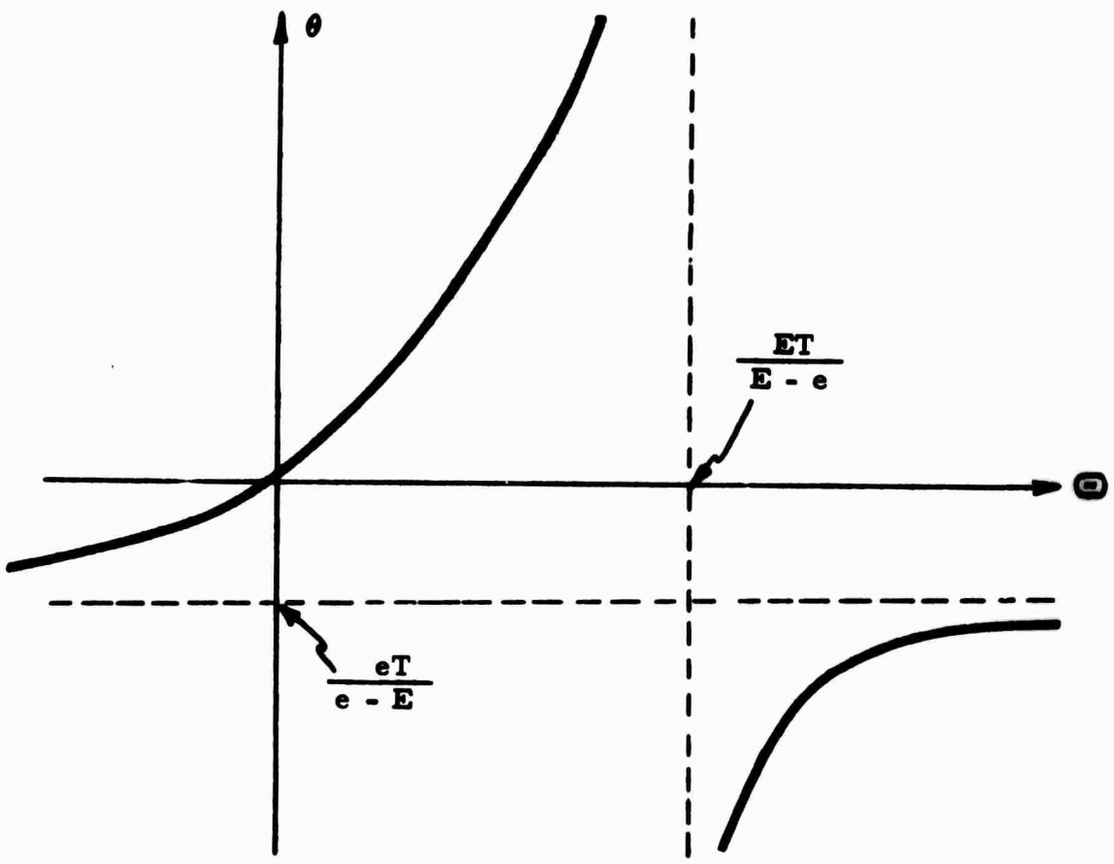

Figure 3.3b. Steady-state vibrational temperatures for interacting system s and S.

by an energy e, while system S has populations N_1 and N_2 in levels 1 and 2, which are separated by an energy E. Assume that level b is pumped at a rate r, and level 2 with a rate R, and that near resonant exchange collisions between the two systems are possible. If the translational mode is in thermodynamic equilibrium at temperature T, the collisional exchange rates will be related by

$$P_{a,2\to b,1} = \exp(\Delta E/kT)\, P_{b,1\to a,2}, \tag{3.30}$$

where $\Delta E = (E - e)$, and the rate equations for the populations n_b and N_2 will be given by

$$\begin{aligned} dn_b/dt &= r + C \\ dN_2/dt &= R - C, \end{aligned} \tag{3.31}$$

where the collision term C is

$$C = n_a N_2 P_{a,2\to b,1} - n_b N_1 P_{b,1\to a,2}. \tag{3.32}$$

If it is assumed that the collision term C is the dominant rate for system s, then r can be neglected, and in the steady state,

$$n_b/n_a = (N_2/N_1)(P_{a,2\to b,1}/P_{b,1\to a,2}) = (N_2/N_1)\exp(\Delta E/kT). \tag{3.33}$$

On the other hand, suppose that the pumping term R is the dominant rate for system S, with collisional loss terms negligible, and assume that R brings the populations N to a temperature Θ:

$$N_2/N_1 = \exp(-E/k\Theta). \tag{3.34}$$

For example, system S could be thought of as being pumped by electrons to a high temperature, $\Theta = T_e$. Eq. (3.33) for the populations of system s becomes

$$n_b/n_a = \exp(\Delta E/kT - E/kT_e) \tag{3.35}$$

Eq. (3.35) has a very interesting structure, for notice that, if

$$(E - e)/T > E/T_e, \tag{3.36}$$

then $n_b/n_a > 1$, corresponding to a situation with <u>total inversion</u>. That is, because of the energy difference $\Delta E = (E-e)$, system S can pump system s to a totally inverted condition in the situation where vibrational cross-relaxation is fast compared with the other pumping and relaxation rates of system s. If a temperature θ is defined for system s, it follows that

$$-\frac{e}{\theta} + \frac{E}{\Theta} = \frac{E - e}{T} \tag{3.37}$$

A plot of this equation is shown in Fig. 3.3, which shows that for values of Θ which are sufficiently large, the corresponding temperature θ becomes negative. Clearly, the effect becomes more pronounced as the kinetic temperature T is decreased, since the Boltzmann factor $\exp(\Delta E/kT)$ that expresses the ratio between the forward and reverse processes increases. That is, for <u>lower</u> translational temperatures, system S can pump system s more efficiently. Schematically, this can be seen in Fig. 3.3, in which the vertical asymptote line would shift toward the left as T is decreased.

Based upon this simple example, it is apparent how rapid V-V-T cross-relaxation can have such profound significance for the kinetics of the vibrational populations in the CO laser system. Since N_2 has larger energy spacings than CO, N_2 can pump the CO levels; furthermore, since the upper vibrational level spacings of CO decrease due to anharmonic effects, molecules in the lower levels of CO can pump molecules which are in the upper levels to higher vibrational temperatures. This is the physical origin of the so-called "anharmonic pumping" mechanism.

There are several theories[43-66] of V-T and V-V-T collision rates, and thus, the dependence of these transition probabilities on vibrational level and translational temperature is one of the greatest uncertainties for constructing a suitable molecular kinetic model. The form of the rates to be used here is taken from a modified form of SSH theory[43-45] with the V-V-T transition rates given by

$$P_{r,s-1\to r-1,s} = \frac{2\pi^2 f_c T}{\theta_1^2 b} \exp\left(\frac{\epsilon}{T}\right)\left(\frac{r}{1-rx_e}\right)\left(\frac{s}{1-sx_e}\right) \times \exp\left(\theta_{rs}/2T\right) F(g_{rs}) \tag{3.38}$$

where x_e was the anharmonicity factor defined by Eq. (2.22), f_c is the kinetic collision frequency, $\theta_{rs} = (E_r - E_{r-1} - E_s + E_{s-1})/k$, and ϵ is a parameter originating from the use of a Lenard-Jones interaction potential. The quantities b and g_{rs} are defined by

$$b = 16\pi^4 \mu \ell^2 k/h^2 \tag{3.39}$$

and

$$g_{rs}^{2} = b\theta_{rs}^{2}/8T \tag{3.40}$$

where μ is the reduced mass, and ℓ is a measure of the effective interaction length, and is typically $\sim .2$ Å, which we shall assume here. If μ is expressed in molecular weight, and ℓ is given in Å, then $b = .8153\,\mu\ell^2$. The function $F(g_{rs})$ is an expression of the "adiabaticity" of the collision,

$$F(g) = g^2 \int_0^\infty d\xi\, e^{-\xi} \operatorname{csch}^2 (g/\sqrt{\xi}), \tag{3.41}$$

and which becomes approximately

$$F(g) \approx 8(\pi/3)^{1/2} g^{7/3} \exp(-3g^{2/3}) \tag{3.42}$$

in the limit that g is large (i.e., off resonant). A modification of the usual SSH theory (which uses Eq. (3.42) for all cases) was suggested by Keck and Carrier[59] and Bray[58] who use an expression

$$F(g) = \frac{1}{2} \exp(-2g/3)\left[3 - \exp(-2g/3)\right], \tag{3.43}$$

which is approximately valid (to within about 20%) for all values of $g < 20$.

For the calculations to be performed here, it is the structure of Eq. (3.38) which is important, since it is necessary to have some assumptions for calculating the V-V-T rates for high vibrational levels in terms of the rate $P_{10\to01}$, which shall be assumed to be known. Thus, Eq. (3.38)

can be written as

$$P_{r,s-1\rightarrow r-1,s} = P_{10\rightarrow 01}\, rs \left(\frac{1 - x_e}{1-rx_e}\right)\left(\frac{1 - x_e}{1 - sx_e}\right)$$

$$\exp(\theta_{rs}/2T)\,\frac{1}{2}\left[3 - \exp(-2g_{rs}/3)\right]\exp(-2g_{rs}/3) \qquad (3.44)$$

Likewise, the rates for V-T processes can be taken from SSH theory, and are given by

$$P_{r\rightarrow r-1} = P_{1\rightarrow 0}\, r\left(\frac{1 - x_e}{1 - rx_e}\right)\exp(\theta_{r,1}/2T)\, F(g_r)/F(g_1) \qquad (3.45)$$

where $\theta_r = (E_r - E_{r-1})/k$, $\theta_{r,1} = \theta_r - \theta_1$, and $g_r = b\theta_r^2/8T$.

Experimental rates for V-T processes have been measured by several workers, and results have been summarized by Millikan[60-62]; some of his results are shown in Figure 3.4 and 3.5 . V-V-T rates, on the other hand, are typically somewhat scarce, and those that are reported are usually measured at high temperatures ($\gtrsim 1000^{\circ}K$), characteristic of shock tube experiments.[64]

Hancock and Smith[66] and Yardley[8] have made some experimental measurements of CO-CO vibrational exchange rates, and we are presently making preparations to infer some of these rates from double-probe and double-Q switch experiments, to be described in a companion report[21]. SSH theory employs the assumption that short-range repulsive interactions (e.g., the Lenard-Jones potential) are the dominant mechanism for V-V-T energy exchange. However, as Mahan[46] has suggested, molecules with large transition dipole matrix elements may be able to transfer vibrational quanta more efficiently by means of resonant processes which result from

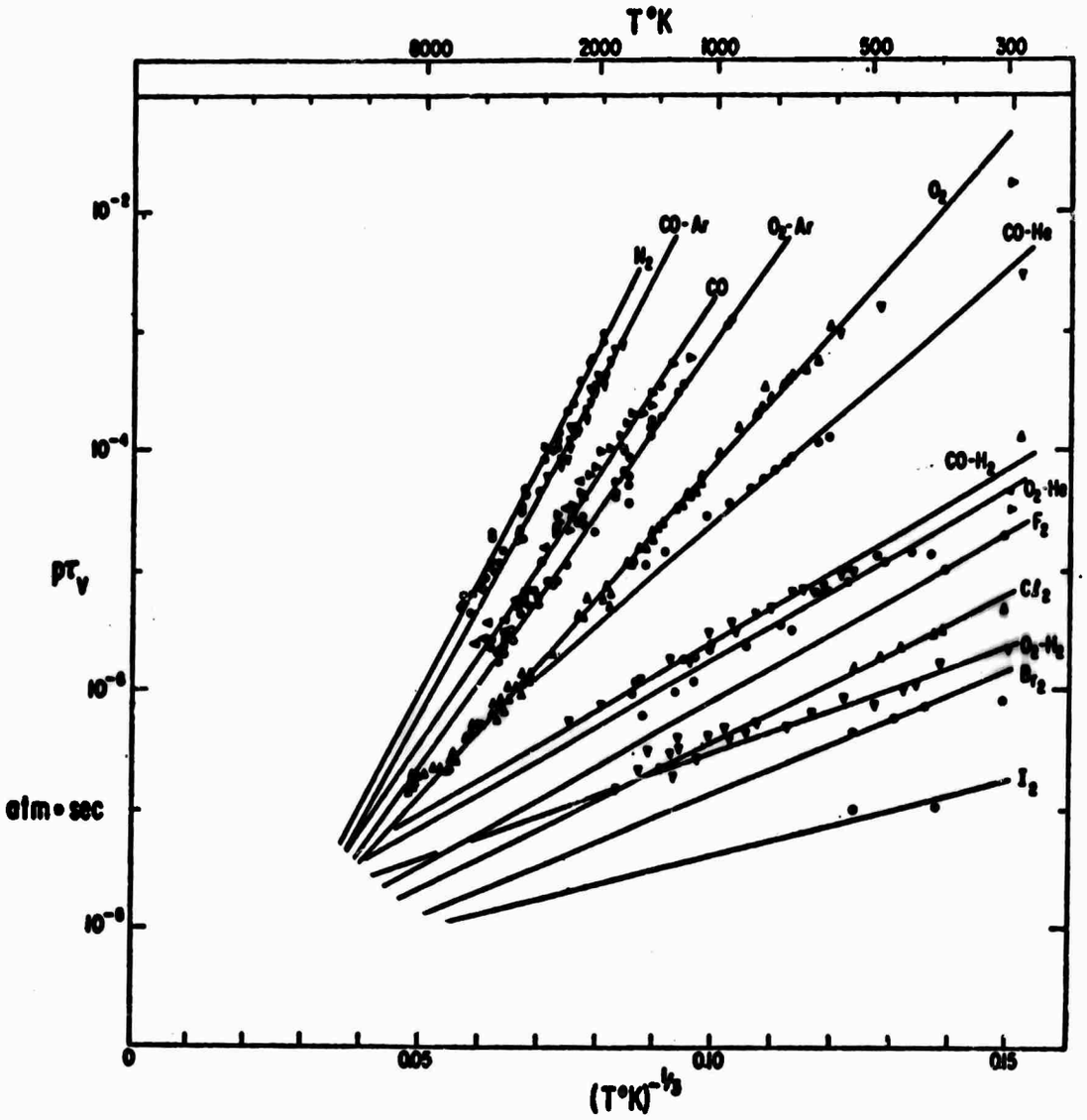

Figure 3.4. V-T Relaxation Rates, taken from Reference 60.

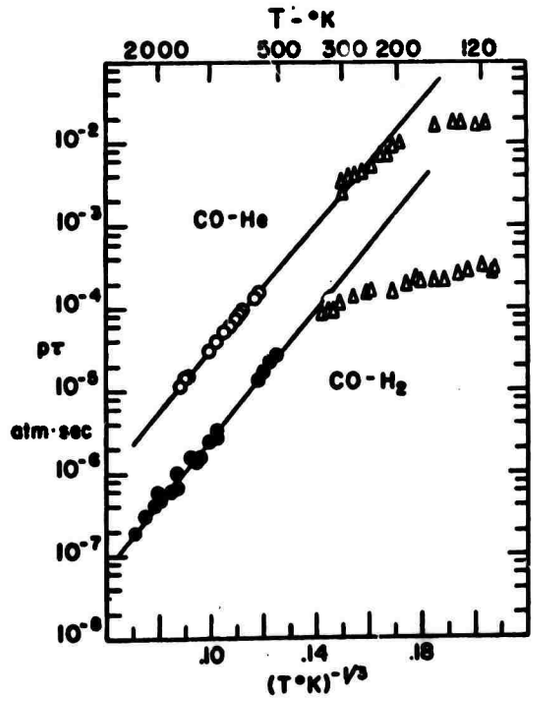

Figure 3.5. V-T Relaxation Rates for CO-He and CO-H_2, taken from Reference 62.

long range dipole-dipole interactions. Sharma[49-53] has made several calculations of the energy transition rates for dipole and multiple coupling, and has shown that the temperature dependence of the transitions may differ markedly from the results that SSH theory predicts. According to Hancock and Smith[66], calculations for CO-CO based on a model similar to Sharma's have been performed by Morley and Smith, and will be published later. Jeffers and Kelley[67] have also recently submitted results of calculations based on both long range and short range interactions. As more reliable data becomes available, it will, of course, be possible to make improvements in the kinetic model for CO. At the present time, the SSH theory is employed, with the calculations to be presented later to be based on Eq. (3.44) and (3.45) for reasonable values of $P_{10\rightarrow 01}$, etc.

3.5 General Discussion. The vibrational levels of A and B are strongly coupled among themselves, and to each other, through the V-V-T exchange collisions. The situation that will result for the population distribution in the steady state will depend, as the master equation (3.16) indicates, upon the relative importance of many different pumping, relaxation, and cross-relaxation rates. In this section, a somewhat qualitative discussion of the molecular kinetics will be given, with the results of computer calculations to be presented subsequently. In spirit, the discussion here will follow the same approach adopted above for the simple model of the two interacting 2-level systems: viz., if any term R_r^i in Eq. (3.1b) for two coupled diatomic species A and B is dominant (with all remaining terms negligible relative to R_r^i), then $R_r^i = 0$ will be the most important condition for determining the form of the equilibrium population distribution.

a) V-T Collisions. If V-T collisions are dominant, the largest term in Eq. (3.1b) will be $R_r^{VT}(A^\dagger, A)$ or $R_r^{VT}(A^\dagger, B)$ or both. If all other rates are neglected in comparison, then the equilibrium vibrational distribution will

be defined by the set of equations

$$(nP_{r+1\to r} + NQ_{r+1\to r})\,(n_{r+1} - e^{-\left(\frac{E_{r+1} - E_r}{kT}\right)} n_r)$$

$$= (nP_{r\to r-1} + NQ_{r\to r-1})\,(n_r - e^{-\left(\frac{E_r - E_{r-1}}{kT}\right)} n_{r-1}). \tag{3.46}$$

For r = 0, only one term enters, viz.,

$$(nP_{1\to 0} + NQ_{1\to 0})\,(n_1 - e^{-\frac{E_1}{kT}} n_o) = 0. \tag{3.47}$$

Thus, the vibrational distribution becomes, under this limiting condition,

$$n_r = n_o e^{-E_r/kT}. \tag{3.48}$$

I.e., the vibrational levels achieve thermal equilibrium at the wall temperature T. Since V-T rates increase with quantum level (both because of the larger transition matrix element, and the smaller amount of energy ΔE that is exchanged with translation), these processes have a cooling effect upon the higher levels.

b) Electron Collisions. If the electron pumping rate R_r^e, given by Eq. (3.18), is the dominant term in Eq. (3.1b), then the population distribution will be determined mainly by setting $R_r^e = 0$, which leads to

$$n_r = n_o \exp(-E_r/kT_e).$$

That is, if electron collision rates are such that other relaxation and cross-relaxation mechanisms are negligible in comparison, then the vibrational levels will be raised to a temperature $\sim T_e$.

c) V-V-T Processes. In the case of V-V-T processes, each set of levels (of both systems A, B) is in a situation where it attempts to equilibrate with itself, and each set is in communication with the other. If V-V-T processes of the type $A^\dagger + A \rightleftharpoons A^\dagger + A^\dagger$ dominate the steady state for species A, and all other mechanisms (including $A^\dagger + B^\dagger \rightleftharpoons A^\dagger + B^\dagger$) are negligible, then the equilibrium state for the vibrational levels of A is defined by $R_r^{VVT}(A^\dagger, A^\dagger) = 0$:

$$\sum_s P_{r+1,\, s-1 \to r,\, s} \left[n_{r+1} n_{s-1} - \exp\left(- \frac{E_{r+1} - E_r + E_{s-1} - E_s}{kT} \right) n_r n_s \right]$$

$$= \sum_s P_{r,\, s \to r-1,\, s+1} \left[n_r n_s - \exp\left(- \frac{E_r - E_{r-1} + E_s - E_{s+1}}{kT} \right) n_{r-1} n_{s+1} \right] \qquad (3.49)$$

It can be verified by direct substitution that a solution to this equation is given by

$$n_r = n_o e^{-r\gamma} \exp(-E_r/kT), \qquad (3.50)$$

where γ is a single parameter for all of the energy levels r(r = 0, 1, 2...). Likewise, if V-V-T processes for species B dominate all other (including even V-V-T collisions of the type $B^\dagger + A \rightleftharpoons B^\dagger + A^\dagger$), then the distribution of populations N_R will be

$$N_R = N_o e^{-R\Gamma} \exp(-F_R/kT). \qquad (3.51)$$

In general, γ need not equal Γ, since the two systems equilibrate independently. If vibrational temperatures θ_r for each level r of

species A are defined by

$$n_r = n_o \exp(-E_r/k\theta_r), \tag{3.52}$$

then

$$\frac{E_r}{k\theta_r} = \frac{E_r}{kT} + r\gamma. \tag{3.53}$$

For r = 1, we get

$$\gamma = \frac{E_1}{k\theta_1} - \frac{E_1}{kT}, \tag{3.54}$$

so that

$$\frac{\theta_r}{T} = \left[\frac{rE_1T}{E_r\theta_1} - \left(\frac{rE_1}{E_r} - 1\right)\right]^{-1}. \tag{3.55}$$

The distribution function (3.50) becomes

$$n_r = n_o \exp\left(-\frac{rE_1}{k\theta_1}\right) \exp\left(\frac{rE_1 - E_r}{kT}\right). \tag{3.56}$$

Clearly, if the levels r describe harmonic oscillators, then $E_r = rE_1$, and the distribution of vibrational levels will be Boltzmann, with some temperature θ, that characterizes the entire set of levels. Likewise for species B. We shall assume for the moment that each species A, B is described by a harmonic oscillator, since it will then be possible to discuss the effects of V-V-T dominance in terms of the convenient qualitative concept of a single vibrational temperature for each species.

Then

$$\gamma = \frac{E_1}{k\theta} - \frac{E_1}{kT}, \tag{3.57a}$$

$$\Gamma = \frac{F_1}{k} - \frac{F_1}{kT}, \tag{3.57b}$$

and

$$n_r = n_o \exp(-rE_1/k\theta), \tag{3.58a}$$

$$N_R = N_o \exp(-RF_1/k\Theta). \tag{3.58b}$$

The result (3.57) was obtained by assuming that V-V-T collisions between A and B of the type (3.21b) are negligible compared to V-V-T collisions of the type (3.21a, c). This would typically be the case if the levels of species B do not have a good resonance match with those of species A, since V-V-T collision rates drop rapidly with an increase in the energy defect that must be exchanged with the translational mode. In general, therefore, the vibrational temperature θ and Θ attained by the levels of A and B under a dominance of V-V-T collisions of types (3.21a, c) would not be equal.

Alternatively, if we assume that all V-V-T processes have rates of the same order of magnitude, then the equilibrium distribution attained by the set of levels of A in a steady state dominated by exchange collisions will be determined instead from

$$R_r^{VVT}(A^\dagger, A^\dagger) + R_r^{VVT}(A^\dagger, B^\dagger) = 0 \tag{3.59}$$

It can be shown that, under this circumstance, the solution for the level populations n_r and N_R of the two species is given by

$$n_r = n_o e^{-r\gamma} \exp\left(-\frac{E_r}{kT}\right), \tag{3.60a}$$

$$N_R = N_0 e^{-R\gamma} \exp\left(-\frac{F_R}{kT}\right), \tag{3.60b}$$

where γ is the <u>same</u> for each set of levels. Thus for harmonic oscillators, if all the V-V-T rates are comparable, the solutions (3.58) give the population distributions subject to the constraint

$$\frac{E_1}{\theta} - \frac{E_1 - F_1}{T} - \frac{F_1}{\Theta} = 0. \tag{3.61}$$

This equation is obtained from (3.57) by setting $\gamma = \Gamma$, and is identical to Eq. (3.37), which was derived earlier for the simple two-level model.

In paragraphs a), b), and c) above, it has been shown how the vibrational levels can achieve quire different distributions, depending upon which of the relative rates for several competing mechanisms is dominant. In actual practice, the equilibrium distribution is determined by an interplay of these processes, and typically, vibrational temperatures of $\lesssim 10,000^{\circ}K$ are attained. For the higher quantum levels, say $r \gtrsim 25$, V-T processes dominate V-V-T processes, and the upper levels can be expected to reach lower local temperatures by increased contact with the wall reservoir.

It was pointed out previously that, due to the smaller energy spacing between the upper vibrational levels of CO, the fast V-V-T cross relaxation processes can excite the upper levels to even higher vibrational temperatures by the

process of "anharmonic pumping." N_2 has levels which are slightly greater than those for CO, and can, therefore, pump the CO levels. Since N_2 does not have a very fast V-T relaxation rate, it can serve as an efficient reservoir for storing vibrational energy, which is subsequently transferred to CO. (Addition of N_2 to an electric discharge system also has important consequences for the plasma characteristics, which will be discussed later.)

Further interesting conclusions can also be obtained by considering rates other than the dominant ones for the system. For example, it is possible to illustrate the effects of N_2 and CO V-V pumping by showing how a "vibrationally cold" system can transfer energy to a "vibrationally hot" one, which may seem paradoxical thermodynamically. Consider the situation where the two species A, B attain quasi-Boltzmann equilibrium distributions separately, with the V-V-T exchange collisions between A and B negligible. (I.e., suppose that, perhaps because of severe energy defect, the off-resonance rates for cross-relaxation between systems A and B are much slower.) Then on a short time scale, the vibrational populations attained by the two species will be expressed by (3.50) and (3.51), where γ and Γ are not, in general, equal. On a longer time scale, the two systems will interact, with the rate of energy change in species A due to V-V-T exchange with B given by

$$\sum_r E_r R_r {}^{VVT}(A^\dagger, B^\dagger) =$$

$$\sum_{R,r} Q_{r+1,R-1\to r,R}\left[n_{r+1}N_{R-1} - \exp\left(-\frac{E_{r+1}-E_r+F_{R-1}-F_R}{kT}\right)n_r N_R\right]E_r$$

$$-\sum_{R,r} E_r Q_{r,R\to r-1,R+1}\left[n_r N_R - \exp\left(-\frac{E_r-E_{r-1}+F_R-F_{R+1}}{kT}\right)n_{r-1}N_{R+1}\right] \qquad (3.62)$$

Assume, for simplicity, that the rates are determined by a dipole-dipole interaction between harmonic oscillators, and are given by $Q_{r, R\to r-1, R+1} \sim r(R+1)Q_{1, 0\to 0, 1}$.

Eq. (3.62) becomes, upon substituting the quasi-steady distributions (3.50), (3.51)

$$E_1 \sum_r rR_r^{VVT}(A^\dagger, B^\dagger) = E_1 Q_{1, 0\to 0, 1} e^{F_1/kT}(e^{\gamma} - e^{\Gamma}) \sum_R RN_R \sum_r rn_r \qquad (3.63)$$

If this expression is negative, then energy is being transferred from A to B through the V-V-T exchange mechanism of Eq. (3.21b). This condition will, therefore, occur when $\Gamma > \gamma$, i.e., for

$$\frac{E_1}{\theta} - \frac{F_1}{\Theta} < \frac{E_1 - F_1}{T} \quad \text{(energy flow: A} \to \text{B)} \qquad (3.64)$$

Alternatively, if $\Gamma < \gamma$, the expression (3.63) is positive, indicating that energy is being supplied to system A by system B:

$$\frac{E_1}{\theta} - \frac{F_1}{\Theta} > \frac{E_1 - F_1}{T} \quad \text{(energy flow: B} \to \text{A)} \qquad (3.65)$$

Figure 3.6 shows a schematic plot of the hyperbola defined by $(E_1/\theta) - (F_1/\Theta) = (E_1 - F_1)/T$ for the case $E_1 < F_1$. In the region above this curve, energy exchange is from A to B, while in the region below, it is from B to A. The straight line corresponds to equal vibrational temperatures, $\theta = \Theta$. Note that, in the shaded region of the curve $\theta > \Theta$ but the energy flow is from B → A. I.e., under this unique situation, energy can flow from the "colder" system to the "hotter" system.

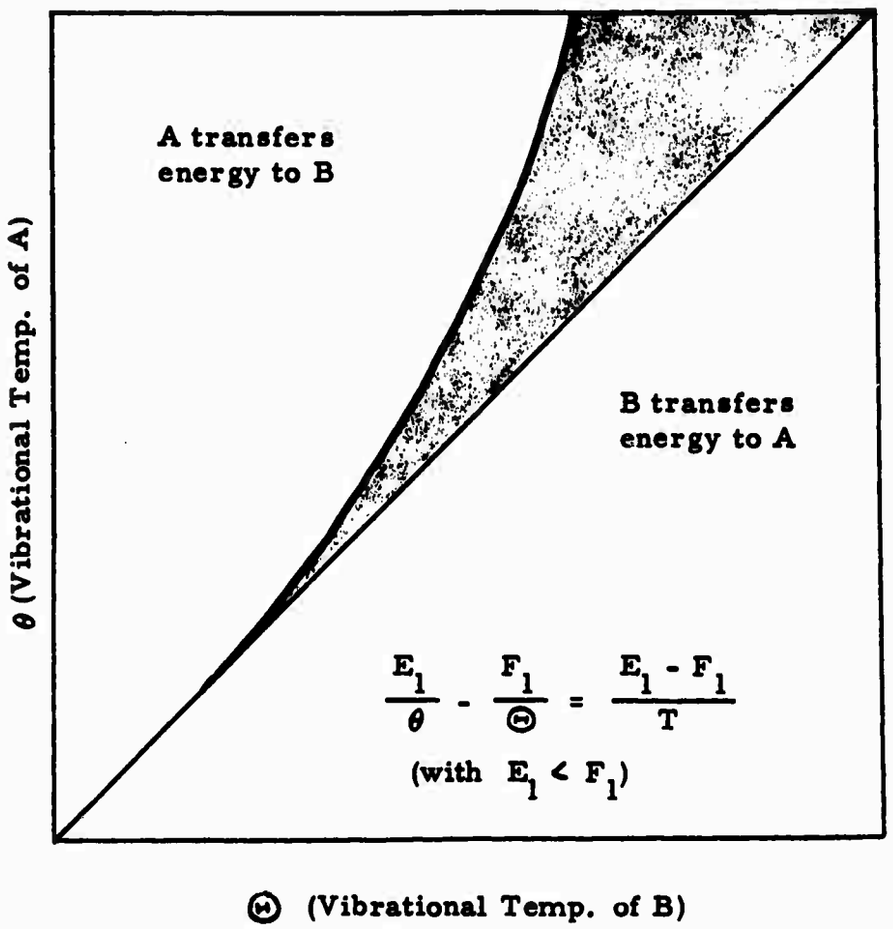

Figure 3.6. V-V-T cross relaxation for two harmonic diatomic species A and B, with energy spacings E_1 and F_1, and vibrational temperatures θ and Θ, respectively, The shaded region corresponds to the case $\theta > \Theta$, and thus represents a situation where the flow of energy (B→A) is from the "colder" to the "hotter" system. (Adapted from Reference 35).

3.6 Computer Calculations and Numerical Results. The computer program that has been developed to analyze the steady state is capable of accepting all of the above inputs, for arbitrary pressures, gas mixtures, temperatures, etc. At the present time, the populations of a second diatomic species such as N_2 (if present) are treated parametrically as specified input, rather than as independent variables to be included in a second coupled set of master equations. (However, if and when it becomes necessary, the program can be easily extended to treat the populations of both of two interacting diatomic species on an equal basis.) The calculation can be carried out for an arbitrary number of CO levels (in practice, usually ≤ 40 is sufficient), and will produce all of the relevant information needed for predicting the characteristics of the laser amplifier medium. The output produced consists of the vibrational population and temperature distribution, the rates of energy transfer through the competing mechanisms present, laser gains, saturation intensities, stimulated energy extraction, and quantum efficiency. Thus, it is possible to obtain small-signal or saturated gains by appropriate input intensities for either single or multiline operation.

3.6.1 Parametric Calculations. In order to perform a preliminary check on the computer program, some initial special cases for which the solution is known in advance were run as part of the debugging procedure. As was pointed out in Section 3.5, turning off all processes except for the electron pumping should result in a distribution for which all of the vibrational temperatures are equal to T_e, and this result was correctly verified. Alternatively, by turning off everything but V-T and V-V-T relaxation, the system should approach a steady state for which all vibrational temperatures equilibrate to the wall temperature T, and this was also confirmed. By turning off the anharmonicity of the diatomic species, an equilibrium distribution whose vibrational temperatures satisfy relation (3.61) should result, providing other processes are negligible, and this also was correctly obtained.

To assess the effects of a variation of parameters on the resulting population distribution in the CO laser, a variety of comparative calculations were performed for a low pressure system, using reasonable assumptions for the relaxation rates and values for electron pumping rates that would be typical of an electrically excited longitudinal discharge configuration. In order to construct a reliable model, it will be necessary to perform measurements of the small signal gain coefficient for several controlled sets of operating parameters, and experimental work toward this objective is now in progress.

In Figure 3.7 , the effects of increasing partial pressure of CO illustrate how anharmonic pumping can cause the excitation to higher v levels. From a different point of view, Figure 3.8 shows how a variation in the rate $P_{10\rightarrow 01}$ of V-V-T cross-relaxation can have a profound effect on the resulting vibrational distribution. In Figure 3.9 the interaction length ℓ, which is critical parameter which measures how fast the off-resonance V-V-T rates decrease, has been varied. Figure 3.10 indicates the effect of increasing the electron number density to increase the pumping rate. Figure 3.11 corresponds to addition of N_2, whose vibrational temperature is parametrically fixed at two different constant temperatures.

3.6. Energy Transfer and Quantum Efficiency. Calculation of the rates of energy transfer for all of the kinetic and radiative mechanisms present in the CO laser amplifier medium are important for predicting detailed rates of heating, electrical energy input, single and multiline extraction capacity, and quantum efficiency. The rates of V-T and V-V-T heating are important parameters for design considerations of high power CO laser devices. The quantum efficiency, which can be defined as the percentage

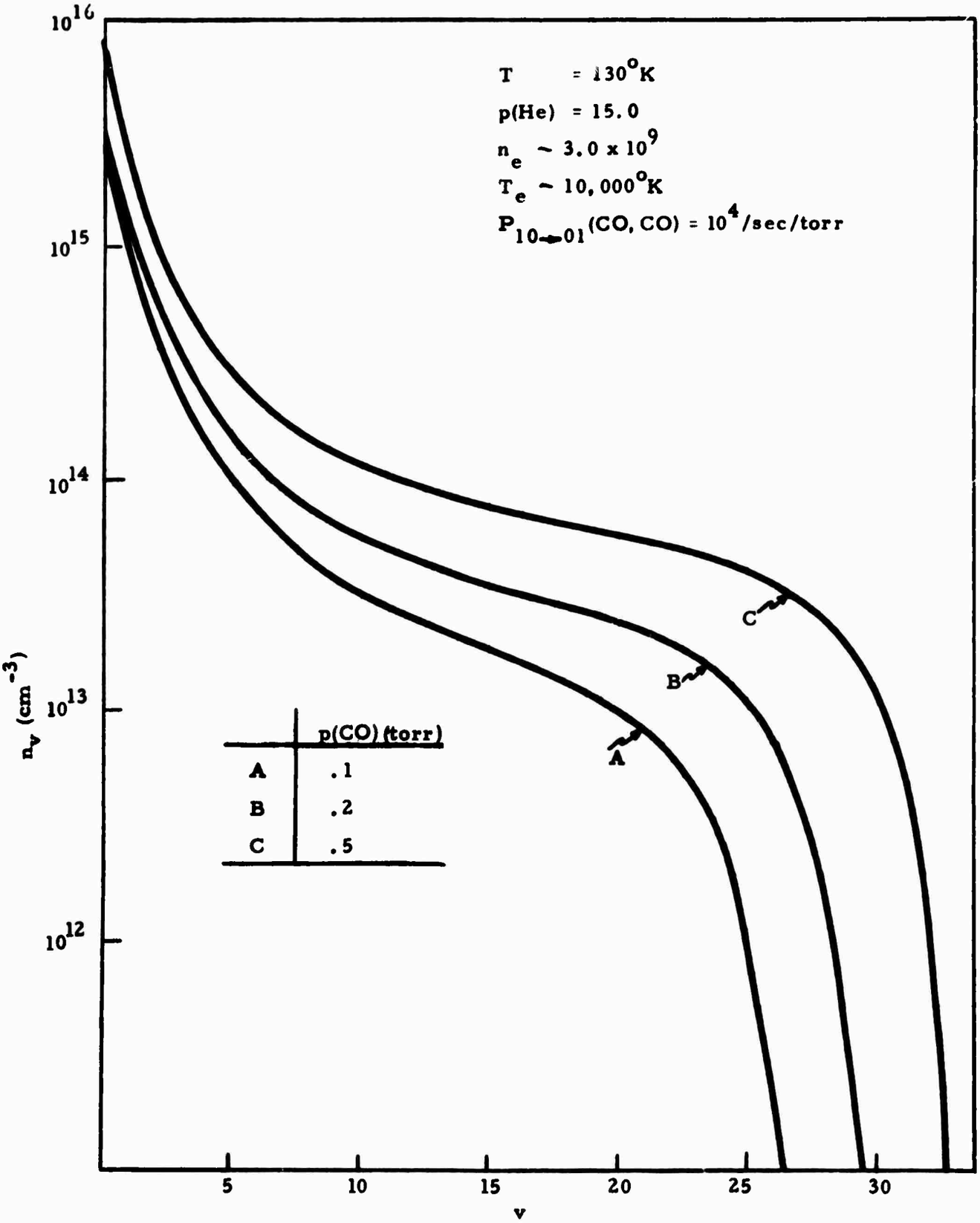

Figure 3.7. Effect of Partial Pressure on CO Vibrational Population Distribution.

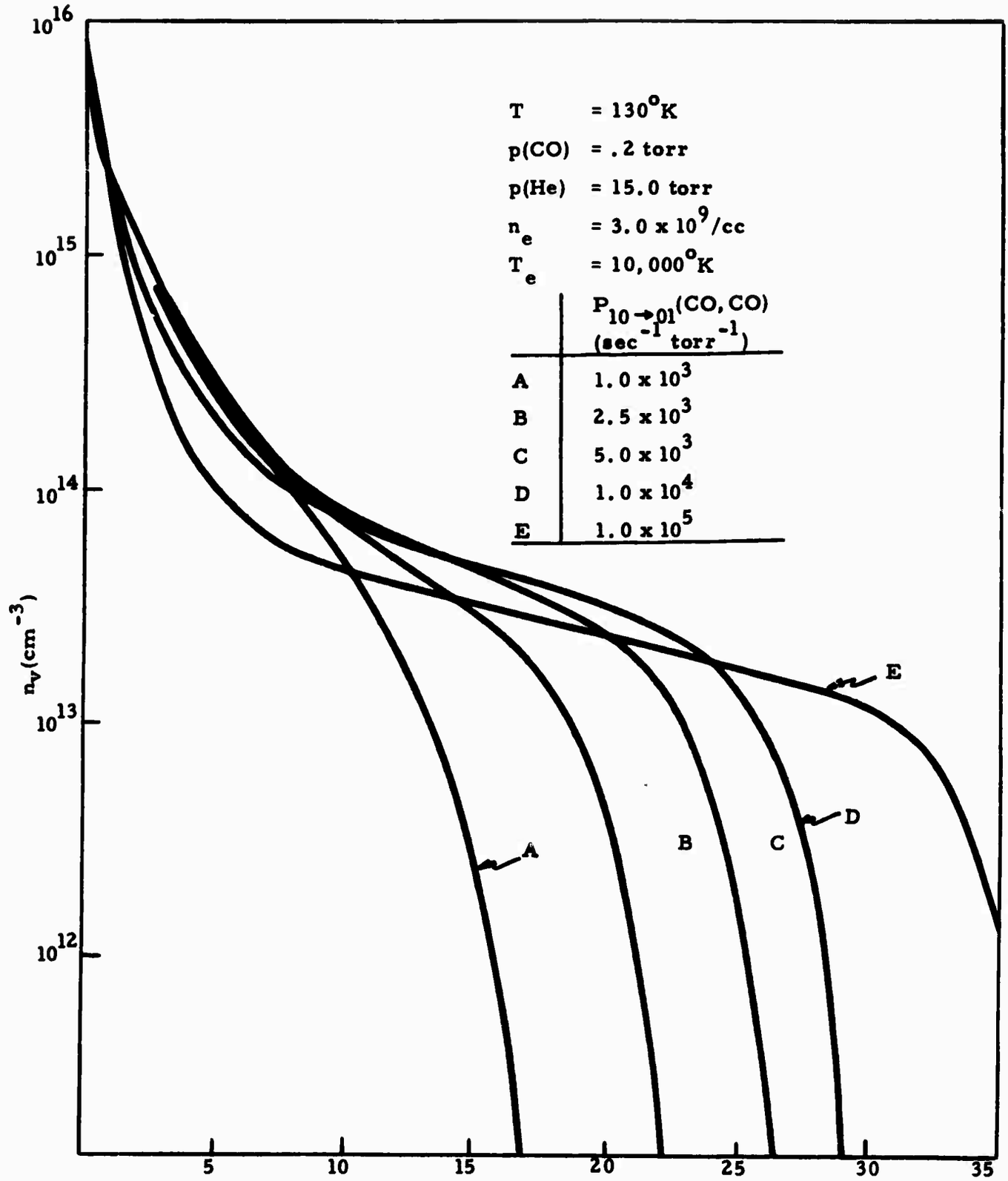

Figure 3.8. Effect of V-V-T Collisional Cross-Relaxation Rate $P_{10 \rightarrow 01}$ on CO Vibrational Population Distribution.

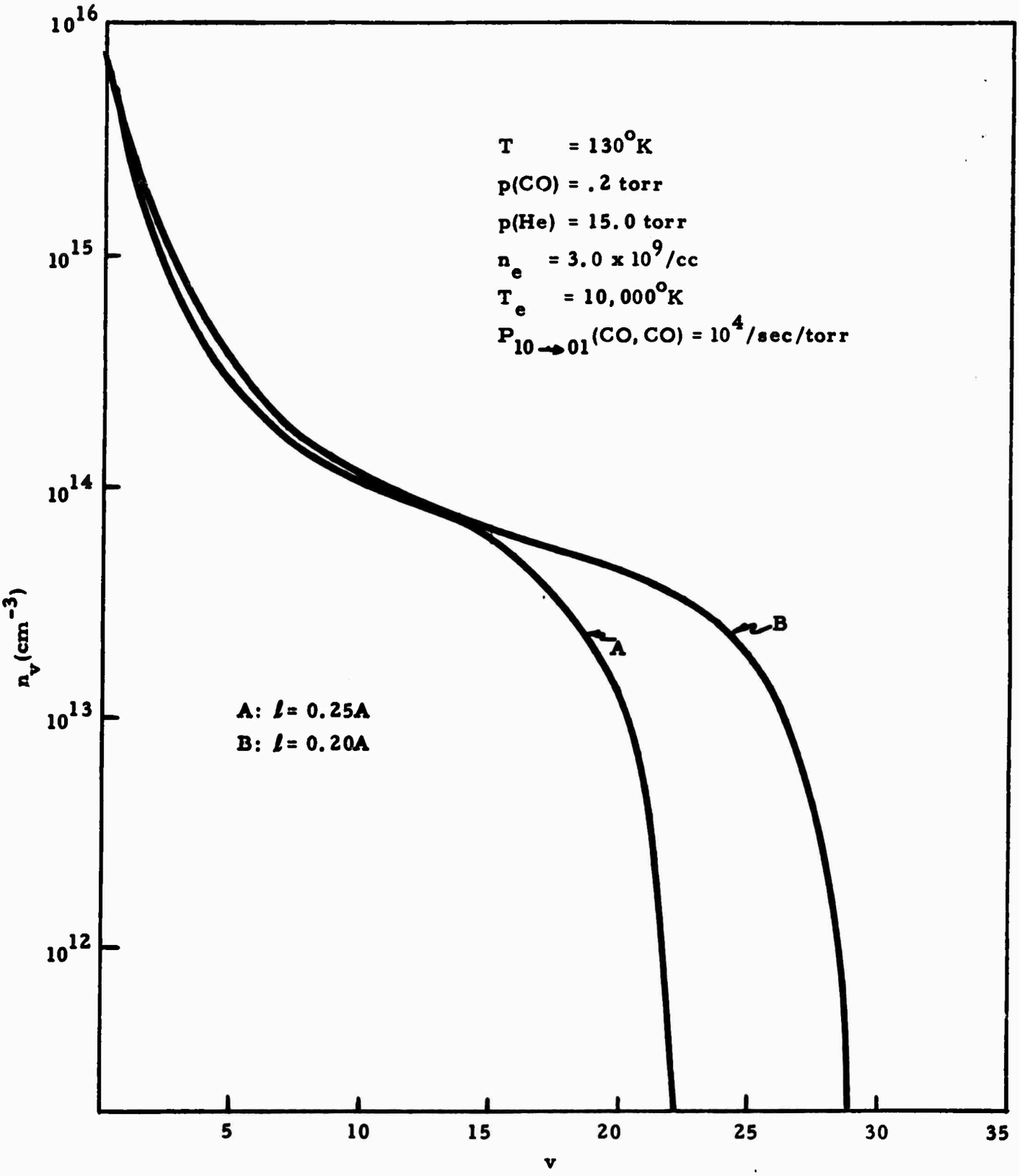

Figure 3.9. Effect of Variation of Interaction Length ℓ of SSH theory on CO Vibrational Population Distribution.

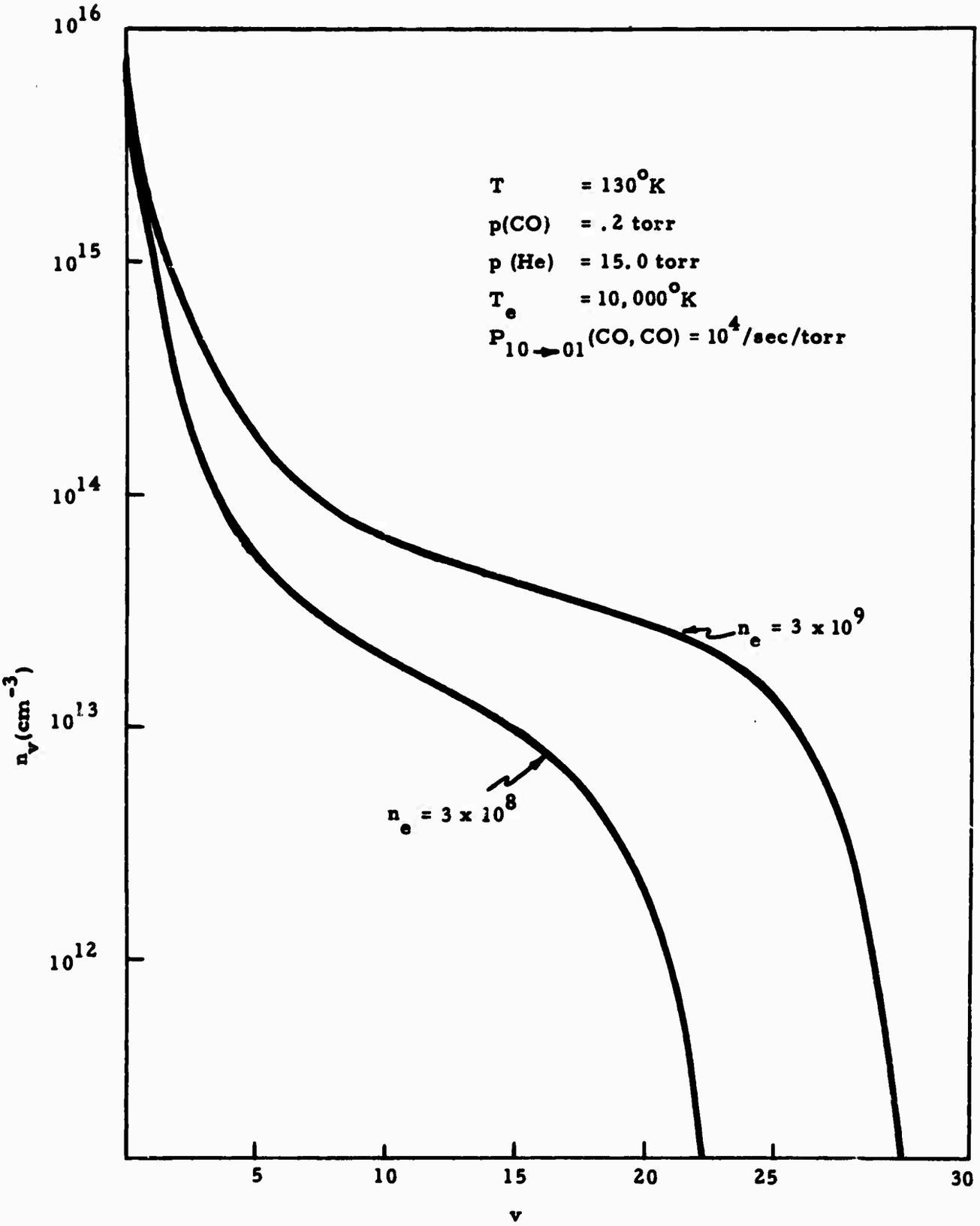

Figure 3.10. Effect of Electron Pumping Rate on CO Vibrational Population Distribution.

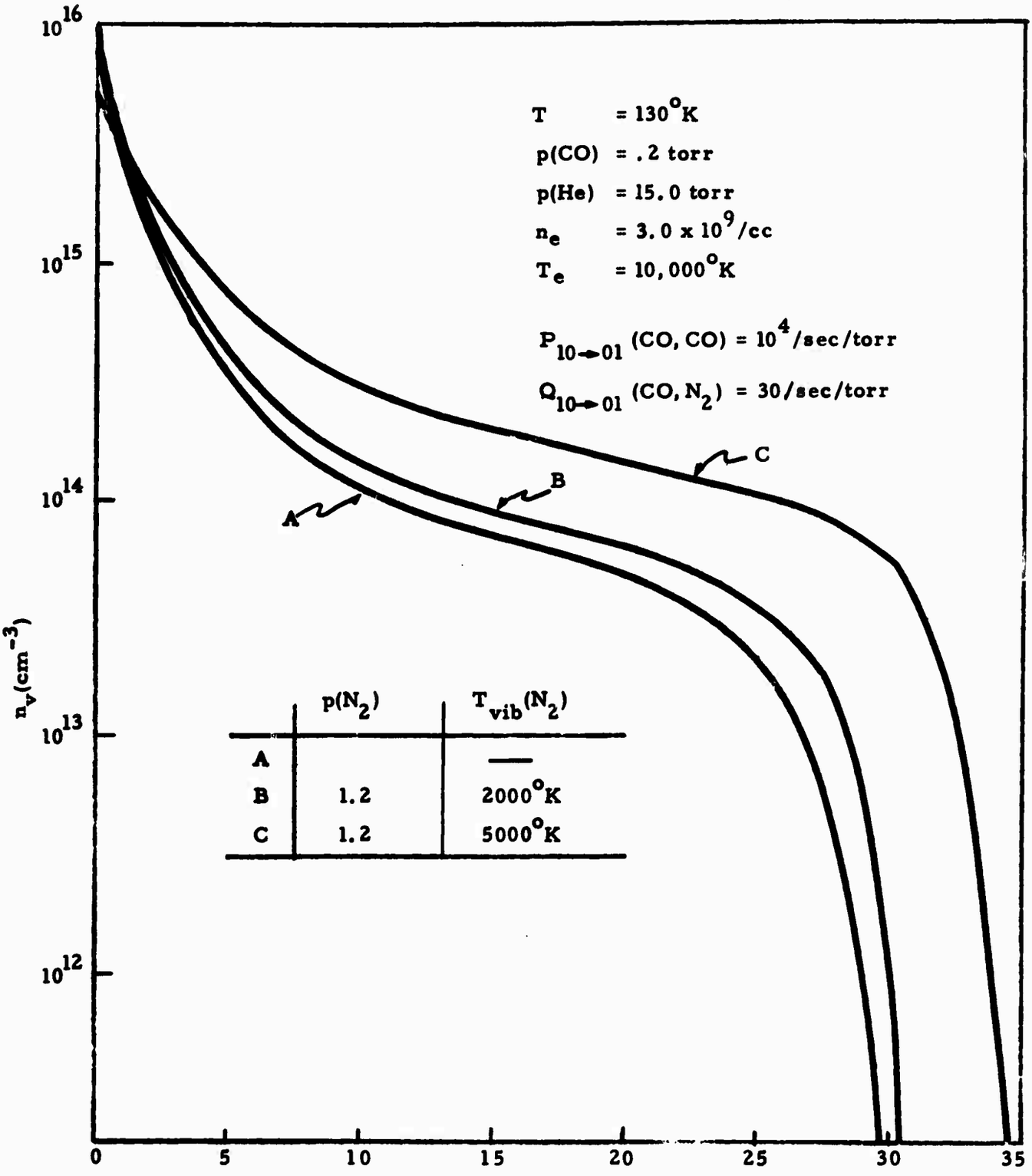

	$p(N_2)$	$T_{vib}(N_2)$
A		—
B	1.2	2000°K
C	1.2	5000°K

Figure 3.11. Effect of N_2 (included parametrically at fixed vibrational temperature) on CO Population Distribution.

of coherent radiation extracted for a given electrical input, is a function of the input line intensities and can be enhanced (approaching the theoretical limit of 100%) if sufficient numbers of lines with intensities near and above saturation are included. Saturation intensities for single or multiline operation can be calculated, as well as volumetric extraction energies, for each line present. The steady-state rates of energy transfer for each of the process considered in Eq. (2.16) are summarized below:

a. Electrical Energy Input. The rate of electrical excitation is given by

$$\dot{U}^{e} = \sum_{r,s} E_r [n_r R^{e}_{r \to s} - n_s R^{e}_{s \to r}] \qquad (3.66)$$

b. V-V-T Heating. For the process $CO(r) + CO(s-1) \to CO(r-1) + CO(s) + \Delta E_{r,s}$, where an amount of energy $\Delta E_{r,s} = (E_r - E_{r-1}) - (E_s - E_{s-1})$ has been transferred to kinetic energy, the rate of V-V-T heating due to the anharmonic defect is given by

$$\dot{U}_1^{VV} = \sum_{r,s} (E_r - E_{r-1})[n_r n_{s-1} P_{r,s-1 \to r-1,s} - n_{r-1} n_s P_{r-1,s \to r,s-1}] \qquad (3.67)$$

If there is another diatomic species B in the gas mixture, then the rate of heat generation for the process $CO(r) + B(R-1) \to CO(r-1) + B(R) + \Delta E_{r,R}$ where $\Delta E_{r,R} = (E_r - E_{r-1}) - (F_R - F_{R-1})$, is given by

$$\dot{U}_2^{VV} = \sum_{r,R} (E_r - E_{r-1} - F_R + F_{R-1}) [n_r N_{R-1} Q_{r,R-1 \to r-1,R} - n_{r-1} N_R Q_{r-1,R \to r,R-1}] \qquad (3.68)$$

c. V-T Heating. For V-T collisional relaxation processes such as $CO(r) + X \rightarrow CO(r-1) + X + \Delta E_r$, where $\Delta E_r = E_r - E_{r-1}$, the rate of V-T heating is given by

$$\dot{U}^{VT} = \sum_r (E_r - E_{r-1}) [n_r P_{r \rightarrow r-1} - n_{r-1} P_{r-1 \rightarrow r}] N_X \qquad (3.69)$$

d. Vibrational Energy Transfer. For a situation where there is a second diatomic gas B included in the mixture, there will be a transfer of energy from one vibrational species to the other. The rate of energy flow from B to CO by the process $CO(r) + B(R-1) \rightarrow CO(r-1) + B(R) + \Delta E_{r,R}$ is given by

$$\dot{U}^{B \rightarrow CO} = - \sum_{r,R} (F_R - F_{R-1}) [n_r N_{R-1} Q_{r, R-1 \rightarrow r-1, R} - n_{r-1} N_R Q_{r-1, R \rightarrow r, R-1}] \qquad (3.70)$$

or equivalently, the transfer of vibrational energy from CO to B is $\dot{U}^{CO \rightarrow B} = - \dot{U}^{B \rightarrow CO}$. It is easy to verify that $\dot{U}^{CO \rightarrow B} + \dot{U}_2^{VV}$ represents the total loss of vibrational energy from CO in a V-V-T exchange collision with B.

e. Spontaneous Radiation. Spontaneous radiation processes represent a pure loss mechanism, and thus, their presence limits the total attainable quantum efficiency to a value less than 100%. For the $\Delta v = 1$ and 2 decay processes considered in the present model, the rate of radiative energy loss is

$$\dot{U}^{sp} = \sum_r n_r (E_r - E_{r-1}) A_{r \rightarrow r-1} + \sum_r n_r (E_r - E_{r-2}) A_{r \rightarrow r-2} \qquad (3.71)$$

f. Stimulated Emission. If stimulated emission processes are important, i.e., if the intensities of the input lines are comparable to or greater than the saturation parameters, the gains for these transitions will saturate.

The extraction power per unit volume will be given by

$$dI/dx = \alpha(I)I \tag{3.72}$$

where I is the input intensity, and $\alpha(I)$ is the saturated gain. The total stimulated extraction from the amplifier medium will be a sum of terms (3.72) for all of the input laser lines present. As an alternative calculation, the total rate of energy transferred to coherent amplified radiation would be given by

$$\dot{U}^{stim} = \sum_r (E_r - E_{r-1})[n_r S_{r \to r-1} - n_{r-1} S_{r-1 \to r}] \tag{3.73}$$

From an initial calculation of the unsaturated amplifier characteristics, for which no stimulated emission processes are included, the small-signal gains can be obtained. Saturation intensities can then be calculated for single or multiline operation from an asymptotic limit,

$$I_s = \lim_{I \to \infty} \alpha(I)\, I/\alpha_o \tag{3.74}$$

where $\alpha(I)$ and α_o are saturated and small-signal gains for any desired transition. In practice, this involves merely that an input value be used for I which is very large (e.g., 10^8 watt/cm^2). The complete generality available for the computer code input description makes it possible to calculate many interesting performance characteristics of the amplifier medium -- e.g., the cross-saturation effects that determine the energy available for extraction/cm^3 on one transition in a situation where other lines are simultaneously being driven to saturation. Knowledge of this sort is extremely important for extrapolating design considerations to a high energy CO laser system, where it is imperative to extract as much useful energy as possible from several simultaneous transitions with desirable characteristics.

In the steady state, the rate of electrical energy input into the vibrational levels must be balanced by all of the energy loss mechanisms which are present. For the case of an unsaturated amplifier, for which all stimulated emission processes are neglected, the dominant mechanism for dissipating the input power is by means of V-V-T heating which results from the anharmonic defect. Since the V-V-T rates as well as the anharmonic defect increase for larger v levels, the population distribution will be pumped up far enough that heating rates can balance electrical excitation rates. Thus, if the electrical pumping is increased, the population distribution will be extended further up the vibrational ladder. When external lines are introduced into the amplifier, with intensities comparable to or greater than saturation, stimulated emission processes enter into the steady state energy balance condition, so that excitation energy is dissipated both by radiative extraction and V-V-T heating processes. In order to maintain the population distribution, of course, V-V-T heating is always present, since the vibrational exchange collisions are the dominant process for the molecular kinetics. Thus, V-V-T heating effects limit the attainable quantum efficiency of conversion of electrical energy to coherent radiation, and can also present difficult heating problems for high power devices. By operating the amplifier for low v-bands, the quantum efficiency is best, and it can be improved by saturated extraction on several v-bands, Preliminary calculations indicate the possibility of achieving quantum efficiencies of 70 - 90% for high pressure CO laser devices.

It has been observed theoretically that the introduction of several P(J) lines corresponding to a single v-band into a CO laser amplifier (assuming that the assumption of rapid rotational cross relaxation is valid) can result in interesting energy transfer possibilities when the incident line intensities

are comparable to or above the saturation intensity. Exploitation of this fact may provide the possibility for rotational line selection, since it is possible to adjust the characteristics of the amplifier medium in such a way that energy from one rotational line is completely transferred to another. The line selection device could be operated at low enough pressures to insure that the lines provided by an oscillator enter with intensities above saturation. Indications of the calculations are that the transfer can be relatively efficient, and that heating difficulties are relatively modest, which would appear to be advantageous for practical control of such parameters as temperature. Basically, this is analogous to a parametric effect, in which the CO medium is pumped by one resonant transition with resulting enhanced characteristics for another.

3.6.3 Numerical Technique. The system of molecular kinetic equations for the steady state is basically a set of simultaneous quadratic algebraic equations. If the variables are regarded as being the relative populations $x_i = n_i/n$, where n is the total CO population, then for an M-level approximation there will be a system of (M+1) equations,

$$
\begin{aligned}
f_1(\vec{x}) &= \sum_{jk} A_{1,jk}\, x_j x_k + \sum_k B_{1,k} x_k = 0 \\
f_2(\vec{x}) &= \sum_{jk} A_{2,jk}\, x_j x_k + \sum_k B_{2,k} x_k = 0 \\
&\vdots \\
f_i(\vec{x}) &= \sum_{jk} A_{i,jk}\, x_j x_k + \sum_k B_{i,k} x_k = 0 \\
&\vdots \\
f_M(\vec{x}) &= \sum_{jk} A_{M,jk}\, x_j x_k + \sum_k B_{M,k} x_k = 0 \\
f_{M+1}(\vec{x}) &= (x_o + x_1 + x_2 + \ldots x_M) - 1 = 0
\end{aligned}
\qquad (3.75)
$$

where $f_1, f_2, \ldots f_M$ are the rates for levels 1, 2, ..., M, and the (M+1) st equation expresses total particle conservation. $\vec{x} = (x_1, x_2, \ldots, x_M, x_o)^T$ is an (M+1) dimension column vector, and if a vector $\vec{f} = (f_1, f_2, \ldots f_M, f_{M+1})^T$ is defined, the molecular kinetic equation can be written concisely as

$$\vec{f}(\vec{x}) = 0. \tag{3.75a}$$

The technique that was employed for solving this system of equations numerically is a generalization of the Newton-Raphson method[68] for solution of nonlinear equations. Define the (M+1) x (M+1) Jacobian matrix

$$J_{ij}(\vec{x}) = \partial f_i(\vec{x}) / \partial x_j. \tag{3.76}$$

If $\vec{x}^o$ is a guess for the solution vector $\vec{\alpha}$ which satisfies $\vec{f}(\vec{\alpha}) = 0$, then a "better" guess is given by the vector $\vec{x}^1$, defined by

$$\vec{x}^1 = \vec{x}^o - J(\vec{x}^o)^{-1} \cdot f(\vec{x}^o) \tag{3.77}$$

Starting with some initial guess vector $\vec{x}^o$, a sequence of vectors $\vec{x}^1, \vec{x}^2, \ldots \vec{x}^n$ is generated in this way, and successive iterations will usually converage to the solution $\vec{\alpha}$, generally with very minimal restrictive conditions. For the present set of equations with M = 40, this procedure typically required $\lesssim$10 iterations to produce a solution accurate to one part in 10^7 for all of the populations, and computation time on a CDC 6600 was about 60 sec. These characteristics correspond to very simple forms for the initial guess $\vec{x}^o$ (e.g., $\vec{x}^o = (0, 0, 0, \ldots 0, 1)^T$), and could probably be improved with a better starting point.

3.6.4 Transient Analysis. For situations where the steady state has not been attained, it is necessary to solve the simultaneous set of nonlinear first order differential equations, Eq. (3.1a), subject to a set of prescribed initial conditions. In that case, the theoretical analysis described in the preceding sections would have to be extended. However, the mode of operation for which such transient effects would be expected to play an important role would be a short pulse regime, where the time scale is typically less than (or comparable to) the fastest relaxation lifetimes that dominate the population distributions. For high pressure molecular gases, the fastest mechanisms that determine that distribution are the near-resonant VVT exchange collisions, with cross-relaxation rates typically of the order of $p\tau \sim 400$ μsec·torr. For a CO partial pressure p_{CO}, it would be expected that a transient analysis based on the set of differential equations would only be required for pulsed operation with times scales $\lesssim (p\tau)/p_{CO}$. Therefore, for long pulse or cw operation, it is to be expected that temporal effects could be treated in a quasi-static approximation, where parameters which are slowly varying functions of time (e.g., the kinetic temperature T(t) varies during a pulse) can be regarded as fixed values which determine, at any given time t, an instantaneously established steady-state population distribution. Thus, in the same spirit, quantities such as gain and saturation intensities will be quasi-steady, slowly varying functions of time during the pulse.

4.0 PLASMA CHARACTERISTICS AND ELECTRON KINETICS

The kinetic model described for calculation of the steady-state vibrational populations has assumed, for the present, that the distribution of electrons in the medium is a Boltzmann function at temperature T_e. In actual practice, this distribution can depart significantly from the Maxwell-Boltzmann form, and it would be an improvement to calculate its energy dependence more accurately. For the weakly ionized plasmas that are characteristic of electrical discharge laser systems (i.e., electron densities much less that neutral molecular densities) it is the inelastic vibrational and electronic excitation processes that dominate the kinetics of the electron gas. The dominant mechanism that determines the form of the electron distribution is collisions between electrons and molecules that result in vibrational or electronic state excitation. The effect of these inelastic collisions is to extract energy from the electrons as they are accelerated across the region of the applied electric field. The combined effect of the electric field and the inelastic collisions is to limit the electron drift velocity, which is determined by the value of (E/N) and the molecular gas composition. Since only low-energy electrons ($\sim$1-3 eV) are effective for vibrational excitation, it is desirable to tailor the (E/N) and the gas composition to optimally achieve this objective.

The structure of the electron distribution will typically reflect the structure of the electron-molecule energy exchange processes, and thus, it will depart most significantly from a Boltzmann in the energy regions where inelastic scattering cross-sections are appreciable. For low density plasmas with mean electron energies of a few eV or less, elastic electron scattering and inelastic electron-molecule rotational excitation have a

negligible effect on the determination of the distribution. Since the electrons for such low energy, weakly ionized plasmas have no mechanism for complete thermalization, a departure from a Boltzmann distribution is to be expected.

For the present situation, the electron kinetic problem involves the solution of the Boltzmann equation[69,70] for the energy distribution function that results for a given gas composition in the presence of an applied electric field E. In general, the solution of the Boltzmann equation is often a practical impossibility, since complete information about all of the collision processes is usually unavailable. However, for the gas constituents (e.g. CO, N_2, CO_2, He, Ar, Xe) and electron energy ranges ($\sim$ few eV) that are typical for molecular laser systems, reliable cross-sections for the important scattering processes have been measured experimentally.[29-31] Nighan et al[71-74] have carried out calculations for the electron energy distribution functions for various gas mixtures, based on the assumptions that the E/N of the plasma is low enough that the average electron energy is only a few eV, and that the electron density is low enough that the approximation of a weakly ionized plasma is valid. Figure 4.1 to 4.3, taken from Reference 71, 74 illustrate the significant departure from Boltzmann form that can result for the electron energy distribution under various conditions.

Knowledge of the electron energy distribution as a function of E/N and gas composition makes it possible to calculate the fractional amounts of electrical energy input that are deposited into each of the possible excitation modes present. The fractional amount of energy transferred to molecular vibrational states, in conjunction with the quantum extraction efficiency discussed previously, will then determine the total efficiency of conversion of electrical input to optical output power. Clearly, it is desirable to operate with

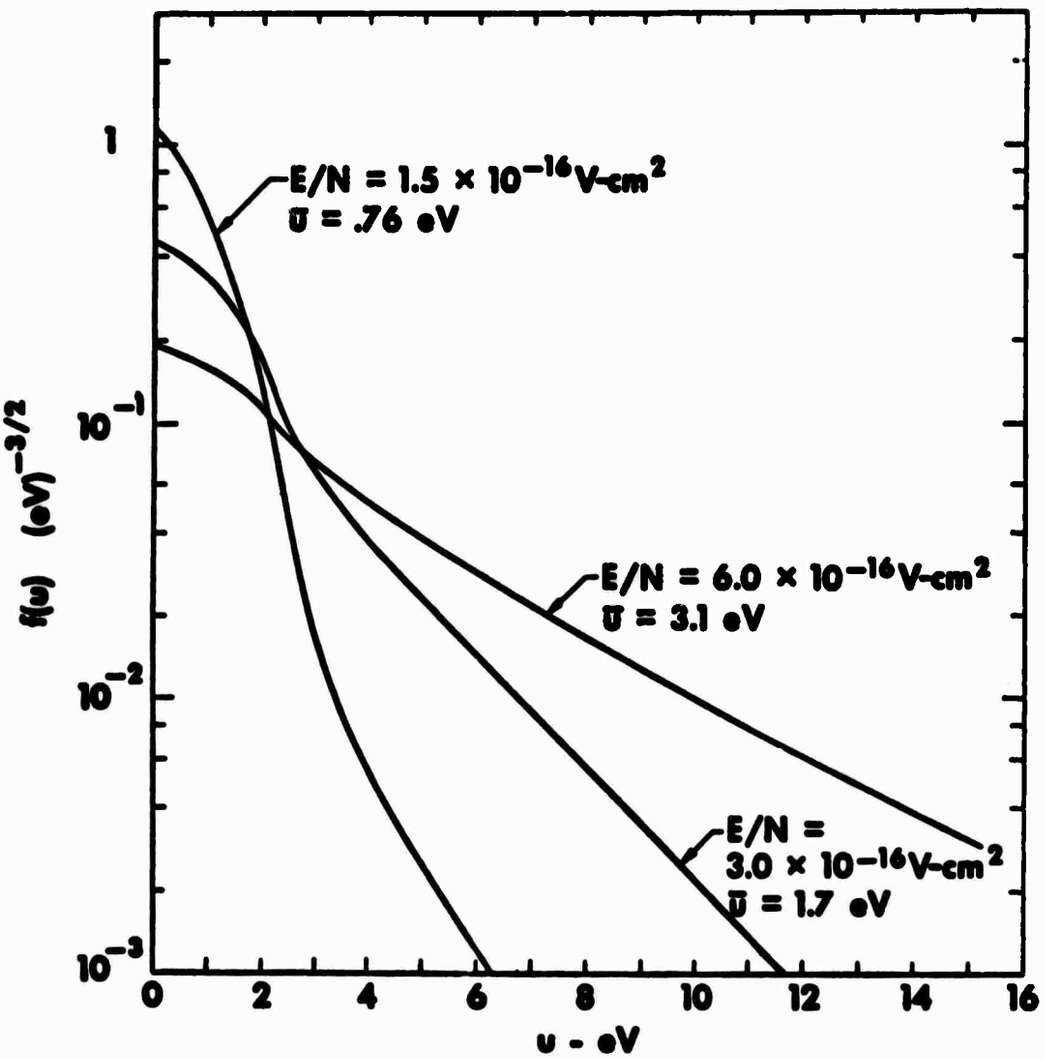

Figure 4.1. Calculated electron energy distributions for a CO_2-N_2-He gas mixture (1-1-8), taken from Reference 71.

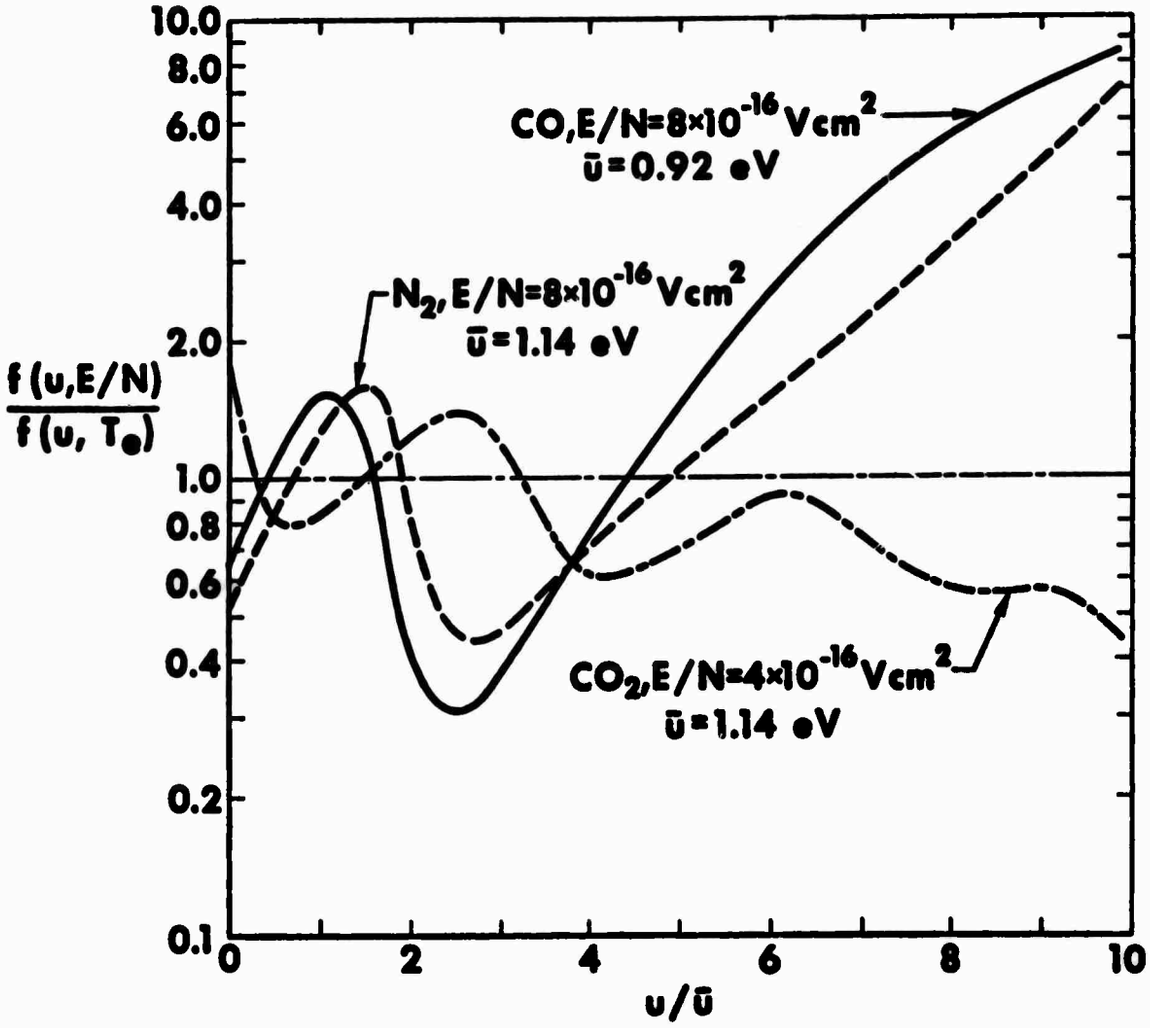

Figure 4.2. Comparison of calculated electron energy distribution functions with a Maxwellian for N_2, CO, and CO_2 (taken from Reference 71). This exhibits the significant departure from a Boltzmann distribution that can occur for a weakly ionized plasma.

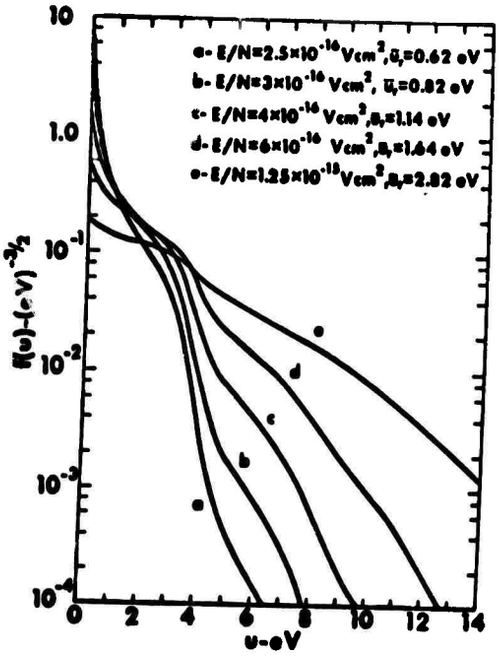

CO_2

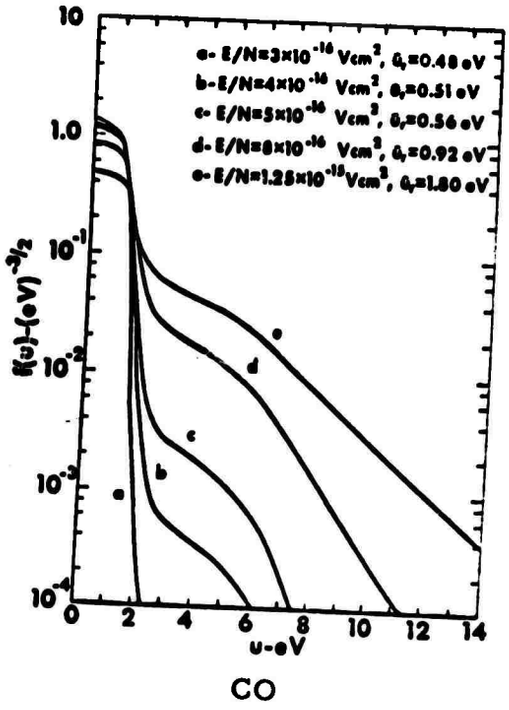

CO

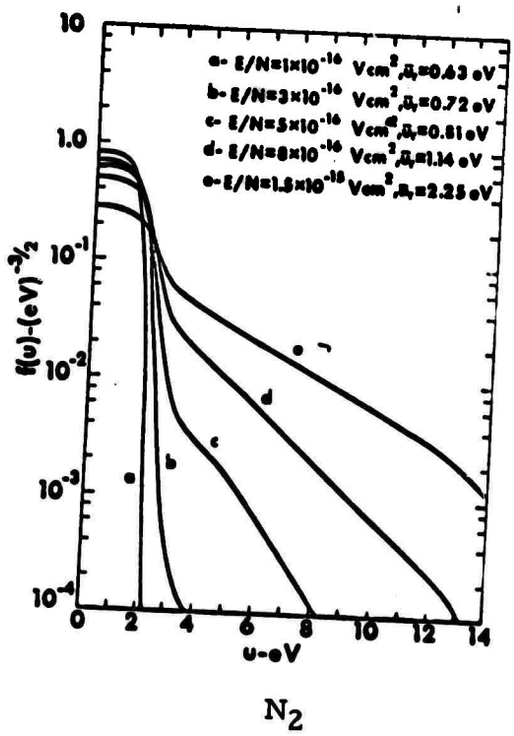

N_2

Figure 4. 3. Electron energy distribution functions for CO_2, CO, and N_2 for various E/N values, taken from Reference 74. (Note that $u^{1/2}f(u)$ corresponds to the distribution function as defined in this report).

discharge characteristics that will optimize the transfer of electrical energy to the vibrational levels, rather than to electronic or ionized states. This is a difficult objective to achieve for the conventional longitudinal electric discharge configurations that are usually employed for conventional CO and CO_2 lasers, since the electron distribution function must adjust itself in such a way that average electron energies are high enough to provide the ionization that is required to sustain the discharge. Thus, one of the ways that is often successfully employed for enhancing gas laser efficiencies is to optimize the mixture with gases that have a low ionization potential, such as Xe or Hg vapor[4,5]. Although plasma control by optimization of gas constitutents is a useful technique for improving laser operating characteristics, the degree of control that this can provide is usually very limited.

The optimum gas mixture for conventional CO lasers contains several other constituents in addition to CO. In a slowly flowing system He is well known to be beneficial for cooling the molecular kinetic temperature. The effect of Xe is to reduce the average electron energy by lowering the high energy tail of the electron energy distribution. Use of Xe is, therefore, a crude method for altering the E/N of the discharge. Since Xe has the lowest ionization potential of any of the constituents typically used in a CO laser mixture, it may also be useful for preventing CO decomposition due to collisions with high energy electrons. According to the measured cross-sections of Shulz[29] (Figure 3.1), electron excitation of CO is effective only for $\lesssim 8$ vibrational quanta. Qualitatively, the cross-sections for excitation of N_2 are quite similar to those for CO, although they are

smaller by about a factor of six. Hence, N_2 would be expected to have an effect on the electron distribution qualitatively similar (in energy dependence) to that for CO. Therefore, addition of N_2 to a CO laser mixture can be of benefit, since for the proper values of E/N, it would be as efficient for storing electrical energy in vibrational states as is CO. Since the levels of N_2 are nearly resonant with those for CO, this vibrational energy can be transferred by V-V-T cross-relaxation to the CO levels and would not be last (since V-T relaxation is much slower). Two important factors to realize, however, are that N_2 can be added to alter the E/N of the plasma without loss of electron-vibration energy transfer efficiency, and its addition does not directly affect the CO-CO V-V-T anharmonic pumping rates, which would have occured if we had merely increased the CO partial pressure. Since V-V-T pumping in the N_2-N_2 system is much slower than that for N_2-CO, most of the transfer from N_2 will be from the lowest level. The beneficial effects that result from the simultaneous pressure of N_2 and Xe may be due to the fact that N_2 and Xe alter the plasma characteristics in qualitatively different ways. For example, the fractional conversion of electrical to vibrational energy is improved not only upon lowering the E/N, but is evidently enhanced also by an optimum gas composition, since the performance can be improved by the simultaneous presence of both of these constituents. An equivalent enhancement cannot be obtained merely by increasing the fractional amount of Xe in the gas mixture. Since the addition of N_2 does not cause degradation of the fractional transfer of energy to vibrations, it may have advantages that an addition of Xe cannot provide. For the plasma characteristics, the effect of the addition of N_2 could probably be accomplished equivalently by increasing the partial pressure of CO (although the average electron energy would not be the same function of E/N). However, the optimum concentration of CO in the laser mixture is also determined by other constraints, such as the rate of V-V-T pumping, V-T relaxation decomposition, etc. Thus, the optimum mixture seems to require several ingredients (typically CO, N_2, He and Xe). The

addition of O_2 often plays a very sensitive role, inasmuch as very small amounts can have a critical effect on the operation. A small amount of O_2 is helpful, because it probably minimizes CO decomposition by driving the reaction $CO \rightleftharpoons C + O$ to the left and prohibits carbon deposits. Beyond a critical amount, the presence of O_2 can have a deleterious effect on the laser performance. This may be due to a drastic alteration of the plasma characteristics (since O_2 has a large electron attachment coefficient of magnitude greater than that for most gases), or it may result in the formation of CO_2 (at least for room temperature operation). Since such minute amounts can have such an important effect, the former explanation is probably correct. Nighan[71 - 74] has shown that for electron energies lower than those necessary for a self-sustaining glow discharge, the efficiency of electrical energy transfer to the vibrational levels can be greatly enhanced, and his analyses show the extreme sensitivity in some cases of the vibrational excitation rates upon plasma characteristics. Figure 4.4 and 4.5, taken from Reference 71-74 illustrate these results. Clearly, in order to best achieve an optimization of the plasma characteristics of a laser system, it would be desirable to have an independent control over the ionization process and the electrical excitation of the molecular vibrational levels, since then the E/N could be adjusted to have the most favorable value. One sophisticated technique for doing that is to obtain the initial pre-ionization with a high energy electron beam, which creates a volume ionized gas of low energy secondary electrons which are then accelerated by an applied electric field to sustain the discharge current. For the case of CO, Figure 4.5 indicates that optimization of energy transfer to vibrational levels is not a sensitive function of E/N below a certain minimum value.

For the case of CO_2 laser systems, the molecular kinetics are much simpler than for the case of CO, where many vibrational levels must be considered. The electron distribution function must depend upon the populations of excited vibrational states of the molecular species if there

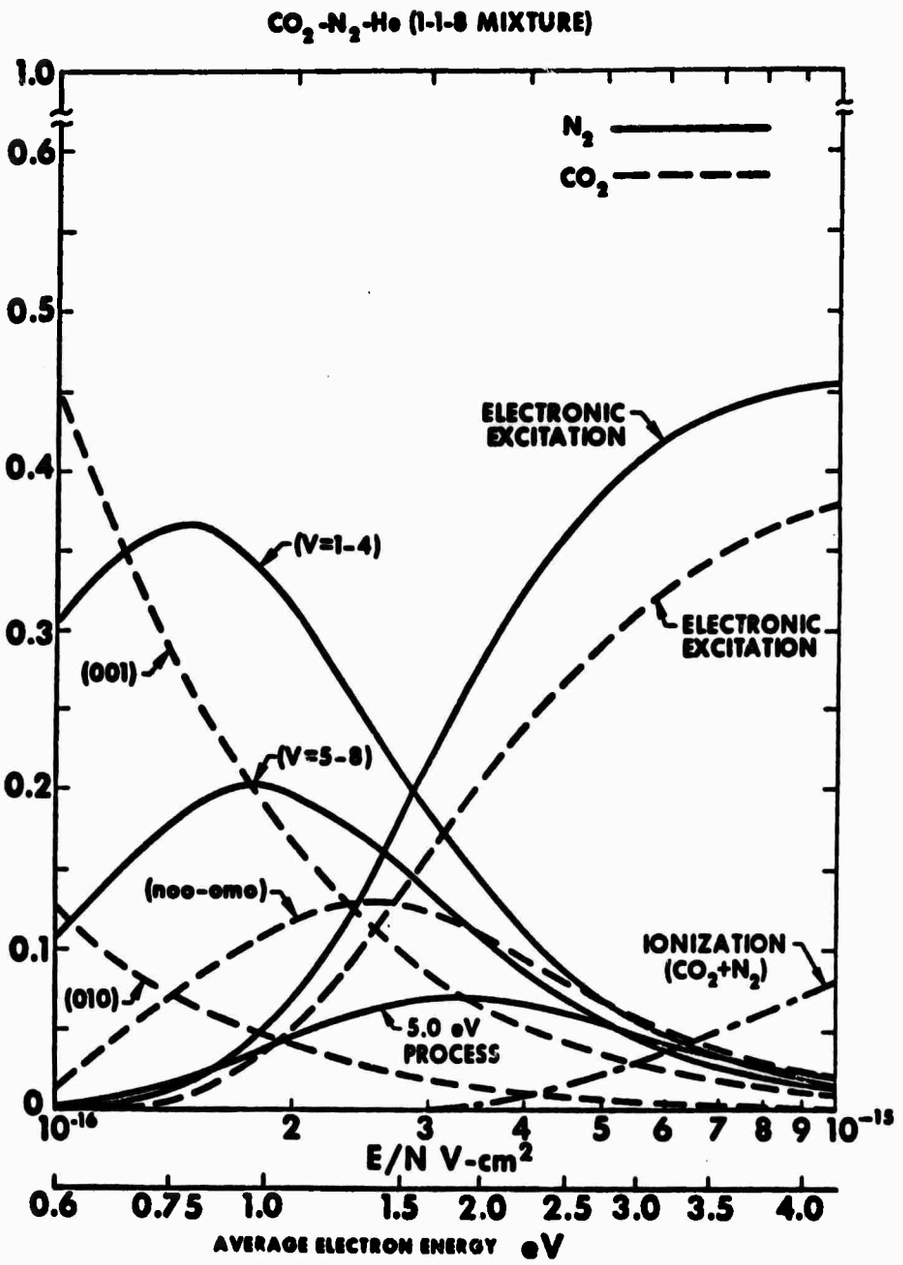

Figure 4.4. Fractional electron power transfer to competing excitation processes for electrically excited CO_2-N_2-He laser mixture, taken from Reference 71.

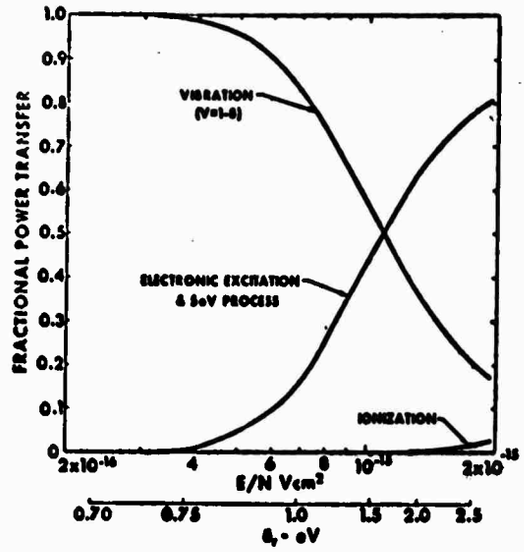

(a)

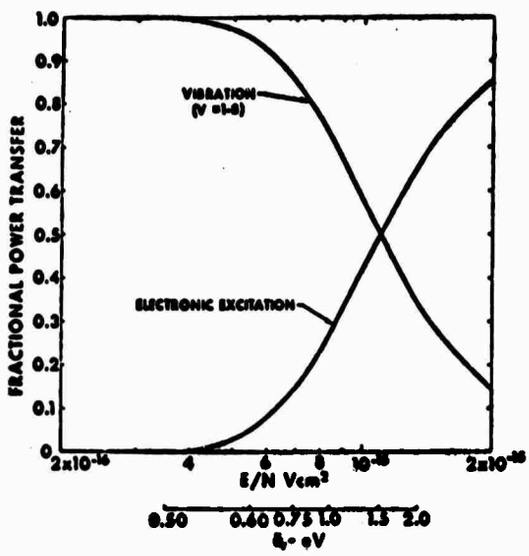

(b)

Figure 4. 5. Fractional electron power transferred to vibrational and electronic state excitation for (a) N_2, and (b) CO (taken from Reference 74).

exist inelastic excitation processes from such states that are important for extracting energy from the electron gas. Thus, a complete model for an electrical discharge CO laser would require a coupled set of equations for the molecular and electron kinetics. Our experiments have shown that the presence or absence of lasing may significantly change the electron distribution function; this was demonstrated by the fact that the visible CO emission from upper electronic states sharply increases when the laser cavity is blocked, suggesting that the average electron energy has been increased by the altered population distribution of the CO vibrational states. Since the vibrational population distribution is different when lasing is prohibited, the relative importance of the vibrational versus electron excitation mechanisms for the electrons would be changed. Nighan[74] has, in fact, carried out calculations for the electron distribution that arises in vibrationally excited N_2, assuming that electron excitation collisions with $N_2(v = 1)$ are also included. Fig. 4.6, taken from Ref. 74, illustrates the effect that the N_2 vibrational population distribution can have on the electron kinetics. Thus, for the CO laser, it is probably not completely accurate to characterize the plasma only by the gas composition and the value of E/N; the details of the vibrational population distribution may also be important for the coupled system of molecules and electrons. For the case of the CO_2 laser system, extremely rapid cross-relaxation processes make it possible to describe the molecular kinetics in terms of only a very few molecular vibrational levels, so that the significant excitation processes that determine the electron distribution occur mainly from the ground state.

In addition to further improvements on the molecular kinetic model for the CO system, it would be desirable to undertake theoretical calculations of the electron energy distribution functions. This would be especially valuable for treating the combined system of molecular and electron kinetics on a consistent and equal basis, and is necessary for constructing a reliable model for electric discharge CO laser systems.

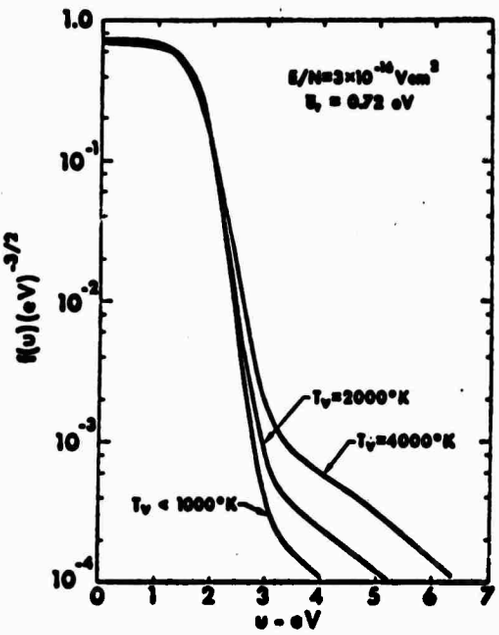

Figure 4.6. Electron energy distribution functions in N_2 calculated for various vibrational temperatures (taken from Reference 74).

5.0 SUMMARY AND CONCLUSIONS

A complete theoretical understanding of the operating characteristics of an electrically excited CO laser system requires a detailed model for the kinetics of both the electrons and the molecular vibrational levels. Although a completely self-consistent analysis should attempt to treat these two coupled systems on an equal basis, there is much useful information that can be obtained by analyzing them independently. The basic reason for this is that the characteristics of one system are only reflected somewhat insensitively in the resulting properties for the other. For example, the detailed structure of the electron energy distribution does not critically affect the integrations over the cross sections that give the rates for electron pumping of the molecular vibrational levels. That is, even though the electron energy distribution function may display very important behaviour in the energy regions of interest for vibrational excitation, use of an (incorrect) Boltzmann distribution can give approximately the correct rates if the electron temperature is selected properly. On the other hand, the detailed structure of the vibrational population distribution does not have a profound effect upon the energy dependence of the electron distribution, although experimental evidence indicates that the plasma characteristics may change in the presence or absence of lasing. The tacit assumption for an independent calculation for the electron distribution is that most of the molecules are in the ground state, and that the significant processes that determine the energy dependence are inelastic excitations from the ground state. To the extent that all of these approximations are valid, a reasonable theoretical picture of electrical CO laser systems can be obtained from results obtained using independent kinetic models for the electrons and the molecular vibrational levels.

As far as the molecular kinetics are concerned, there are several processes of pumping, relaxation, and cross-relaxation that must be included to explain theoretically the population distributions that are produced. Although

the initial source of energy input is the electrical excitation of the lowest vibrational levels, the dominant vibration-vibration exchange collisions (i.e., the "anharmonic pumping" mechanism) are responsible for rapid redistribution of this energy to higher levels. In this report, a discussion of several important aspects of the CO laser has been given, along with a description of the molecular kinetic model and computer program that has been constructed at NCL for calculations of the characteristics of a steady-state CO laser amplifier system. Although there presently remains a need for refining some of the experimental constants and theories of rates needed for this model, the program is essentially complete. From a reasonably general input description of the experimental conditions, it is designed to calculate all of the information about the vibrational population distribution that is necessary to completely describe the radiative characteristics. Small-signal gain measurements as well as measurements of relaxation rates using double Q-switching and double probe techniques are planned for the near future[21], and should help to finalize some of the constants required for construction of a reliable model.

For completeness, a discussion of several important aspects of the CO laser has been given. In addition to a qualitative and quantitative discussion of the molecular and electron kinetics, with formulation and numerical solution of the master equation for the steady state vibrational populations, several useful equations for the spectroscopic and radiative properties have also been included. The purpose for expanding the scope of this report somewhat beyond the specific topic of molecular kinetics has been to present a unified treatment of the physics of the electrically excited CO laser, as well as to provide a convenient summary of several relevant equations and references.

6.0 REFERENCES

1. M. L. Bhaumik, W. B. Lacina, and M. M. Mann, "Characteristics of a Room Temperature CO Laser," presented at CLEA, June 1971.

2. W. B. Lacina, M. M. Mann, R. G. Eguchi, and M. L. Bhaumik, "Efficiency Enhancement and Room Temperature Operation of the CO Laser," presented at the International Quant. Elect. Conf., September 1970.

3. M. L. Bhaumik, "High Efficiency CO Laser at Room Temperature," Appl. Phys. Lett. 17, 188 (1970).

4. M. L. Bhaumik, W. B. Lacina, and M. M. Mann, "Enchancement of the CO Laser Efficiency by Addition of Xenon," IEEE Journ. Quant. Elect. QE-6, 575 (1970).

5. M. M. Mann, M. L. Bhaumik, and W. B. Lacina, "Room Temperature CO Laser," Appl. Phys. Lett. 16, 430 (1970).

6. C. K. N. Patel, "Vibrational-Rotational Laser Action in Carbon Monoxide," Phys. Rev. 141, 71 (1966).

7. C. K. N. Patel, "CW Laser on Vibrational-Rotational Transitions of CO," Appl. Phys. Lett. 7, 246 (1965).

8. J. T. Yardley, "Vibrational Energy Transfer in CO-He Lasers," J. Chem. Phys. 52, 3983 (1970).

9. M. A. Pollack, "Laser Oscillation in Chemically Formed CO," Appl. Phys. Lett. 8, 237 (1966).

10. F. Legay, N. Legay-Sommaire, and G. Taieb, "Mechanism of a CO-N_2 Laser I. Study of the Vibrational Populations," Can. J. Phys. 48, 1949 (1970).

11. G. Taieb and F. Legay, "Mechanism of a CO-N_2 Laser II. Study by Electronic Spectroscopy," Can. J. Phys. 48, 1956 (1970).

12. N. Legay-Sommaire and F. Legay, "Vibrational Distribution of Populations and Kinetics of the CO-N_2^+ System in the Fundamental and Harmonic Regions," Can. J. Phys. 48, 1966 (1970).

13. R. M. Osgood and W. C. Eppers, Appl. Phys. Lett. 13, 409 (1968).

14. R. M. Osgood, Jr., W. C. Eppers, and E. R. Nichols, "An Investigation of the High-Power CO Laser," J. Quant. Elect. QE-6, 145 (1970).

15. P. K. Cheo and H. G. Cooper, "Excitation Mechanisms of Population Inversion in CO and N_2 Pulsed Lasers," Appl. Phys. Lett. 5, 42 (1964).

16. F. Legay, "Excitation des Molecules Par Transfert d'Energie Vibrationelle en Phase Gazeuse," J. Chim. Phys. (France) 64, 9 (1967).

17. F. Legay, G. Taieb, and N. Legay-Sommaire, "Vibrational and Electronic Processes Involved in the Mechanism of the CO-N_2 Laser," J. Quant. Elect. QE-6, 181 (1970).

18. F. Legay and N. Legay-Sommaire, Comptus Rendus 259, 99 (1964); 260, 3339 (1965); 266, 855 (1968).

19. C. Freed, "Sealed-Off Operation of Stable CO Lasers," presented at Conference on Laser Eng. Appl., Washington, D. C., June 1971.

20. L. E. S. Mathias and J. T. Parker, Phys. Lett. (Neth.) 2, 194 (1963).

21. M. L. Bhaumik, "Carbon Monoxide Laser Studies," NCL Report 71-31R, August 5, 1971.

22. P. H. Krupenie, "The Band Spectrum of Carbon Monoxide," Nat'l. Bureau of Standards Report, NSRDS-NBS5 (1966).

23. G. Herzberg, Spectra of Diatomic Molecules (D. Van Nostrand, 1959).

24. S. S. Penner, Quantitative Molecular Spectroscopy and Gas Emissivities (Addison-Wesley, 1959).

25. W. S. Benedict, R. Herman, G. E. Moore, and S. Silverman, Astrophys. J. 135, 277 (1962).

26. P. W. Anderson, "Pressure Braodening in the Microwave and Infrared Region," Phys. Rev. 76, 647 (1949).

27. J. H. Van Vleck and Henry Margenau, "Collision Theories of Pressure Broadening of Spectral Lines," Phys. Rev. 76, 1211 (1949).

28. C. K. N. Patel, "Continuous-Wave Laser Action on Vibrational-Rotational Transitions of CO_2," Phys. Rev. 136A, 1187 (1964).

29. G. J. Schulz, "Vibrational Excitation of N_2, CO, and H_2 by Electron Impact," Phys. Rev. A135, 988 (1964).

30. M. J. W. Boness and G. J. Schulz, "Vibrational Excitation of CO_2 by Electron Impact," Phys. Rev. Lett. 21, 1031 (1968).

31. A. V. Phelps, "Rotational and Vibrational Excitation of Molecules by Low-Energy Electrons," Rev. Mod. Phys. 40, 399 (1968).

32. A. Herzenberg and F. Mandl, "Vibrational Excitation of Molecules by Resonance Scattering of Electrons," Proc. Roy. Soc. (London) A270, 48 (1962).

33. J. C. Y. Chen, "Theory of Subexcitation Electron Scattering by Molecules. I. Formalism and the Compound Negative-Ion States," J. Chem. Phys. 40, 3507, and "... II. Excitation and De-Excitation of Molecular Vibration," J. Chem. Phys. 40, 3513 (1964).

34. C. E. Treanor, J. W. Rich, and R. G. Rehm, "Vibrational Relaxation of Anharmonic Oscillators with Exchange-Dominated Collisions," J. Chem. Phys. 48, 1798 (1968).

35. J. D. Teare, R. L. Taylor, and Von Rosenberg, "Observation of Vibration-Vibration Energy Pumping Between Diatomic Molecules," Nature, 225, 240 (1970).

36. C. T. Hsu andF. H. Maillie, "Vibrational Relaxation of Anharmonic Oscillators with Vibration-Vibration and Vibration-Translation Energy Exchanges," J. Chem.Phys. 52, 1767 (1970).

37. R. Fisher and R. H. Kummler, "Relaxation by Vibration-Vibration Exchange Processes. Part I. Pure Gas Case, and Part II. Binary Mixtures," J. Chem. Phys. 49, 1075, 1085 (1968).

38. Kurt E. Shuler, "Relaxation of an Isolated Ensemble of Harmonic Oscillators," J. Chem. Phys. 32, 1692 (1960).

39. C. A. Brau, G. E. Caledonia, and R. E. Center, "Nonequilibrium Vibrational Distribution Functions in Infrared Active Anharmonic Oscillators," J. Chem. Phys. 52, 4306 (1970).

40. R. L. McKenzie, "Vibrational Relaxation and Radiative Gain in Expanding Flows of Anharmonic Oscillators," NASA Technical Note, NASA TN D-7050, March 1971.

41. J. W. Rich, "Kinetic Modeling of the High Power Carbon Monoxide Laser," J. Appl. Phys. 42, 2719 (1971).

42. A. Javan, "Collision Effects and Approach to Partial Thermal Equilibrium within Excited Atomic Levels," in Quantum Optics and Electronics, 1964 (Gordon & Breach), p. 393.

43. K. F. Herzfeld and T. A. Litovitz, Absorption and Dispersion of Ultrasonic Waves, (Academic Press, 1959).

44. R. N. Schwartz, Z. I. Slawsky, and K. F. Herzfeld, "Calculation of Vibrational Relaxation Times in Gases," J. Chem. Phys. 20, 1591 (1952).

45. R. N. Schwartz and K. F. Herzfeld, J. Chem. Phys., 22, 767 (1954).

46. Bruce M. Mahan, "Resonant Transfer of Vibrational Energy in Molecular Collisions," J. Chem. Phys. 46, 98 (1967).

47. James T. Yardley, "Nonresonant Vibration-to-Vibration Energy Transfer due to Dipole-Dipole Interactions," J. Chem. Phys. 50, 2464 (1969).

48. J. C. Stephenson, R. E. Wood, and C. Bradley Moore, "Near-Resonant Energy Transfer between Infrared-Active Vibrations," J. Chem. Phys. 48, 4790 (1968).

49. R. D. Sharma and C. A. Brau, "Near-Resonant Vibrational Energy Transfer in N_2-CO_2 Mixtures," Phys. Rev. Lett. 19, 1273 (1967).

50. R. D. Sharma, "Deactivation of Bending Mode of CO_2 by Hydrogen and Deuterium," J. Chem. Phys. 50, 919 (1969).

51. R. D. Sharma and C. A. Brau, "Energy Transfer in Near-Resonant Molecular Collisions due to Long-Range Forces with Application to Transfer of Vibrational Energy from ν_3 Mode of CO_2 to N_2," J. Chem. Phys. 50, 924 (1969).

52. R. D. Sharma, "Near-Resonant Vibrational Energy Transfer among Isotopes of CO_2," Phys. Rev. 177, 102 (1969).

53. R. D. Sharma, "Transfer of Vibrational Energy from Asymmetric Stretch of CO_2 to ν_3 of N_2)," Phys. Rev. A2, 173 (1970).

54. Donald Rapp and Thomas Kassal, "The Theory of Vibrational Energy Transfer between Simple Molecules in Non-Reactive Collisions," Chemical Reviews, Feb., 1969, p 61.

55. Donald Rapp and P. Englander-Golden, "Resonant and Near-Resonant Vibrational-Vibrational Energy Transfer between Molecules in Collisions," J. Chem. Phys. 40, 573 (1964).

56. Donald Rapp and P. Englander-Golden, "Erratum: Resonant and Near-Resonant Vibrational-Vibrational Energy Transfer between Molecules in Collisions," J. Chem. Phys. 40, 3120 (1964).

57. Donald Rapp, "Interchange of Vibrational Energy between Molecules in Collisions," J. Chem. Phys. 43, 316 (1965).

58. K. N. C. Bray, "Vibrational Relaxation of Anharmonic Oscillator Molecules: Relaxation under Isothermal Conditions," J. Phys. B (Proc. Phys. Soc.), 1, 705 (1968).

59. J. Keck and G. Carrier, "Diffusion Theory of Nonequilibrium Dissociation and Recombination," J. Chem. Phys. 43, 2284 (1965).

60. Roger C. Millikan and Donald R. White, "Systematics of Vibrational Relaxation," J. Chem. Phys. 39, 3209 (1963).

61. Roger C. Millikan, "Vibrational Fluorescence of Carbon Monoxide," J. Chem. Phys. 38, 2855 (1963).

62. Donald J. Miller and Roger C. Millikan, "Vibrational Relaxation of Carbon Monoxide by Hydrogen and Helium down to 100°K," J. Chem. Phys. 53, 3384 (1970).

63. F. A. Gianturco and R. Marriott, "A Recalculation of Vibrational Excitation in Carbon Monoxide," J. Phys. B (Atom, Molec. Phys.), 2, 1332 (1969).

64. Yukinori Sato and Soji Tsuchiya, "Shock-Wave Study of Vibrational Energy Exchange between Diatomic Molecules," J. Chem. Phys. 50, 1911 (1969).

65. R. J. Cross and R. G. Gorden, "Long-Range Scattering from Anisotropic Potentials: Diopole-Dipole Scattering," and "Dipole-Dipole Scattering in Molecular Beams. Variation of Total Cross Section with Velocity and Rotational Overlap," J. Chem. Phys. 45, 3571, 3582 (1966).

66. G. Hancock and I. W. M. Smith, "Quenching of Infrared Chemiluminescence," Appl. Optics, Special Issue, August, 1971.

67. W. Q. Jeffers and J. D. Kelley, "Calculations of V-V Transfer Probabilities in CO-CO Collisions," (preprint, submitted for publication).

68. B. Carnahan, H. A. Luther, and J. O. Wilkes, Applied Numerical Methods (Wiley, N.Y.).

69. T. Holstein, "Energy Distribution of Electrons in High Frequency Gas Discharges," Phys. Rev. 70, 367 (1946).

70. I. P. Shkarofsky, T. W. Johnston, and M. P. Bachynski, The Particle Kinetics of Plasmas (Addison Wesley, 1966).

71. W. L. Nighan, W. J. Wiegand, M. C. Fowler, and R. H. Bullis, "Investigation of Plasma Properties of High Energy Gas Discharge Lasers," United Aircraft Report, 1970.

72. William L. Nighan and John H. Bennett, "Electron Energy Distribution Functions and Vibrational Excitation Rates in CO_2 Laser Mixtures," Appl. Phys. Lett. 14, 240 (1969).

73. William J. Nighan, "Effect of Molecular Dissociation and Vibrational Excitation on Electronic Energy Transfer in CO_2 Laser Plasmas," Appl. Phys. Lett. 15, 355 (1969).

74. W. L. Nighan, "Electron Energy Distributions and Collision Rates in Electrically Excited N_2, CO, and CO_2, Phys. Rev., 2A, 1989 (1970).